

Copyright
by
Antônio Nemer Kanaan Neto
1996

MAGNETISM AND PULSATING STARS

by

ANTÔNIO NEMER KANAAN NETO, B.S., Ms. Sc.

DISSERTATION

Presented to the Faculty of the Graduate School of

The University of Texas at Austin

in Partial Fulfillment

of the Requirements

for the Degree of

DOCTOR OF PHILOSOPHY

THE UNIVERSITY OF TEXAS AT AUSTIN

December 1996

MAGNETISM AND PULSATING STARS

APPROVED BY
DISSERTATION COMMITTEE:

Supervisor: _____

Acknowledgements

Many people have directly helped me along this project. Some helped in the project, some helped me to keep doing the project.

In this last category Lisi has been the most important figure — as well as in the rest of my life. Astronomers work pretty hard and for many and odd hours. I have no complaints about that (especially comparing it to the amount of work, in many times not so good working conditions, I grew up used to see), in fact I have enjoyed every minute of doing astronomy. I have however, many times felt like giving up because I never got used to the extremes that competition has brought the Astronomical community to — and the US society in general. In those hours, when I felt like I would be better off elsewhere Lisi was always there to remind me how much I liked doing what I do and that these “giant contests” are actually petty little fights for insignificant matters. To her and her acute critical world view I owe much.

Don Winget, my advisor (the third actually) has played a rôle in both fronts. At a time when I was feeling highly frustrated for having produced nothing in my first two years of graduate school we started working together. Don’s passion for Astronomy and little care for politics and the need to impress other people were vital for me at that time.

Driving back from the Observatory I met Artie Hatzes. From that

day on we started a very productive relationship. We did together all of the research reported on the chapter about the rapidly oscillating Ap star γ Equulei. We have done other research as well which we are now working on. And I hope we will do lots of stuff in the future.

Kepler was my advisor back in Brazil and helped me much when I was getting started. Once I started working on my Ph. D. we continued interacting very much and much of this work is a result of his help.

I thank my committee members Ed Nather, David Lambert, Verne Smith and Jim Liebert for interesting conversations and all the suggestions they had while I worked on this project.

While doing the radial velocity measurements on γ Equ Bill Cochran helped me many times to better understand the technique of radial velocity measurements as well as the use of his software to do all the data analysis.

When I was still back in the “ghetto” (the big office two floors below the rest of the department where first year students are corralled into) I met Mike. Mike is one of the most knowledgeable students I have met and yet the least pretentious of all. Our conversations were always filled with questioning everything, either questioning the physics or our understanding of it — and what was even more startling this would also happen when we talked about many other subjects. That combination I really liked and we started interacting a lot. I must admit that it was thanks to him that I became a real part of our lab. I must also thank him for always being ready to run some pulsation or evolutionary model whenever I needed and also helping me to digest some

theoretical papers with to hairy a math for my observational skills. Scot and I have interacted much in the last few years. Even though our work has not overlapped much I always enjoyed running ideas by him, he was always a great help because he would give me the two things you want from people when you run ideas by them: encouragement and critical appraisal. Scot was also very generous in sharing (that is “giving” me) the office and Hovis (his computer). Atsuko has been a great person to work with. She has been very supportive in some difficult moments and was always fun to discuss about problems we wanted to have a better understanding.

Anand, whose love for physics made him leave astronomy, was a great friend whom I am glad to have met. We could always have conversations ranging from physics and astronomy to memories of our childhood or just about anything. His interest for physics was always refreshing to me and our interaction has helped me many times to deepen my understanding of the world (in general).

At the observatory many nights were saved by the early visits of Dave Doss who always had a fix for problems. His help showing how things work also helped me to better understand, and therefore use, the whole observatory. Marian Frueh and Earl Green were also very helpful in getting things working as well as showing me things, many times without my asking, just because they figured I would be glad to see them.

In many cloudy nights when I felt down Frank Cianciolo invited me over his place (later on I would come even with no invitation). Kevin Mace,

Mark Wetzel and Anil Dosaj were usually together in our meetings playing cards or just talking. I thank them all for providing entertainment (which kept me away from those horrible depressions typical of cloudy nights) as well for making me feel English as a real language for the first time.

Back in Brazil my good friend Odilon Giovannini kept providing me support and practical help. Our conversations over the years have always been very exciting to me. I thank him for letting me use some of his data on BPM 37093 (Chapter 3) and also letting me borrow some of the white dwarf spectra I show on Chapter 6 (GD 31 and 40EriB).

When I started working on the project of the origin of magnetic fields in white dwarfs I talked to Chuck Claver about the best way to find white dwarfs in open clusters. Some time later Chuck and Jim Liebert found the first magnetic white dwarf in a star cluster: EG 61 in the Praesepe. He and Jim knowing how excited I would be with this finding invited me to collaborate with them on that finding. I thank them both for sharing that finding with me.

I would also like to thank my mother for all the support she has given me to become an astronomer. It was very important that she always told me: “do what you love and you will be fine”. I took that to heart and just kept at it. I vividly remember how much she — and I, and all the children involved — liked doing plays for children (which was her professional activity), and one of the most important lessons she always gave us while practicing: “don’t just stick to the script, let your imagination fly”.

Gabriel has been a marvellous person to interact during the last three

years. He is always been interested about my “trabalhinho” (art-work in Portuguese baby speech a word which was transferred from his art-work at the day care. The same word, without the diminutive, “trabalho” means job, work) and was very understanding (as much as a toddler can be) every time I had to leave for a week’s observing. At the final stages of doing this dissertation I spent much less time with him than I am used to, but he was again very understanding and I thank him for bringing me his Bambi to calm me down the day before my defense.

Preface

Each chapter has been written to be a self contained paper. Chapter 2 is to be submitted to the Astrophysical Journal. Chapter 3 will be reformulated somewhat to fit in an Astrophysical Journal Letter, (Winget, Kepler, Kanaan) where more emphasis will be given to the possible finding of crystallizing pulsators and a little less emphasis on BPM 37093. Chapter 4 will be submitted to the Astronomical Journal. Chapter 5 will be submitted to the Astrophysical Journal (Kanaan and Hatzes). Chapter 6 is going to be a part of a comprehensive study of the Praesepe white dwarfs (Claver, Liebert, Bergeron and Kanaan).

Because of this structure there may be a fair amount of repetition in each chapter of this thesis. It has however the advantage that each chapter is self-contained therefore the reader can always go to one chapter and find all the relevant information in there.

MAGNETISM AND PULSATING STARS

Publication No. _____

Antônio Nemer Kanaan Neto, Ph.D.
The University of Texas at Austin, 1996

Supervisor: D.E. Winget

In this work I have approached two fundamental problems with the ZZ Ceti instability strip. First, I have proved that the lack of pulsating stars below the temperature of 11,000 K is real and not the result of a selection effect. Pulsation models indicate pulsations should be present at temperatures as low as 8,000 K. Theory and observation agree in that pulsations have longer periods (as well as larger amplitudes) at lower temperatures, starting with periods of 2–4 minutes at 13,000 K and having the longest observed periods at around 15 minutes at 11,000 K. Observers have never found any pulsations below the temperature of 11,000 K. However, previous surveys have concentrated in searching for shorter periods and typical observing runs were at most three hours long. Doing differential photometry using a CCD camera and observing each star for one whole night I have surveyed 17 stars and proved that none of them is variable.

BPM 37093 is a special ZZ Ceti star. Of all stars in this category it is the only one which deviates from the period–amplitude relationship: it has a long pulsation period but very small amplitudes. I analyze two possibilities

to explain why it is so: 1) that it is reaching the red-edge of the instability strip; 2) that it is a crystallized star. The odds of the second hypothesis seem much higher. This star is very massive ($1.0 - 1.1 M_{\odot}$), and, for such a high mass, crystallization is expected to happen at temperatures even higher than that of the ZZ Ceti stars. As this star is the only known pulsating star which is expected to be crystallized, it presents an opportunity for testing the predictions of crystallization theory in a single object. Future white dwarf luminosity functions will show whether or not crystallization is important for the cooling of white dwarfs, but will not teach us anything about the characteristics of individual objects.

The second problem with the ZZ Ceti instability strip is the presence of non-pulsating stars in the same temperature range as the pulsating ones. This problem is not particular to the ZZ Ceti stars. We see this in all other instability strips. The hope is that, because the contamination with non-variables is much lower among the ZZ Ceti stars and because these objects are physically simpler than the other known pulsating stars, we can discover the physical characteristic that distinguishes the variables from the non-variables. The hypothesis that magnetic fields suppress pulsations has been ruled out by my observations of three non-variable stars. These objects do not show any magnetic fields down to the detection limit of 25 kG, a value smaller than that needed to suppress pulsations.

One excellent laboratory to study the interactions of magnetic fields with pulsations is the rapidly oscillating Ap stars. I have observed one of these

stars using high precision (50 m/s) time resolved (1 minute) spectroscopy and uncovered very revealing information. Before our observations, there had been a few reports of different values for the radial velocity modulations caused by pulsations in these objects. We now understand why that was. Different spectral lines show different modulations. The amplitude of the modulations are anticorrelated with the equivalent width of the lines. It is also true that some elements (Cr, Ti) systematically exhibit larger radial velocity modulations than others (Fe).

To finalize I propose an observational program to test the validity of the old claim that all magnetic white dwarfs are descendants from the magnetic Ap stars. This program consists in looking for magnetic white dwarfs in young clusters where the Ap stars have not yet evolved to the white dwarf stage. If the fields in magnetic white dwarfs are only fossil remnants from the Ap stars then no magnetic white dwarfs should be found among these young clusters. The finding of a magnetic white dwarf in a young cluster would disprove this hypothesis. Among older clusters the Ap stars have already evolved to white dwarfs, and magnetic white dwarfs should be found in these clusters. The first magnetic white dwarf in a cluster has now been found and it belongs to the Praesepe. The Praesepe has its main-sequence turnoff mass around $2.2 M_{\odot}$ and therefore this magnetic star can be the descendant of an Ap star. The fossil field hypothesis has survived this first test. If in the future we continue finding magnetic white dwarfs among old clusters and not among young clusters then we can consider the fossil field hypothesis reliable.

Table of Contents

Acknowledgements	iv
Preface	ix
Abstract	x
Table of Tables	xv
List of Figures	xvi
Chapter 1. Introduction	1
Chapter 2. Observational Definition of the ZZ Ceti Red Edge	7
1. Introduction	7
2. Observations	10
3. Data Reductions	11
4. Results	12
Chapter 3. BPM37093: a different ZZ Ceti	26
1. Introduction	26
2. BPM37093 and the others	28
3. Observations	30
3.1. Analysis of the 1996 data	31
4. Why?	33
4.1. Crystallization	33
4.2. Red Edge	35
4.3. High Mass	35
5. Conclusion	35

Chapter 4. Magnetic Fields are not Suppressing Pulsations in ZZ Ceti Stars	46
1. Introduction	46
2. The Observational Technique	51
3. Observations	56
4. Results	56
5. Temperatures	59
6. Conclusion	60
 Chapter 5. Pulsations and Radial Velocity Variations in Magnetic Pulsating Ap Stars. Analysis of γ Equulei	 89
1. Introduction	89
2. Observations	92
3. Analysis	93
4. Discussion	96
 Chapter 6. A Proposed Test of Models for the Origin of Magnetic White Dwarf Stars	 114
1. Introduction	114
2. Our Method	116
3. Feasibility	117
4. First Results	120
5. A Closer Look at the Distribution of Magnetic White Dwarfs	123
6. Other Connections	125
6.1. A Few More Ideas	127
7. Conclusion	128
 Chapter 7. Conclusions	 140
 Appendices	
 Appendix A. Line Identifications for γ Equulei	 145
 Bibliography	 156
 Vita	 163

Table of Tables

2.1	Selected Cool DAs.	17
2.2	Photometric limits on variability for cool DAs.	18
4.1	Observing Log	64
4.2	Results.	65
4.3	Dolez et al. non variables in the strip.	66
4.4	Cool DAs	67
4.5	ZZ Ceti temperatures.	68
4.6	ZZ Ceti temperatures (continued).	69
4.7	ZZ Ceti temperatures relative to G117-B15A.	70
4.8	ZZ Ceti temperatures relative to G226-29.	71
4.9	ZZ Ceti temperatures relative to BPM 37093	72
5.1	Radial velocity amplitudes for Cr lines.	100
5.1	Radial velocity amplitudes for Cr lines.	101
6.1	White Dwarfs in Clusters.	130
6.1	White Dwarfs in Clusters.	131
6.1	White Dwarfs in Clusters.	132
6.2	Clusters to be observed I	133
6.3	Clusters to be observed II.	134

List of Figures

2.1	This figure shows the period-amplitude-temperature relationship in three steps. Part c) displays temperature against periods. b) temperature against amplitude and a) amplitude against period.	19
2.2	We show here the effect of using different apperture sizes on the light curves. The star observed is G111-71 a non-variable DA star ($m_V = 16.6$) observed on February 3, 1995 under photometric conditions. The bottom panel is for a 2 pixel radius aperture. The aperture radius increases by one pixel at each panel, the top one being at 7 pixels. The seeing on that night was 3 arcsec (= 3 pixels) The aperture which minimizes the scatter in the data is the one at 3 pixel radius.	20
2.3	The root mean scatter of each panel in the previous figure. Apertures of three to four pixels radius maximize the signal to noise in the light curve.	21
2.4	The worst and the best. Top panel shows the Fourier transform for the star G61-17. The bottom panel shows the Fourier transform of G1-45. The solid line on each plot represents the amplitude above which the probability of false alarm would be less than 1/100.	22
2.5	The light curve for G61-17 on the night of March 9, 1995. . . .	23
2.6	The light curve for G1-45 on the night of September 24, 1994. .	24
2.7	On this figure we repeat part b) of figure 1 but also including the non-variables below the red edge of the instability strip. It is clearly visible that the amplitudes abruptly fall down to an undetectable level (4mmag for plotting purposes). This indicates that the mechanism shutting pulsations off is more of an on/off nature than a smooth damping process. The filled circles represent the known ZZ Ceti variables. The filled squares the non-variable cool DAs we have observed.	25
3.1	This figure shows the period-amplitude-temperature relationship in three steps. Part a) displays temperature against periods. b) total power against temperature c) total power against period. BPM 37093 is shown with the star symbol.	38
3.2	We show here the Fourier transforms of our data for each year.	39

3.3	We show here the daily Fourier transforms during our 1996 run on BPM 37093.	40
3.4	Phase versus time for the 1.766 mHz mode. Only the first six nights are on this plot because this mode disappears in the last four nights.	41
3.5	Amplitude versus time for the 1.766 mHz mode.	42
3.6	Phase versus time for the 1.716 mHz mode. We have plotted data from the second night till the seventh. For other nights this mode was not present.	43
3.7	Amplitude versus time for the 1.716 mHz mode.	44
3.8	The rectangle in the center represents the range of masses and temperatures found for BPM 37093. The lower right corner is the determination of Bergeron et al. (1995), the top left corner is the determination of Giovannini (1996). The formal temperature uncertainties from each author are much less than their discrepancies. The lines represent the limits where crystallization reaches 10% (top line) and 90% (bottom line). The continuous line is for an oxygen core. The long-short dash is for a pure carbon core.	45
4.1	A gaussian with a full width at half maximum of 1 Å looks very similar to the absorption core of H $_{\alpha}$ in a white dwarf. Such a line can have the width it has either because of rotation or a combination of rotation and a magnetic field.	73
4.2	The sum of three 1 Å wide lines split by a 25 kG magnetic field (0.5 Å in both directions) produces a wider line whose full width at half maximum is 1.5 Å. Measuring this width it is possible to set an upper limit of 37.5 kG to the presence of a magnetic field.	74
4.3	The sum of three 1 Å wide lines split by a 50 kG magnetic field (1 Å in both directions) produces a wider line whose full width at half maximum is 2.8 Å. Measuring this width it is possible to set an upper limit of 71 kG to the presence of a magnetic field. In very high signal to noise spectra it would be possible to see the triplet at the bottom of the line, however this would not be the case with our low signal to noise spectra.	75
4.4	The ZZ Ceti G29-38.	76
4.5	The spectrum of the cool DA G1-45.	77
4.6	The spectrum of the cool DA G19-20.	78
4.7	The cool binary degenerate L870-2. Spectra are separated by 0.5h intervals, beginning at the bottom.	79

4.8	The ZZ Ceti G29-38.	80
4.9	The ZZ Ceti G185-32.	81
4.10	The ZZ Ceti R548.	82
4.11	The ZZ Ceti G226-29.	83
4.12	The non-variable G67-23.	84
4.13	The non-variable PG1022+050.	85
4.14	The non-variable G8-8.	86
4.15	This figure shows the results of our compilation of temperature determinations for the ZZ Ceti instability strip. We show it only for the two most recent temperature determinations. That of Giovannini (1996) which uses Koester model atmospheres and that of Bergeron et al (1995) which uses ML2 convection with $\alpha = 0.6$. BPM 37093 was used as the fiducial point. Of the 10 stars they have in common three suffer shifts bigger than 500 K.	87
4.16	The ZZ Ceti instability strip according to Giovannini (1996). The Solid line represents the computations of Bradley and Winget. The dashed line is the same but shifted by 300 K to include all the variable stars. Open circles represent the pulsating ZZ Ceti stars. Filled circles are non variable stars. Theoretical models were computed only till $0.8 M_{\odot}$, this is why the line becomes vertical at $0.8 M_{\odot}$	88
5.1	On this figure we show the part of the spectrum of γ Equulei which was accessible to us with our instrument. Due to small size of our detector we do not have complete wavelength coverage.	102
5.2	The Fourier transforms at each spectral order is shown on this figure. All boxes have the same scale. This is the first clear proof of our point: different spectral regions do have different velocities.	103
5.3	The phase diagrams for the radial velocity measurements on each spectral order.	104
5.4	Fourier transforms for two iron lines. Iron 5555.00 and iron 5295.20. Note the big difference in the noise between each.	105
5.5	The amplitudes of all unblended CrI and CrII lines as a function of equivalent width. The filled are circles are lines of CrI. The open circles are lines of CrII.	106
5.6	The amplitudes of all unblended FeI lines as a function of equivalent width.	107
5.7	The amplitudes of all unblended FeII lines as a function of equivalent width.	108

5.8	The amplitudes of all unblended TiI and TiII lines as a function of equivalent width.	109
5.9	The amplitudes of all unblended CrI and CrII lines as a function of wavelength.	110
5.10	The amplitudes of all unblended FeI lines as a function of wavelength.	111
5.11	The amplitudes of all unblended FeII lines as a function of wavelength.	112
5.12	The amplitudes of all unblended TiI and TiII lines as a function of wavelength.	113
6.1	Spectra of a magnetic white dwarf (2 MG) at different signal-to-noise ratios. All spectra have a dispersion of 8.6\AA per pixel. . .	135
6.2	Spectra of three white dwarfs. 40 Eri is a $0.4 M_{\odot}$ and 16,000 K. GD 31 is $1.0 M_{\odot}$ and at 16,600 K. EG 61 is $0.9 M_{\odot}$ and 21,000 K and has a magnetic field of 2 MG.	136
6.3	Spectrum of the recently discovered white dwarf in the Praesepe. A field of 2 MG has been derived for this star from the splitting at the bottom of H_{β} and H_{γ}	137
6.4	The distribution of magnetic field strengths as a function of effective temperature.	138
6.5	The distribution of magnetic field strengths as a function of effective temperature (log plot).	139
A.1	Line identifications in the region from 5132\AA to 5153\AA . In this figure we mark the lines used in our analysis. All of the Fe, Cr and Ti lines studied are marked on the spectra from figure . . .	146
A.2	Line identifications in the region from 5210\AA to 5231\AA	147
A.3	Line identifications in the region from 5290\AA to 5310\AA	148
A.4	Line identifications in the region from 5374\AA to 5395\AA	149
A.5	Line identifications in the region from 5459\AA to 5481\AA	150
A.6	Line identifications in the region from 5547\AA to 5568\AA	151
A.7	Line identifications in the region from 5638\AA to 5660\AA	152
A.8	Line identifications in the region from 5732\AA to 5755\AA	153
A.9	Line identifications in the region from 5830\AA to 5852\AA	154
A.10	Line identifications in the region from 6034\AA to 6057\AA	155

Chapter 1

Introduction

The study of astronomy is full of examples of the most refined forms of abstraction where inferences are made about every single observable phenomenon. After we have played long enough with our abstractions they finally become to us a concrete reality. There is a long series of connections from looking up at bright dots on the sky up to the point where we can say they are stars, immense balls of gas whose energy is provided by nuclear reactions. All these connections however, are made from observations of stellar surfaces. For stellar evolution it is extremely important to have knowledge of the stellar interior. The amount of information about the stellar interior available to the astronomer is however, very small. The only instance where we have direct access to the stellar interior is with the solar neutrino detections.

Asteroseismology changes this picture by allowing us to probe the stellar interior, not directly but by physically interpreting vibrational motions present in some special stars. This kind of study was first applied to our own planet and is called seismology. Since the recognition of δ Cephei as a variable star in 1784 by Goodricke almost a hundred years passed until Ritter in 1879 suggested that these variations might be caused by pulsations. By that time he also developed the first rudiments of pulsation theory. His hypothesis, however,

competed with the binary hypothesis for many years. Apparently Shapley was responsible for consolidating the pulsation hypothesis in an article published in the *Astrophysical Journal* in 1914. There he pointed out the problems with the binary hypothesis, and how many of these problems could be solved using the pulsation hypothesis. After Shapley, Eddington developed the theory even further. And finally in the late 50's Ledoux and Walraven in an article in the “*Handbuch der Physik*” presented what is to this date the “complete” theory of stellar pulsations.

We now know a wealth of groups of pulsating stars, from the horizontal branch Cepheids to the degenerate white dwarfs. We understand that pulsations in most of these objects are driven by the partial ionization of some abundant element near the surface. For some stars it is helium, for some hydrogen, and for some a combination of both.

Our models for pulsation fit the observed picture very well: the temperature range where pulsations are observed can be reproduced by theoretical models — and has even been predicted in one instance. However, two problems seem to plague the theory for almost all types of pulsators: 1) there seems to be always non-pulsating stars whose physical characteristics are the same as the pulsating ones; 2) the range of temperature where we see pulsations is always smaller than theory can explain, the maximum temperature can be reproduced correctly but the minimum is always much lower than the observed minimum.

Having these two problems in mind I decided to study the behavior of hydrogen white dwarfs in the ZZ Ceti instability strip.

On this strip we seem to have a few non-pulsating stars in the same temperature range as the pulsating ones and the question to arise immediately is what could be the difference between these non-pulsating stars from their pulsating counterparts?

One of the mechanisms which could possibly shut the pulsations off is the constraining of mass motions by a magnetic field. We have computed that a field strength around 10^5 G is necessary to shut off convection and pulsations as well. We then set off to observe the non-variable DAs to search for the existence of magnetic fields. By doing high resolution spectroscopy of the core of their $H\alpha$ lines we can set upper limits on the magnetic fields as low as 25kG. We have observed 3 known non-pulsators in the strip as well as 7 other DAs and have found no evidence for the existence of a magnetic field, so if any field exists in these objects it has to be weaker than 25kG. While this work was being done Schmidt and Smith (1995) published the results of their comprehensive survey for magnetic fields among hydrogen white dwarfs. The sensitivity of their measurements was as good as ours; however, their measurements are only sensitive to the longitudinal component of the field, while ours is sensitive to the global field.

It also happens that the ZZ Ceti's seem to stop pulsating at temperatures much higher than predicted by theory. However, in this case, there might be an observational selection effect. It is well known that the ZZ Ceti's follow a period–luminosity relationship which is better represented as period–temperature. The brighter, bluer and hotter pulsators pulsate with shorter periods and lower amplitudes. The cooler, redder and dimmer stars with longer periods and higher amplitudes. All searches for pulsations among

DA stars of temperature around the instability strip have been done using high speed photoelectric photometry and observing runs which were at most 3 hours long. We decided to survey a group of DA stars cooler than the current ($\approx 11,500\text{K}$) red edge limit for long pulsation periods. To do that we used a CCD photometer on the McDonald Observatory 0.9m telescope. This instrument allowed us a field of view of 4 arcmin which, at the faint magnitude of our objects, always allowed us to have at least one or more comparison stars in the same field as the white dwarf.

During the time we worked on this project we came to realize that the study of the interaction between pulsations and magnetic fields could be extremely fruitful for both fields. As we know of only one pulsating magnetic white dwarf (GD358) we decided to investigate the magnetic rapidly oscillating Ap (roAp) stars. Ap stars are apparently near main sequence objects which possess a magnetic field (100 G – 30,000 G) and show very high abundances of elements of the rare earths group. roAp stars are a subgroup of the Ap stars which display pulsations. Their pulsations are believed to be high overtone p -mode pulsations of low l index. In spite of all the differences between roAp stars and ZZ Ceti stars their light curves are extremely similar: periods ranging from 4 to 12 minutes and amplitudes of a few millimagnitudes.

We have observed the star γ Equulei using the cross dispersed coude spectrograph of the 2.7 m telescope at McDonald Observatory. Our data show different spectral lines having different radial velocity modulations, one result which by itself is very unexpected and clarifying as it solves the previous conflicting reports on the radial velocity amplitudes caused by the pulsations. Also, it is now apparent that there is a correlation between the radial velocity

modulations and the equivalent width of the lines being observed. It was also observed that chromium lines display higher average velocity modulations than the iron lines. We interpret these results in the light of the oblique pulsator model of Kurtz. Our point is that the motions of the atoms may be constrained by the magnetic field.

Considerations of the pulsations in magnetic white dwarfs and the magnetic rapidly oscillating Ap stars, led me to one of the many origin questions arising in astrophysics: where did the magnetic fields of white dwarfs come from? And by the same token, where did the magnetic fields of Ap stars come from? In 1981 Angel et al. argued that the space densities of magnetic white dwarfs were compatible with their being descendants of the Ap stars. Computing the space densities of white dwarfs in the solar neighborhood and comparing it to the expected space density of Ap star remnants, they find them to be very similar. This is indeed suggestive, but far from conclusive. We have devised a test that will, once and for all, answer the question of whether or not the magnetic white dwarfs descend from the Ap stars.

This test exploits the special opportunity provided by clusters. Stellar clusters have always been very useful because they provide astronomers with groups of stars with more or less homogeneous characteristics. The one characteristic we are interested in this case is their age. Suppose we observe two groups of stellar clusters: young ones where the Ap stars have not yet evolved away from the main sequence, and old ones where the Ap stars have already evolved into white dwarfs. If the magnetic white dwarfs do descend from the Aps we would find magnetic white dwarfs in the old clusters and no magnetic white dwarfs in the young clusters. In any case my test will determine

if the magnetic fields of white dwarfs are inherited from the Ap stars.

The origin of magnetic fields in Ap stars can be approached in the same way as with the white dwarfs. Abt (1979) showed that the fraction of A/Ap stars in stellar clusters is directly proportional to the cluster age reaching the same ratio as the field stars after a threshold age of 100 Myr. This strongly suggests that the Ap phenomenon arises as the stars age. Because the presence of peculiarities in Ap stars is always associated with a magnetic field, it is appropriate to ask whether the magnetic fields are being generated during the main sequence phase (and diffusion acts quickly afterwards bringing all the “peculiar” elements to the surface), or if they were in place by the time the star arrived to the main sequence (therefore implying diffusion has to be a slow process). I propose observations of the normal A stars in young clusters as a form to verify whether the magnetic fields are being generated during the main sequence. If the magnetic fields of Ap stars are fossil fields then the number ratio of magnetic normal A stars to non-magnetic normal A stars in young clusters should be the same as the number ratio Ap/A in older clusters.

Chapter 2

Observational Definition of the ZZ Ceti Red Edge

1. Introduction

The understanding of pulsational mechanisms in stars has helped us learn about both the physics and the interiors of stars. Once we understood Cepheid luminosity variations to be caused by pulsations, our understanding of the mechanisms leading to this phenomenon vastly improved. Entire new groups of pulsating stars have been found and for most of them we find that the same mechanism (see e.g. Cox, 1980, Cox & Giuli, 1968) can be invoked to explain the presence of pulsations: the $\kappa - \gamma$ mechanism acting on the partial ionization of some abundant element under the surface of these stars.

Even though we understand how pulsations happen, we do not understand why they sometimes do not happen. There are at least two instances where we do not know why pulsations do not happen. First, we see groups of stars apparently sharing the same physical characteristics in which some stars pulsate, while others do not. We assume that some physical characteristic we are unaware of is responsible for the difference, although so far we have identified no such characteristic. This problem is well substantiated

for the roAp stars (Martinez, 1993), for the δ Scuti (Breger, 1979) for the Cepheids (Bidelman, 1985) and for the ZZ Ceti (Kepler and Nelan, 1993). The second problem is more of a theoretical nature. Computations of stellar pulsation models trying to predict the temperature range where stars should pulsate normally indicate a broader range than observed. While fine tuning of parameters, especially convective efficiency, often can give a good match to the blue (hot) edge of the instability strips, the theoretical red (cold) edge is always much colder than the observed one.

Among the white dwarf stars, we know of three kinds of pulsators: the DAVs (or ZZ Ceti stars) having pure hydrogen atmospheres at $\approx 12,000$ K; the DBVs having pure helium atmospheres at $\approx 25,000$ K; and the DOVs and PNNV which are pre-white dwarfs showing lines of nitrogen, carbon, oxygen and helium, and are hotter than $100,000$ K, the latter being still shrouded by a planetary nebula.

With the ZZ Ceti stars, pulsation models are unable to predict a red edge before a temperature as low as $8,000$ K (Winget, 1981, Winget et al., 1982a, Dolez and Vauclair 1981, Hansen et al, 1985). As the models are computed at lower and lower temperatures longer period pulsations become excited. The models stop having excited modes with periods shorter or equal to $1,500$ seconds at temperatures of $8,000$ K. That however, does not mean that longer period modes could exist at temperatures even lower than that. According to Hansen et al. (1985) pulsations with periods longer than $10,000$ seconds should suffer from energy leakage and therefore not be excited. ZZ Ceti models have that time scale at effective temperatures between $9,000$ and $10,000$ K. Observations have shown no pulsating DA cooler than $11,000$ K

(McGraw, 1979, Fontaine et al., 1982, Greenstein, 1982, Kepler and Nelan, 1993). Among the DAVs, a clear correlation between temperature, amplitude, and period is observed: the cooler the star, the longer its pulsation period and the larger its pulsational amplitudes. Figure 2.1 (based on data from the literature and the Whole Earth Telescope, presented in Clemens, 1994 and with temperatures coming from Bergeron et al. 1995) shows this in three steps. The plots are easier to look at using power instead of amplitude, power is simply the amplitude squared. Part c) shows the temperature *vs.* period effect; part b) shows amplitude *vs.* temperature; part a) shows amplitude *vs.* period. This effect is understood as a consequence of the movement of the partial ionization zone of hydrogen into deeper layers of the star caused by evolutionary cooling (Winget, 1981, Winget et al., 1982, Clemens, 1994). As the partial ionization layer moves in deeper, the thermal timescale becomes longer and the amount of energy available for driving increases correspondingly.

The reality of the observed red edge has been questioned, as all surveys for pulsations among DAs have been carried out using high-speed photometry (Hansen et al, 1985). Past surveys for variability among ZZ Ceti stars were done with short observing runs, where a star would be observed for at most three hours. Long period variations of the order of 1 to 3 hours would be hard to detect using such short runs. To probe for long periods we decided to observe several white dwarfs at and cooler than the currently accepted observational red edge for the instability strip of DAs. For this survey we used a CCD photometer which allows us to constantly compare the brightness of our target relative to one or more stars in the same field of view, therefore correcting for extinction variations during the night. This technique has been

described by other authors in the literature (see *e. g.* Gilliland and Brown, 1988, Abbott, 1992) and we are not going to describe it in here. Taking short exposures we were able to probe for long and short periods as well.

Object selection:

Even though the absolute temperature determination of cool white dwarfs is uncertain (Bergeron et al, 1995), we can at least claim with certainty that the stars we selected are indeed cooler than the stars on the red edge. In Table 2.1 we list the stars we selected to observe along with their spectroscopic or photometric temperatures as well as the bibliographical reference for those values.

2. Observations

From June 1994 to May 1995 I observed 17 cool white dwarfs with the f/13 0.9 m telescope of McDonald Observatory. We used a Cassegrain focus CCD camera equipped with a Tektronix 512² detector with 27 μ m pixels. We binned the pixels 2 by 2 resulting in a plate scale of 0.95 arc seconds per pixel. In order to probe for longer periods we decided to observe each star for at least one whole night allowing for many cycles to be observed in case long period pulsations were present. The typical length of previous surveys was 3 hours, in this survey the average run length was 6 hours.

In order to minimize the color difference between the observed objects we chose to do the observations through a V filter, which gives the most number of counts given the blue spectrum of our targets and the red sensitivity of our detector. To minimize differential extinction we selected the least red

star in the field as our comparison star. This was found by interrupting the time series every 1.5 hours to take B and R frames. We used 1 minute integration time plus 20 seconds of dead time spent between readout and write time. This integration time places the Nyquist frequency at 6.25 mHz (160 seconds) which is a bit longer than the period of the fastest DAV, (G226-29, 109.2s; Kepler et al, 1983) which is a hot star. Among the cool DAVs, all known pulsation periods are longer than 5 minutes, being as long as 1189s for GD154 (Robinson et al, 1978).

With this choice of equipment and exposure times, we were able to probe for long period pulsations, as well as the well known reasonably short period pulsations, and with sensitivity comparable to previous surveys.

3. Data Reductions

At the telescope, as each frame arrives at the computer a copy of it is saved to a directory separate from the one where the original data are. On this directory we have previously prepared a bias image, and a flat field image. Immediately after the image is recorded, it is automatically trimmed and corrected for bias and flat field effects. Next we obtain our preliminary photometry on the field. For each star we determine the number of counts inside an aperture twice the FWHM of the images (see later for aperture size choice) and then the number of counts in an annulus around the star's aperture to determine sky brightness. Sky counts are subtracted from star counts and we are left with the net number of star counts. A table with heliocentric Julian date and counts for each star is created. This table is plotted on the computer every time a new point on the light curve is received. Currently we are able to do up to 20 seconds time

resolution with real time data reductions. We can improve our time resolution by using a program specific to this task instead of using the script language of IRAF (Image Reduction and Analysis Facilities) we have been using so far.

On the day following the observations we then decide upon what is the best form to reduce our data. The main question is the choice of the aperture size to be used. To do that we currently generate several light curves, one for each aperture size. In figure 2.2 we show the effect of changing the aperture radius from 2 to 7 (FWHM was 3 pixels on that night) pixels in steps of 1 pixel. For each datum, we compute: $r_t = I_t / \sum_{i=1}^{N_{stars}} I_i$ where I_t is the intensity of the target star and I_i the intensity of each comparison star. The ratio r_t is then the relative intensity of the target star relative to the sum of the comparison stars. We choose the light curve which produces the least scattering in the light curve as being our best light curve, in this case it was the one obtained with an aperture of 3 pixel radius (see also figure 2.3 where we plot the measured root mean scatter against aperture radius). The results are insensitive to the sky annulus size. Only in very crowded fields we have problems with sky subtraction, in which case we use a program designed for photometry in crowded fields (in IRAF, DAOPHOT developed by Stetson, 1987) to deal with the entire photometry. We have not needed to use it for this project.

4. Results

On figure 2.4 we show the Fourier transform of our best and worst data set. Superposed on the Fourier transform we plot a line representing the amplitude above which a peak on the transform would have a chance of less than 0.01

of having been created by chance. Note that for the star G1-45 we have a peak above this limit, however, its period of eight hours is, first of all, of the same length as our run; second it is longer than what we can correct for with our observation scheme as we do not try to make correction for differential extinction (we are correcting for extinction when dividing the target by the comparison stars but are not applying any correction to compensate for their color difference).

The false alarm probability is calculated using (Scargle, 1982):

$$P_F = 1 - (1 - e^{-\frac{P_{obs}}{\bar{P}}})^{N_i} \simeq N_i e^{-\frac{P_{obs}}{\bar{P}}}$$

or,

$$P_{obs} = \ln \left(\frac{N_i}{P_F} \right) \bar{P}$$

where P_F is the probability that a given peak in the Fourier transform be false. P_{obs} is the power of the peak (power equals amplitude squared) and \bar{P} is the average power in the Fourier transform. N_i is the number of independent peaks in the Fourier transform.

$$N_i = \frac{N_f}{RES}$$

where N_f is the Nyquist frequency and RES is the resolution of the frequency spectrum and given by $RES = 1/T$ where T is the length of the data string.

We then compute P_{obs} for $P_F = 0.01$ any peak above this limit would have one chance in 100 of being created by a random process.

Figures 2.5 and 2.6 show the light curves used to produce the two previous Fourier transforms. The light curve for G1-45 has a much lower scatter for two reasons: it is much brighter than G61-17 (14.0 and 15.8 magnitudes respectively) and better weather conditions.

In table 2.2 we show the results of our photometry. None of these objects pulsates with an amplitude larger than 5 mmag in periods shorter than 2 hours. Our limits for several of these stars are actually better than this. In figure 2.7 (which is the same as figure 2.1 part a with the addition of the non-variable stars) we present our results in a graphical form. The horizontal line connecting the points represents the 5 mmag limit.

We have proven that these cooler white dwarfs do not pulsate with amplitudes higher than 5 mmag as was expected from theoretical models.

One possible mechanism for the advent of the red edge could be the generation of magnetic fields ($\approx 10^5$ G) by the convective motions which are supposed to become stronger as the stars cool down. We have explored this possibility in detail and will publish those results separately. We used high resolution spectroscopy to look at the narrow core of the $H\alpha$ line in several of the stars observed for this project and have set a firm upper limit of 25 kG for the presence of any magnetic field in these objects.

A possible explanation was proposed by Hansen et al. (1985). They suggest that periods either too long or too short might not be stable because those waves would not be completely reflected at the stellar surface, thereby causing energy leakage eventually resulting in damping of pulsations. However, the long period edge found by them implies a temperature much lower than

the observed limit.

The interaction between pulsations and convection has been invoked with reasonable success to understand the red edge of Cepheids and RR Lyrae stars (Deupree, 1980, Deupree, 1977). We still wait a consistent treatment of convection pulsation interaction in white dwarfs.

Another mechanism to shut pulsations down is the dredge up of helium caused by convection at lower temperatures (Winget and Fontaine, 1982). Bergeron et al. 1990 have shown that most DA stars cooler than the ZZ Ceti instability strip have the high Balmer lines wider than we would expect for a $0.6M_{\odot}$ white dwarf. This could be explained by saying that on average these objects are more massive than their warmer relatives by $0.1M_{\odot}$. This is plausible in the sense that cooler white dwarfs being older may have more massive ancestors (Reimers and Koester, 1982). They suggest instead helium is being dredged up to the surface; the presence of helium increases the pressure broadening on the hydrogen lines therefore mimicking a higher gravity. However, the mass determinations of Bergeron et al. 1990 were all based on the ML1 parameterization of convection (following the notation of Fontaine et al, 1981) and they have not been redone with ML2 or ML3 (convective efficiency increases from ML1 to ML3). For the ZZ Ceti's, the inferred mean mass changes from 0.698 ± 0.086 to 0.575 ± 0.068 to 0.511 ± 0.062 and to 0.649 ± 0.076 going from ML1 to ML2 to ML3 and to $ML2/\alpha=0.6$. Assuming similar changes occur in models of cool DAs it is easy to admit that the mass increase deduced for the cool DAs is caused by different choices of the mixing length parameters. It is also probably not correct to use the same set of mixing length parameters from temperatures varying from the hot to the cool end of

the instability strip as the efficiency of convection is expected to increase as the stars cool. The helium dredge up as an hypothesis for the end of pulsations is interesting because it has an extra prediction (other than the shutdown of pulsations) however, we do not believe we can yet determine if helium is present in the atmosphere of the cool DAs.

Our contribution to this question has been to definitively prove that the red edge to the ZZ Ceti instability is real and not an observational selection effect.

Table 2.1. Selected Cool DAs.

WD	Alias	Temperature	Mass	Reference
0032-175	G266-135	9980	—	Dolez et al, 1991
0033+016	G001-007	11184	0.93	Giovannini, 1996
0101+084	G001-045	8750	—	Fontaine et al., 1985
0135-052	L870-002	8700	0.41	Bergeron et al, 1995
0816+387	G111-071	7710	0.67	Bergeron et al, 1995
0913+442	G116-016	8750	1.01	Bergeron et al, 1995
0955+247	G049-033	8600	0.60	Bergeron et al. 1990
1147+255	G121-022	10317	0.53	Giovannini, 1996
1244+149	G061-017	11068	0.50	Giovannini, 1996
1507-105	GD176	10640	0.35	Giovannini, 1996
1537+651	GD348	9910	0.53	Giovannini, 1996
1539-035	GD189	10457	0.67	Giovannini, 1996
1655+215	G169-34	9578	0.51	Giovannini, 1996
1840-111	G155-34	10389	0.61	Giovannini, 1996
1857+119	G141-54	10182	0.57	Giovannini, 1996
2136+229	G126-018	10652	0.63	Giovannini, 1996
2246+223	G067-023	11131	1.01	Giovannini, 1996

Table 2.2. Photometric limits on variability for cool DAs.

WD	Alias	Length (h)	Limit (mmag)
0032-175	G226-135	4.8	< 2
0033+016	G001-007	5.5	< 3
0101+048	G001-045	6.7	< 2
0135-052	L870-002	4.5	< 3
0816+387	G111-071	6.6	< 3
0913+442	G116-016	8.9	< 2
0955+247	G049-033	9.2	< 2
1147+255	G121-022	8.0	< 3
1244+149	G061-017	4.8	< 5
1507-105	GD176	4.2	< 3
1537+651	GD348	5.0	< 2
1539-035	GD189	7.1	< 2
1655+215	G169-34	4.5	< 5
1840-111	G155-34	5.0	< 3
1857+119	G141-54	3.5	< 5
2136+229	G126-018	7.5	< 2
2246+223	G067-023	6.1	< 2

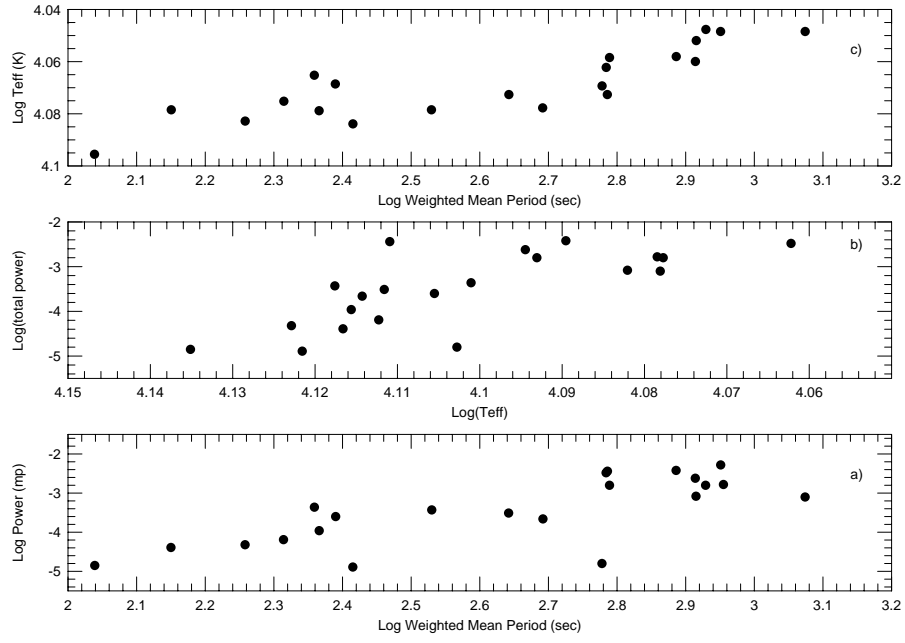


Fig. 2.1.— This figure shows the period-amplitude-temperature relationship in three steps. Part c) displays temperature against periods. b) temperature against amplitude and a) amplitude against period.

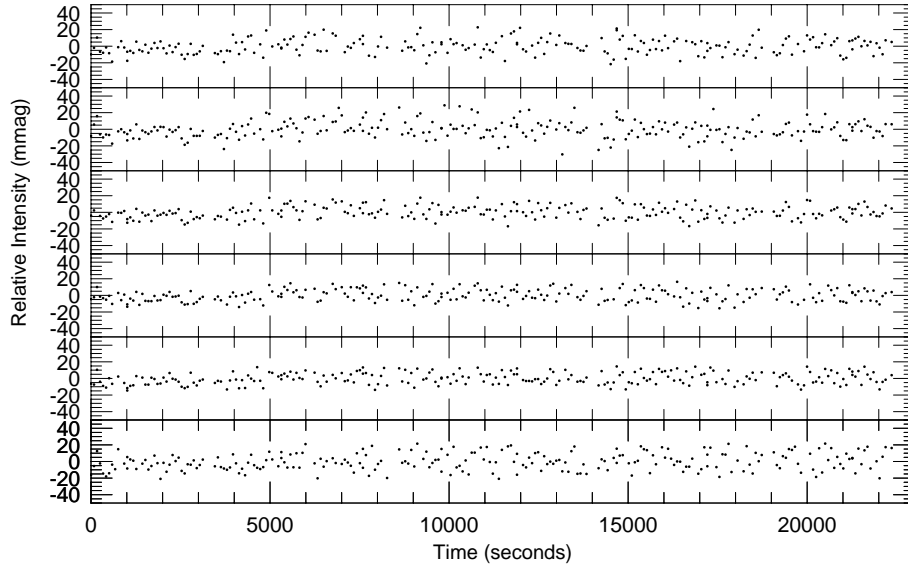


Fig. 2.2.— We show here the effect of using different apperture sizes on the light curves. The star observed is G111-71 a non-variable DA star ($m_V = 16.6$) observed on February 3, 1995 under photometric conditions. The bottom panel is for a 2 pixel radius aperture. The aperture radius increases by one pixel at each panel, the top one being at 7 pixels. The seeing on that night was 3 arcsec ($= 3$ pixels) The aperture which minimizes the scatter in the data is the one at 3 pixel radius.

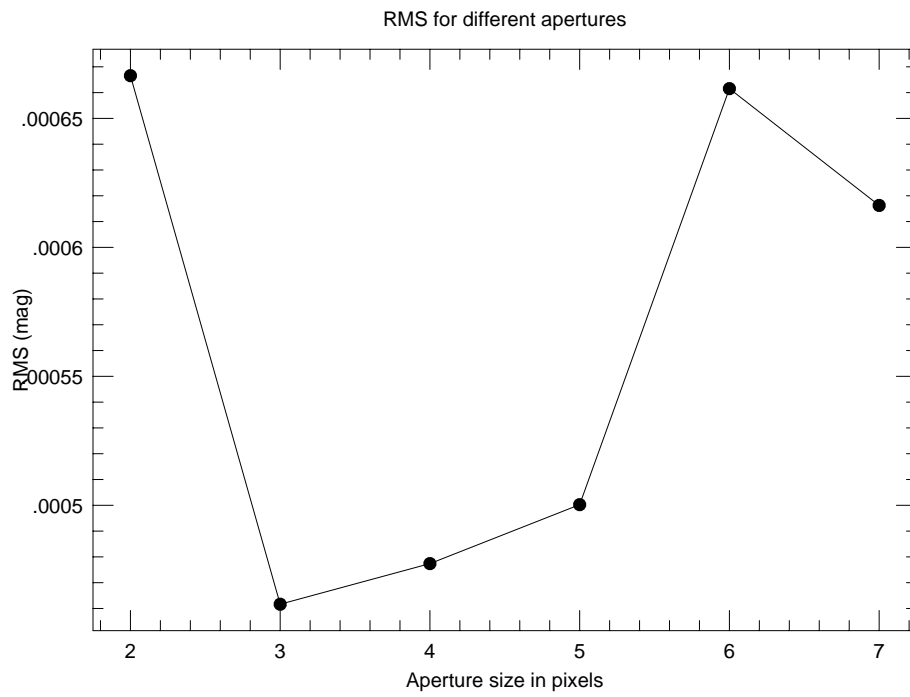


Fig. 2.3.— The root mean scatter of each panel in the previous figure. Apertures of three to four pixels radius maximize the signal to noise in the light curve.

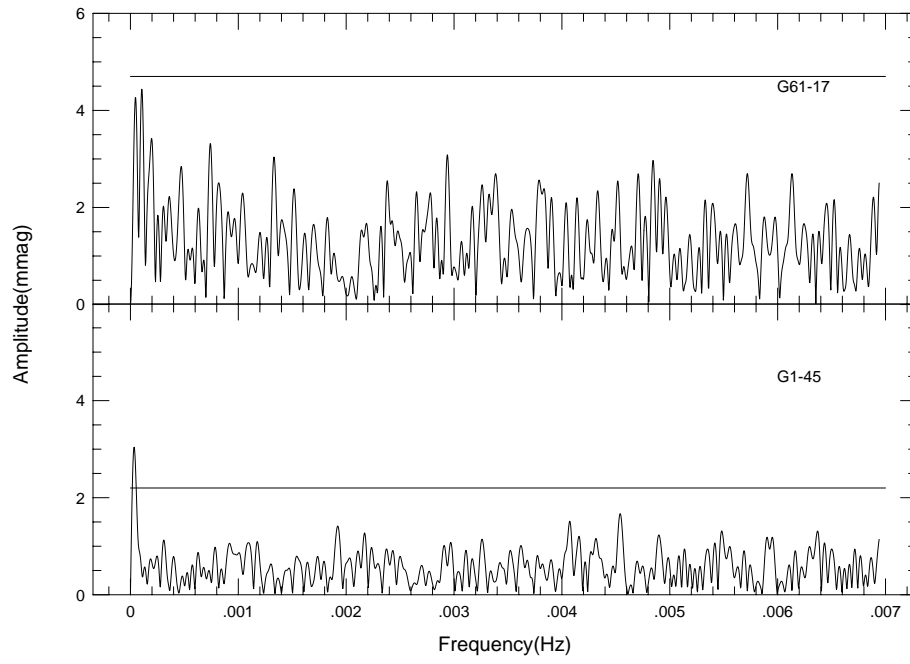


Fig. 2.4.— The worst and the best. Top panel shows the Fourier transform for the star G61-17. The bottom panel shows the Fourier transform of G1-45. The solid line on each plot represents the amplitude above which the probability of false alarm would be less than 1/100.

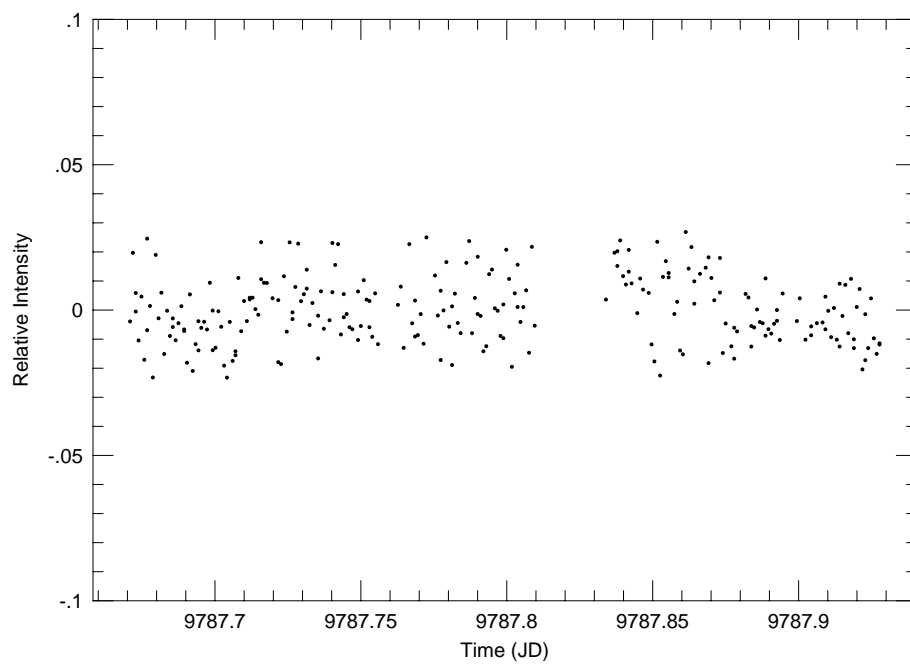


Fig. 2.5.— The light curve for G61-17 on the night of March 9, 1995.

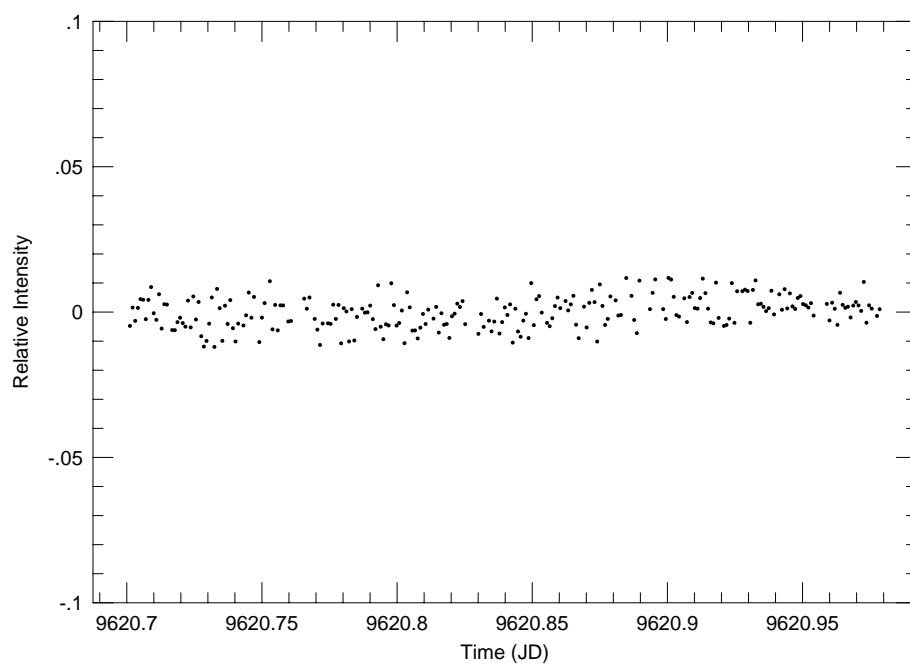


Fig. 2.6.— The light curve for G1-45 on the night of September 24, 1994.

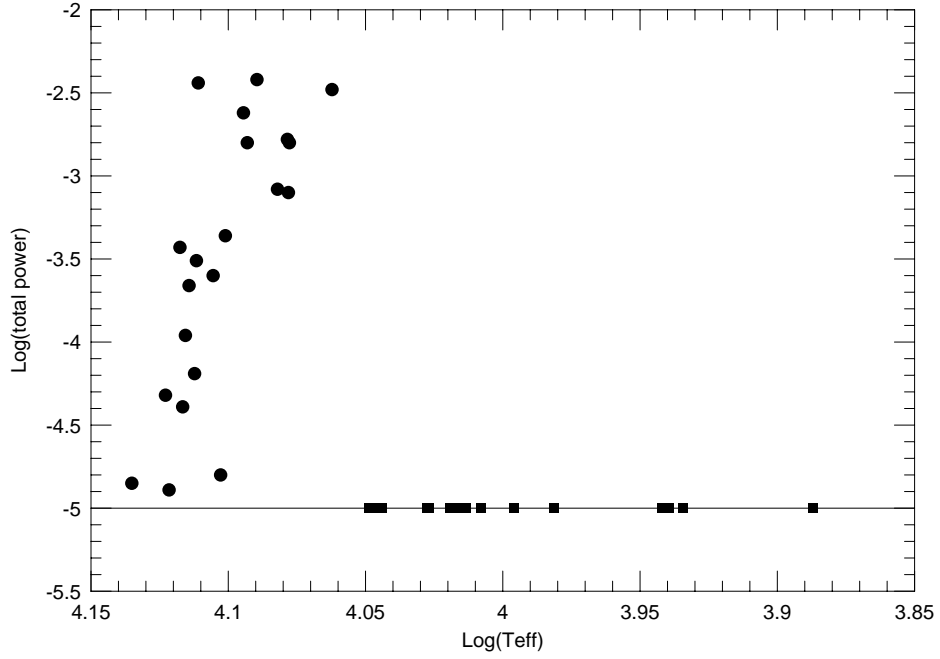


Fig. 2.7.— On this figure we repeat part b) of figure 1 but also including the non-variables below the red edge of the instability strip. It is clearly visible that the amplitudes abruptly fall down to an undetectable level (4mmag for plotting purposes). This indicates that the mechanism shutting pulsations off is more of an on/off nature than a smooth damping process. The filled circles represent the known ZZ Ceti variables. The filled squares the non-variable cool DAs we have observed.

Chapter 3

BPM37093: a different ZZ Ceti

1. Introduction

Since 1961 (Abrikosov, 1961, Salpeter, 1961) most astronomers have agreed that cool white dwarfs must crystallize. This process would start when the electrostatic interaction between the ions becomes much larger than the thermal energy. This conclusion is based on such well known physics that it has become widely accepted without ever having been tested.

In measuring the luminosity function of white dwarfs there is hope of seeing a signature of crystallization. Crystallization is a phase transition which has a latent heat associated, therefore the cooling of a crystallizing white dwarf should be slowed down during crystallization. This should in turn imply a higher space density of white dwarfs at the corresponding luminosity (Wood, 1990). However, our current luminosity function is not good enough to see such a bump, which is expected to be small. More accurate luminosity functions should show us the bump, if it exists. Surveys like the Texas white dwarf survey (Claver, 1994) will increase the number of known white dwarfs by a factor of 10 and it is expected that when it is completed a definitive answer about the existence of a bump will be reached.

In 1987, Winget et al. used for the first time, the white dwarf luminosity function to measure the age of the Galactic disk at the solar neighborhood. As pointed out by Mestel (1952), thanks to the lack of energy generation in white dwarfs, there is a simple mapping between luminosities and ages. The tie between the two quantities comes from the cooling rates. These rates are, however, essentially theoretical values. One excellent form of verifying our theoretical rates of cooling is by comparing them against rates of period change for pulsating white dwarfs (Winget et al., 1983). As these stars cool their pulsation periods become longer, and the observational task is to measure the speed of this change. This is, of course, not a direct measure of cooling but is an independent way of computing it based on an observed quantity. The tie between rate of period change and cooling rates also depends on the ℓ index of the pulsation mode. ℓ determination can be achieved through multicolor photometry as described by Robinson et al (1995). The ZZ Ceti star G117-B15A provides us with observational constraints on these cooling rates (Kepler et al., 1995), though not yet a measurement. A value of $\dot{P} = (1.2 \pm 2.9) \times 10^{-15}$ s/s was found by Kepler et al. This number is consistent with the theoretical models of Bradley et al., 1992. This proves that G117-B15A is not currently in the phase of Debye cooling, where, owing to the rapid cooling, pulsation periods should change quickly. This is a reassuring result but it is no surprise. We do not expect a star like G117-B15A ($T_{eff} = 11,620$ K, $M=0.59 M_{\odot}$, Bergeron et al., 1995) to be even starting to crystallize. The two instability strips, DBV and DAV, will someday provide us with the cooling rates. However, both probe the same phase of cooling, namely the Mestel cooling phase.

BPM37093 is a ZZ Ceti star (Kanaan et al. 1991) of very high mass ($1.09M_{\odot}$ Bergeron et al., 1995, $1.01M_{\odot}$ Giovannini, 1996). More massive white dwarfs are subject to much higher pressures in their core and it is expected that for $1.0M_{\odot}$ white dwarfs crystallization starts at temperatures well within the ZZ Ceti instability strip (Wood, 1990).

In this paper we will discuss the observed properties of BPM 37093 and discuss why we consider it a special object. We then will review the evidence for its being crystallized and will finally elaborate on what we can learn from this object, and any other high mass ZZ Ceti star to be identified in the future.

2. BPM37093 and the others

Before we get into a more detailed description of pulsations in BPM37093 we want to put it in the context of other ZZ Ceti stars. To do that all we need to say at this point is that its light curve is dominated by a mode of period close to 600 seconds and of very low amplitude, of order of 5 mmag.

Among the DAVs, a clear correlation between temperature, amplitude, and period is observed: the cooler the star, the longer its pulsation period and the larger its pulsational amplitudes. Figure 3.1 (based on data from the literature and the Whole Earth Telescope, presented by Clemens, 1994) shows this in three steps: part a) shows the temperature *vs.* period effect; part b) total power *vs.* temperature; part c) total power *vs.* period. This effect is understood as a consequence of the movement of the partial ionization zone of hydrogen into deeper layers of the star caused by evolutionary cooling (Winget, 1981, Winget et al., 1982, Clemens, 1994). As the partial ionization

layer moves in deeper, the thermal timescale becomes longer and the amount of energy available for driving increases correspondingly. BPM37093 is the only star to deviate significantly from the general trends shown on these plots.

According to Bradley and Winget, 1994 there should be an instability strip for each mass of ZZ Ceti. The more massive ones would start pulsating at higher temperatures and the less massive ones at lower temperatures. This would probably lead to a similar effect on the red edge, namely the more massive ones would stop pulsating earlier than the less massive. However, from their models, they are unable to make such a prediction. Giovannini (1996) has shown that the effect predicted by Bradley and Winget (1994) for the blue edge as well as for the red edge can be seen in his extensive survey for photometric variability and temperatures of white dwarfs in and out of the ZZ Ceti instability strip. BPM 37093 defines the red edge of his $1.0M_{\odot}$ mass bin.

While this star's temperature and mass can always be questioned, its pulsational period and amplitudes are measured quantities, rather than derived — as are temperature and mass. One could argue that its not fitting on parts a and b of figure 3.1 is caused by uncertainties in its temperature and/or mass determination. Part c, however, depends only on period and amplitude, and BPM37093 is a clear outlier on that plot as well.

Independent of its temperature determination, BPM 37093 does behave very differently in the amplitude *vs.* period plot. Having a long period and a low amplitude, as well as being close to the observed red edge of the observed instability strip, has made us think of the possibility that it is at the very red edge of the instability strip, and its pulsations are being shut off. However, it is

known that other red edge ZZ Ceti stars pass through phases of low amplitude in their pulsations and then come back to high amplitude (Kleinman, 1995a) — which is their normal state. As the only data on BPM 37093 available were the data from the discovery paper (Kanaan et al. 1991) we decided to re-observe this object. Our first priority is to verify if it is *always* a low amplitude pulsator and not just at a temporary low amplitude phase. We did have an indication that this is not the case. It had been observed before (McGraw, 1976) and no pulsations had been detected. The discovery paper shows the object had the same pulsation mode (610s) at the same amplitude in observations taken 2.5 months apart in 1991. In 1992 Giovannini (private communication) observed this object for 2.5 hours and also found the same mode at the same amplitude. We also want to know if this star is really stopping its pulsations. If so, we should see changes in its behavior. As the most sensitive method of detecting changes in the internal structure of a star is by measuring the rate of change of its pulsation periods, we plan to measure its period accurately every year to build a good ($O - C$) diagram for its pulsations.

3. Observations

We observed BPM 37093 for four hours in 1995, cloudy skies prevailed during the rest of our five night observing run. We reobserved BPM 37093 in April 1996 for ten nights using the 0.9 m telescope at CTIO. This time we used one of CTIO's Cassegrain Focus CCD (CFCCD) cameras with a B filter. A filter is used to minimize effects of differential extinction as well as minimizing the effects of seeing disc variations for stars of different colors. The B filter

was used mainly because of consistency: we have observed this star before with blue sensitive photomultipliers without filters, whose spectral response is roughly equivalent to a B filter, and have observed all other pulsating white dwarfs with the same kind of equipment. Another reason for choosing the B filter is that the amplitude of pulsations increases at shorter wavelengths (Robinson et al., 1982). We used a Tektronix 1024² chip and binned the pixels 2x2 resulting in pixels 0.8 arcsec in size. Integration time was 20 seconds and cycle time was 25 seconds resulting in a duty cycle of 80%. Such a high efficiency is only possible thanks to the use of four amplifiers which share the job of reading the whole chip simultaneously.

From the very little data we had collected before we had the impression that pulsations on this object were stable. We had observed it twice in 1991; once in 1992; and once in 1995. On every occasion we could gather only a few hours of data on different nights, but those data showed two low amplitude modes having periods of roughly 614 and 560 seconds (see figure 3.2). We were in for a surprise.

3.1. Analysis of the 1996 data

On figure 3.3 we show our daily Fourier transforms. It is immediately apparent that something is happening to the pulsations. During the course of these ten nights we can say three pulsation modes can be identified: at 560 seconds (1.766 mHz), at 583 seconds (1.716 mHz) and at 614 seconds (1.634 mHz). The first and the last modes had been seen before and the 583 seconds had not. Even at the low resolution of our transforms we should have seen it. Significant changes in amplitude and phase are seen in all of the identified

modes. Even more impressive is the total disappearance of pulsations after May 1st. In our last night on May 2nd we reobserved BPM 37093 and again found absolutely no variations down to a limit of 1 mmag. Had we observed it for the first time on one of those two nights and we would have classified it as a non-pulsating star. Note that McGraw in 1979 had classified this object as non-pulsating, however, his observations were not sensitive enough to have detected the 4–5 mmag modulations we normally see in this star.

In figure 3.3, four modes are easily identifiable for the 1996 data set. Looking at the daily Fourier transforms we see that the 1.766 mHz mode is present from April 24 to April 29. The 1.716 mHz mode is present from April 25 till April 30. On April 30 a mode compatible with being the same 1.634 mHz mode seen in previous years is present and disappears the next day. On the first of May there is power in the same frequency region but the center of the peak is not at any frequency we have seen before.

The next step in our analysis is a close look at the behavior of the phases and amplitudes of the two main modes. On figure 3.4 we show the phase as a function of time for the 1.766 mHz mode. The phase is clearly shifting during the first four days and seems to reach a stable value on the fifth day and then turns back down. The amplitudes also change during those four days but the change is not as clear (see figure 3.5). We also present the phases and amplitudes for the 1.716mHz, in figures 3.6 and 3.7. Neither of these plots can be explained in terms of beating between close modes. Let alone explaining the disappearing of a given mode for several days. If beating were the case, we should, first of all, see these modes on the Fourier transform as we have a long enough data set; secondly the amplitude and phase changes

should be correlated.

4. Why?

We have shown how BPM 37093 is an outlier in the period–amplitude–temperature relation. We have also shown how its pulsations are unusually unstable in a short timescale. We now want to explore why this might be so.

4.1. Crystallization

According to Bergeron (1995), BPM 37093 mass is $1.1M_{\odot}$ similar results are obtained by Giovannini (1996). According to the evolutionary models of Wood (1990) this implies a crystallized core for any assumed internal composition heavier than helium. The percentage of the core crystallized depends on what we assume for the internal stellar composition. On figure 3.8 (based on models from Wood 1990) we show a diagram of how much crystallization we expect for different (possible) combinations of the physical parameters of BPM 37093.

From figure 3.8 we see that BPM 37093 core must be at least 10% crystallized if its core composition is pure carbon and up to 90% if its core is pure oxygen. For even heavier compositions, the core should be totally crystallized.

At $1.1 M_{\odot}$ BPM 37093 is at the limit mass for having an O/Ne core (Iben, 1991). If the core is really composed of a mix of O/Ne then BPM 37093 should be more than 98% crystallized. If this star is completely crystallized then its pulsation spectrum must be quite different than other non-crystallized ZZ Ceti stars, as a fraction of the outer stellar layers which take part in the

pulsation motions will be crystallized. No models for that kind of star exist yet and the only handle on the problem in a near future is to observe BPM 37093 and find as many pulsation modes as possible to compare its properties to those of other known pulsators.

Another revealing way of studying this object would be the measurement of the rates of period change of its pulsation modes. It is expected that cooling rates be greatly accelerated when the star enters the Debye cooling phase. We should in principle be able to tell between the phase of Debye cooling and the two other cooling regimes which are likely at this stage. Normal cooling is the phase where the star spends most of its life and is a slow cooling process where the star radiates its internal heat away into space. After normal cooling the star will start crystallizing and as latent heat of crystallization is released, the temperature at the crystallization front stays almost constant; above the crystallization front, the star continues cooling normally, and the net effect is a very small decrease in the cooling rate.

Our recent results show, however, that getting that kind of information is going to be harder than we previously expected. To measure \dot{P} it is imperative to have a stable mode. For G29-38 we have seen that some of its modes come and go while others are stable (Kleinman, 1995a). The unstable modes are the highest amplitude modes, around 50 mmag, while stable modes have amplitudes of a few millimagnitudes. If BPM 37093 is similar we need to acquire data that allow us to see very low amplitude modes. We have observed this star for ten nights using a 0.9 m telescope and reached a sensitivity of 0.5 mmag, that is we could have detected any pulsation of amplitude larger than 0.5 mmag. In a period of 2 hours the sensitivity on the 0.9 m telescope

is 2.5 mmag. On the 1.5 m telescope in CTIO we have reached a limit of 0.8 mmag in 2 hours. The use of a larger telescope will definitely be useful in improving the current limit.

4.2. Red Edge

Other red edge ZZ Ceti share with BPM 37093 the instability in their pulsation modes. Modes come and go — and come back. Phase shifts are seen without change in amplitude. From another point of view they are completely different from BPM 37093, they have many pulsation modes, and their amplitudes are large. Also all the changes in the red edge pulsators happen in a time-scale of months, not days as we have seen with BPM 37093.

4.3. High Mass

Other higher than average mass ZZ Ceti are known. They do not have anything in common with BPM 37093. Their pulsational modes are just like other ZZ Ceti, and the pulsation models for more massive ZZ Ceti do not show any particularity when compared with less massive stars. It is true though that the next massive ZZ Ceti (G207-9, Bergeron et al., 1995) is only $0.83 M_{\odot}$ and it is conceivable that strange effects only happen at much higher masses. Of course, the number one effect that only happens at very high masses is crystallization.

5. Conclusion

We have now proved that BPM 37093 is a black-sheep among the herd of ZZ Ceti stars. Not only does it not fit in the period–luminosity–amplitude

relation, it also has an unstable amplitude spectrum, characteristic of the red edge pulsators with whom it only shares a long period. Even its instability is not the same kind as we see with the red edge pulsators because the latter objects are unstable in a timescale of months, not days.

We are faced with a unique ZZ Ceti star in many respects. As the only ultra massive ZZ Ceti, it is only reasonable to think that to be the cause for all the difference. We expect the key to be in crystallization as a massive ZZ Ceti like BPM 37093 should be either crystallizing or completely crystallized.

One possibility, strange as it may sound, is that pulsations in BPM 37093 ceased. We do not expect that to happen in a timescale of two days as we have seen, so we have “faith” pulsations will come back. We plan to reobserve it as soon as possible to check whether or not pulsations have returned to their normal state.

Very high signal-to-noise data gathered by large telescopes will allow us to detect lower amplitude modes. Yet another possibility is the use of the Hubble Space Telescope, we can then observe the pulsations in the ultra violet where the amplitudes are much larger. If we find several pulsation modes we will then be able to compare BPM 37093 properties to other normal ZZ Ceti stars. We hope then to find signatures of crystallization in its pulsations. If we find stable modes we will then be able to measure a rate of period change for BPM 37093 and finally have a grip on the rates of cooling of crystallizing/ed white dwarfs.

In the future surveys for ZZ Ceti stars should turn other above solar mass objects. These will be essential to test whether the behavior of

BPM 37093 is common to massive ZZ Ceti.

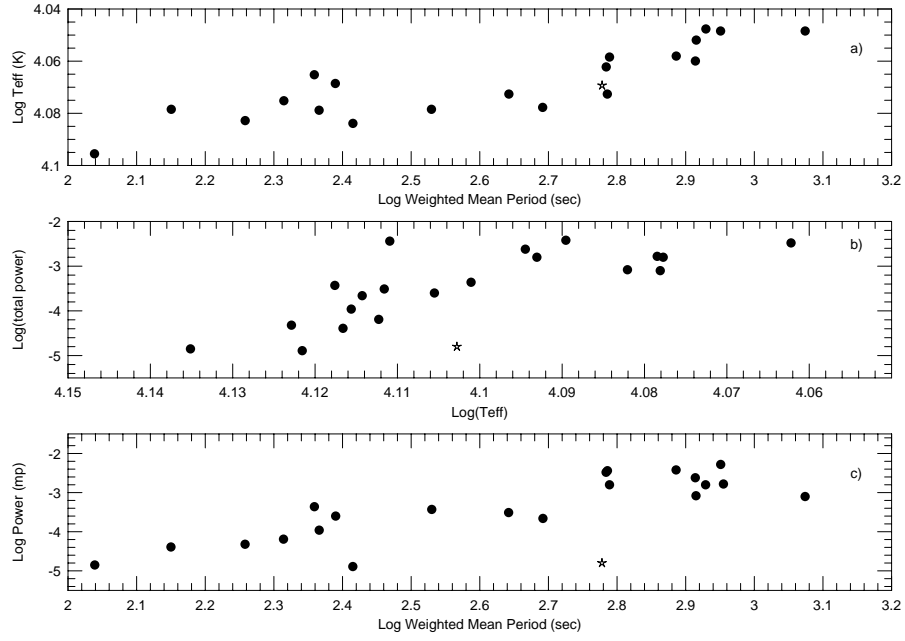


Fig. 3.1.— This figure shows the period-amplitude-temperature relationship in three steps. Part a) displays temperature against periods. b) total power against temperature c) total power against period. BPM 37093 is shown with the star symbol.

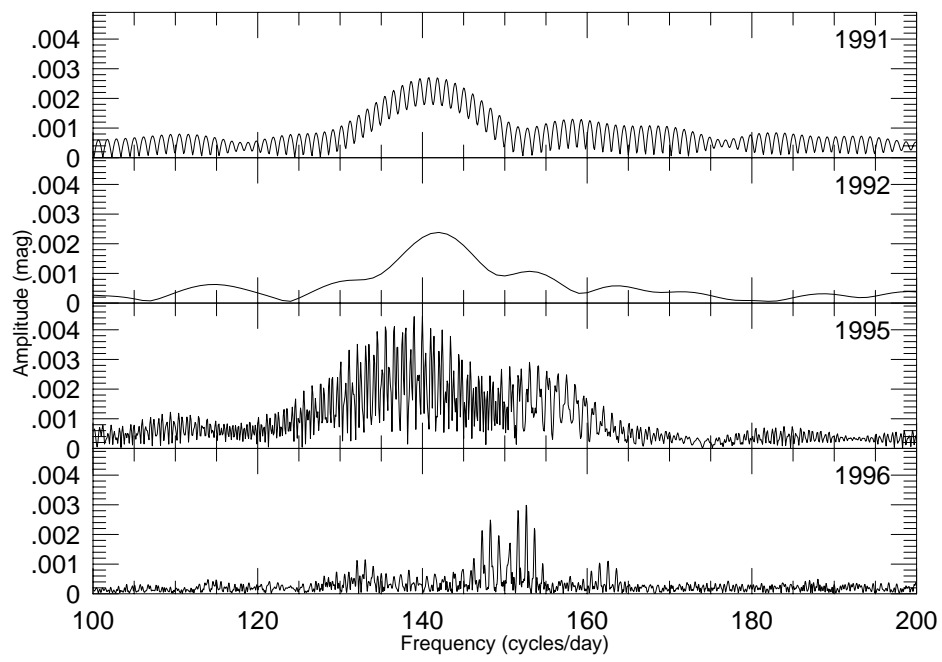


Fig. 3.2.— We show here the Fourier transforms of our data for each year.

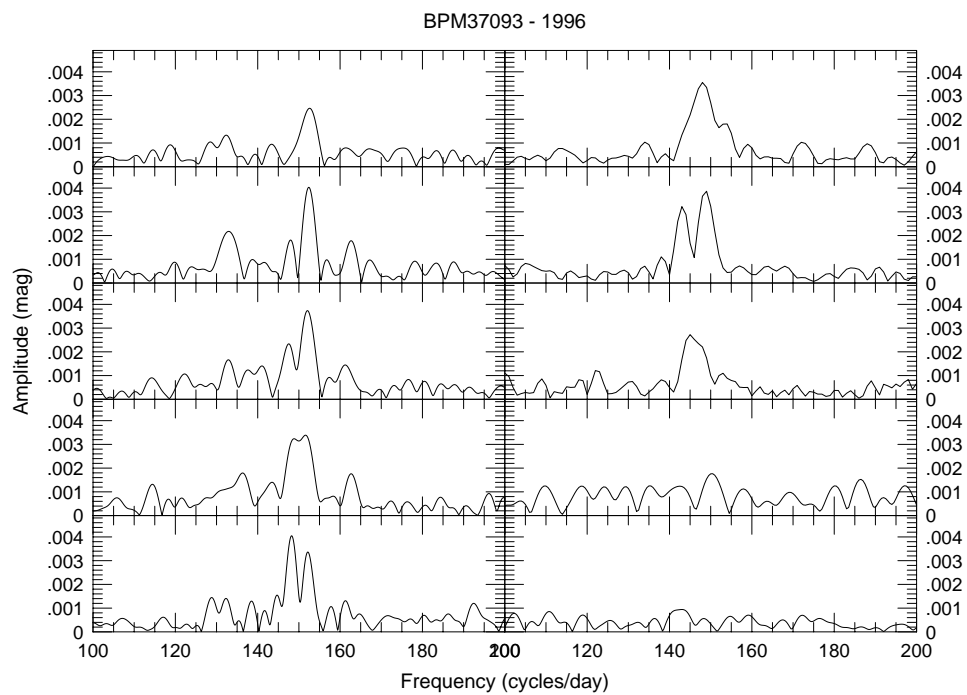


Fig. 3.3.— We show here the daily Fourier transforms during our 1996 run on BPM 37093.

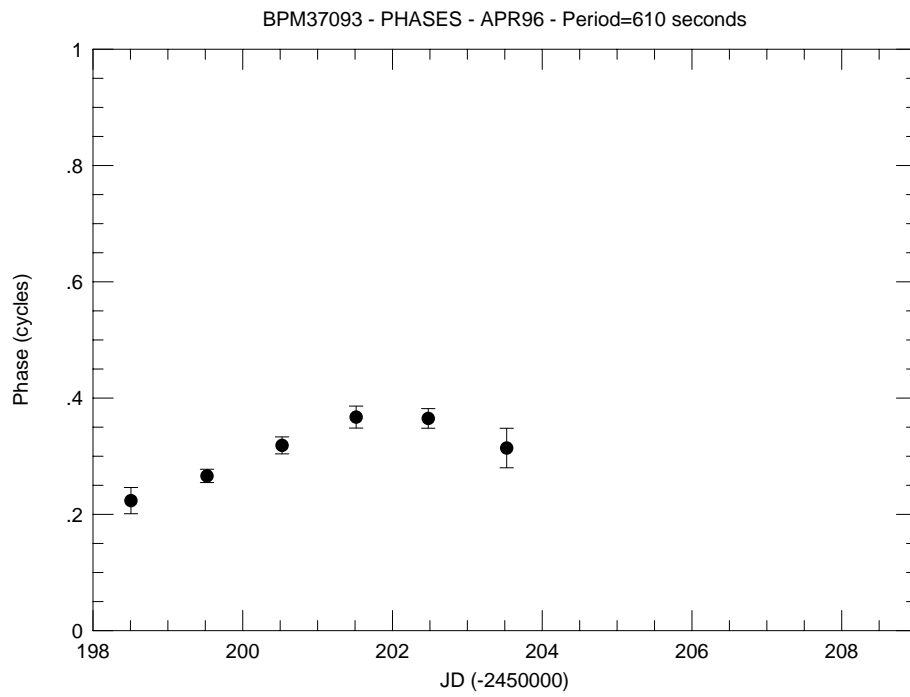


Fig. 3.4.— Phase versus time for the 1.766 mHz mode. Only the first six nights are on this plot because this mode disappears in the last four nights.

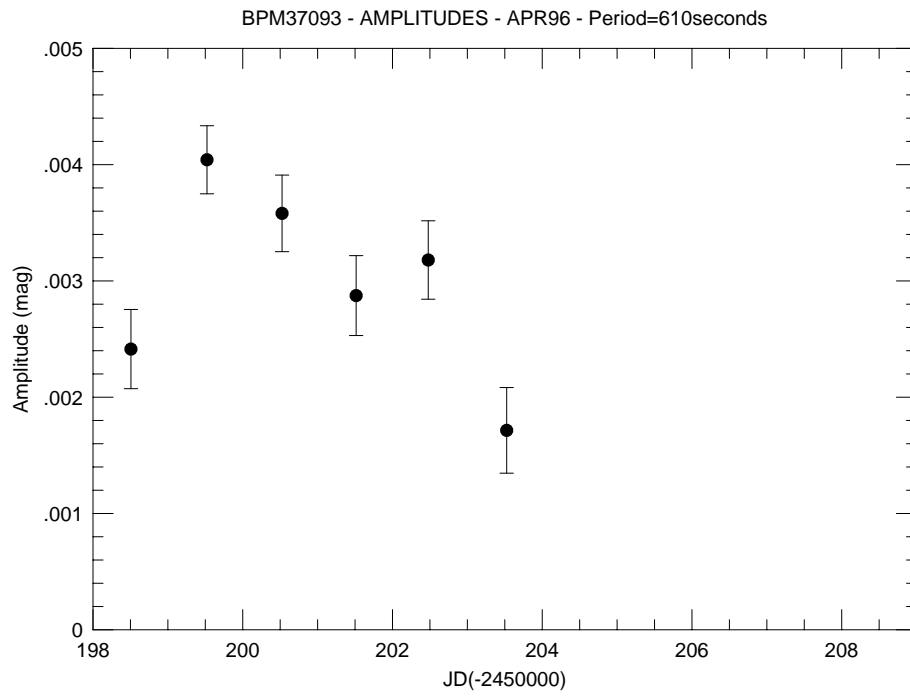


Fig. 3.5.— Amplitude versus time for the 1.766 mHz mode.

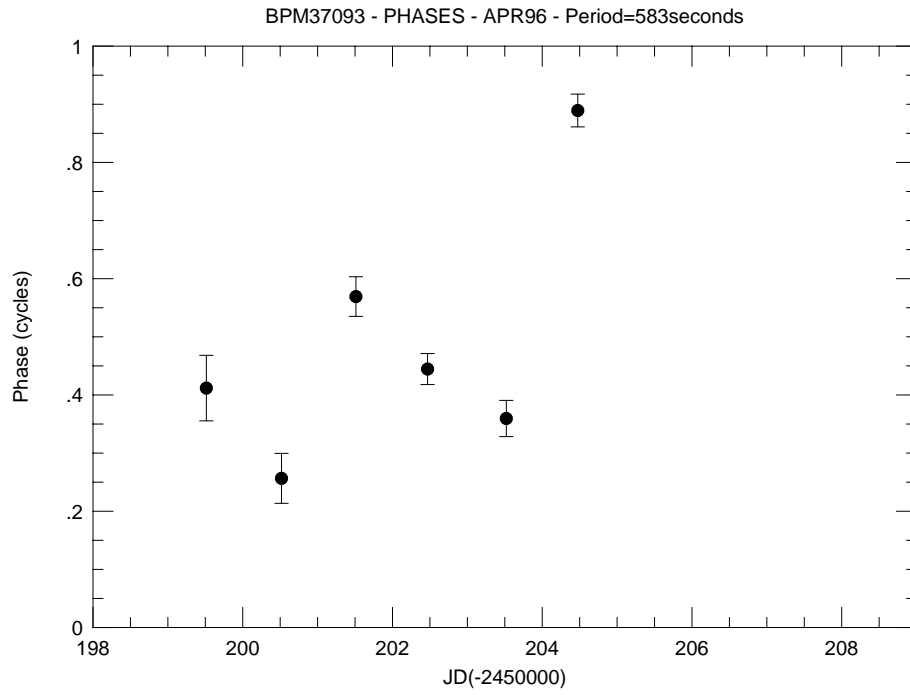


Fig. 3.6.— Phase versus time for the 1.716 mHz mode. We have plotted data from the second night till the seventh. For other nights this mode was not present.

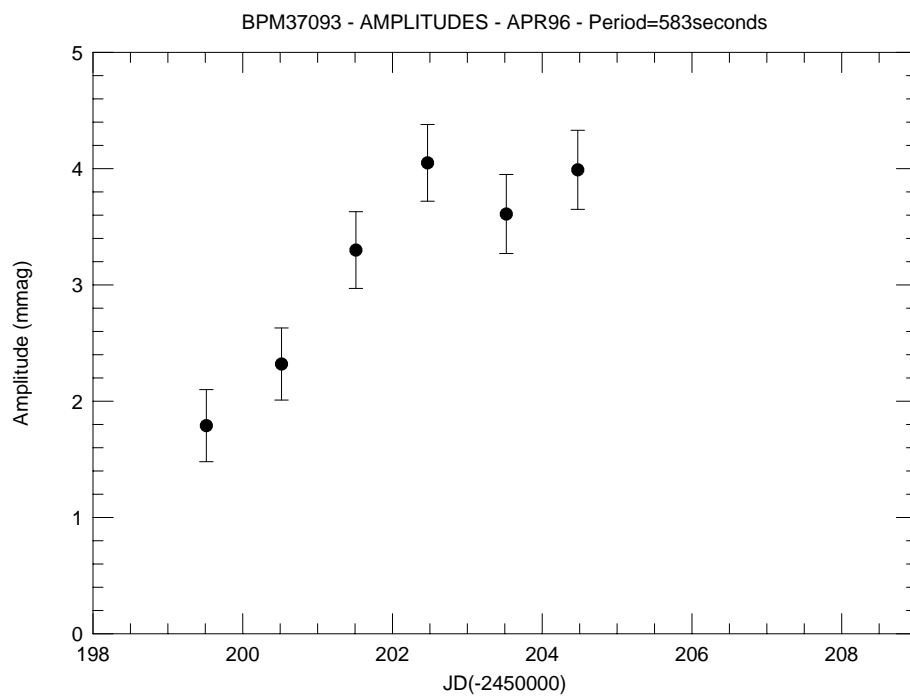


Fig. 3.7.— Amplitude versus time for the 1.716 mHz mode.

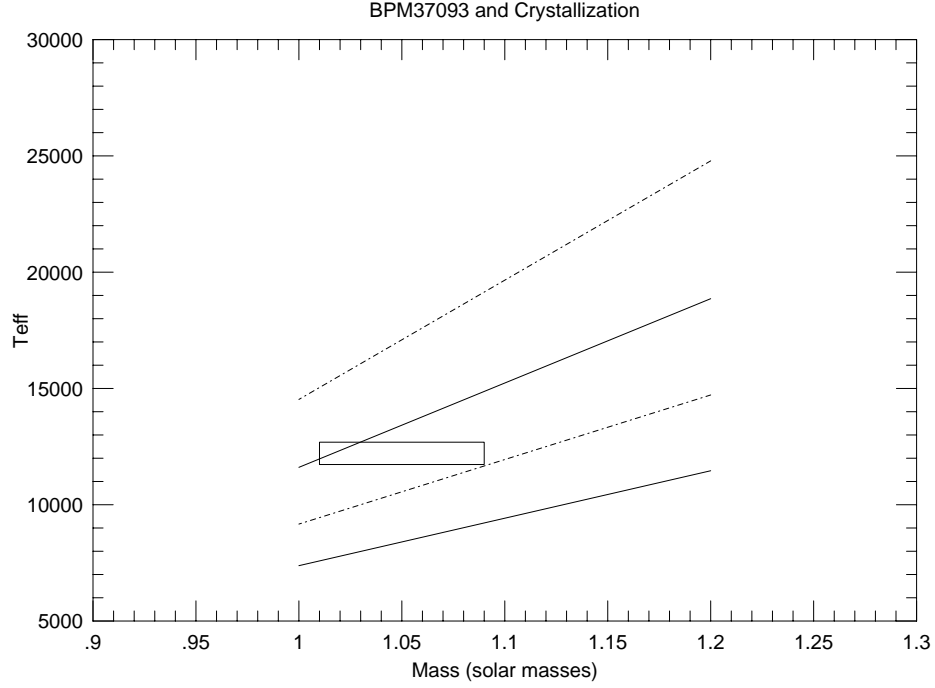


Fig. 3.8.— The rectangle in the center represents the range of masses and temperatures found for BPM 37093. The lower right corner is the determination of Bergeron et al. (1995), the top left corner is the determination of Giovannini (1996). The formal temperature uncertainties from each author are much less than their discrepancies. The lines represent the limits where crystallization reaches 10% (top line) and 90% (bottom line). The continuous line is for an oxygen core. The long-short dash is for a pure carbon core.

Chapter 4

Magnetic Fields are not Suppressing Pulsations in ZZ Ceti Stars

1. Introduction

The ZZ Ceti stars are pure hydrogen atmosphere white dwarfs presenting non-radial g mode pulsations on time scales ranging from 100 seconds to 1000 seconds. They are found in a narrow strip on the Hertzsprung Russell diagram centered at 11,500 K and having a total width of 1,000 K (Bergeron et al., 1995).

Compared to other instability strips the ZZ Ceti is the most pristine one. It is so pure that most astronomers have for many years, and many are still not completely convinced otherwise, thought of temperature as a unique predictor of ZZ Ceti variability (Greenstein, 1982). The situation with other pulsating variables is quite different. For the δ Scuti variables, many non-variables are found in the strip (Breger, 1979). The same is true for the rapidly oscillating Ap stars (Martinez, 1993), and for the Cepheids (Bidelman, 1985).

The question of whether all stars in the ZZ Ceti instability strip pulsate was highly stressed in the early days of white dwarf seismology. People wanted

to know if what they learned about the stellar interiors of these pulsators applied to all white dwarfs, and consequently to the past of all low mass (below $8M_{\odot}$, Reimers and Koester, 1982) main sequence stars. If all white dwarfs in a temperature range do pulsate, it is then natural to suppose that pulsation is a phenomenon dependent only on the evolutionary stage of the star. From the work of several astronomers (*e. g.* Fontaine et al., 1982, Greenstein, 1982, McGraw, 1979) it became clear that pulsation was a commonplace among stars in the instability strip. This reassured most astronomers of the normalcy of these objects, convincing the community of the usefulness of studying them.

We are now convinced that the ZZ Ceti phenomenon is evolutionary. However, Kepler and Nelan (1993), using ultraviolet spectra from the International Ultraviolet Explorer (IUE), determined the temperatures of many objects in the instability strip vicinity and obtained high speed photometry on them. They found six non-pulsating stars in the instability strip. Using optical spectra for temperature determination and high speed photometry for variability studies Dolez et al. (1991) found 7 non-variables in the strip, 3 of which are in the middle of the strip. There must be a physical distinction between the pulsating and the non-pulsating inhabitants of the ZZ Ceti instability strip. We hope to identify this physics and afterwards infer the difference in the evolutionary histories of these two groups.

It is widely accepted that magnetic fields are the cause for sunspots, inhibiting convection (Moss, 1986) and therefore making those regions affected cooler and darker. This argument has been extended to stellar convection as well (Gough and Tayler, 1966). It is plausible that whenever the energy density in the magnetic field is comparable to the energy density of convection,

the magnetic field will start having disturbing effects on the convection. The same argument can be applied to the pulsation motions as well.

This energy condition can be written as:

$$\frac{B^2}{8\pi} > \frac{1}{2}\rho v^2.$$

The first point to note here is where we must compute these quantities. The most important region is at the base of the partial ionization zone, as that is where pulsations are actually driven (Winget, 1981). If pulsations are suppressed here, there will be no pulsations at all.

A dipole field, as observed in virtually all of the magnetic white dwarfs, has a change in intensity of only a factor of two from the magnetic poles to the equator. The radial dependence is extremely weak and can be neglected. As a consequence, our estimates will be for an average surface field, an observable quantity, but similar to the value at the base of the partial ionization zone. ρ is the gas density in the same region, while v is the pulsational velocity. Using pulsation models similar to those described in Bradley (1993), at a temperature of 11,000 K, and using the ML2 description of convection (following the notation of Fontaine et al, 1981), we find $\rho \simeq 10^{-3}$ g and $v \simeq 10^5$ cm/s. Such values in the above energy equation imply that a magnetic field of at least $B \simeq 10^4$ G is needed to shut off pulsations.

As such fields are not readily detectable in low resolution spectra, we thought they could be present, suppressing pulsations but going undetected. We decided then to survey some of the non-variable DA stars in the instability strip for fields of this order. As at the time of our observations 25 kG was

the best possible measurement of a magnetic field, as demonstrated below, we decided to go ahead and probe those non-variable stars for the presence of such fields. It is important to stress that 10^4 G is the value for a magnetic energy *equal* to the pulsational energy, and a stronger field will be necessary to completely shut off the pulsations.

In order to do a meaningful test, it is necessary to observe the non-pulsating as well as several pulsating stars. If we find magnetic fields in the non-pulsating objects, we must demonstrate that the pulsators do not have substantial magnetic fields before concluding that magnetic fields shut down pulsations. Another issue, already assessed in chapter 2, is the lack of pulsations in stars below the temperature of 11,000 K. Theoretical models predict pulsations in models as cool as 8,000 K. One hypothesis raised is that magnetic fields can be generated or amplified as these stars cool and develop deep convection zones, and that these fields could be the reason for the red edge at temperatures higher than expected theoretically. Recently Markiel et al. (1996) published detailed models of magnetic fields generated by the convection zone in cool DA stars models with similar amounts of differential rotation as the inferred from the asteroseismological observations of GD 358 (see next paragraph). The field strengths inferred by them are much lower than what we expected to shut off pulsations.

An important issue was raised by Jones et al. (1989), who suggested that weak magnetic fields break the symmetric frequency splitting in a multiplet of modes. For example, in 1994 (Winget et al., 1994) Winget et al. (1994) found this behavior in the multiplets of the DBV star GD 358 and interpreted it as being caused by a $\simeq 1$ kG magnetic field. They suggested

that the observed variation in frequency and amplitude on one of the large amplitude modes of GD 358 is caused by a varying magnetic field. It was also observed on GD 358 that the average splitting of modes of different k (the radial overtone index) grows with k . As modes of higher k are believed to be most influenced by layers close to the surface this was interpreted as due to differential rotation, the inner layers rotating with a period of ≈ 1.6 days and the outer layers with a period of ≈ 0.8 days. So GD 358 has the necessary ingredients for a dynamo: a convection zone (all the pulsating white dwarfs have one), and differential rotation. Markiel et al. (1994) worked out the details for an $\alpha\omega$ dynamo generated at the convective zone of this star using the same amount of differential rotation as suggested by Winget et al.

According to Jones et al., if the rotation rates are very slow and the magnetic fields are strong, one should observe doublets in the power spectra of pulsating white dwarfs. We do see doublets in some of the ZZ Ceti stars. From a frequency splitting $\Delta f = 8.03 \times 10^{-6}$ Hz and $\Delta f = 6.95 \times 10^{-6}$ Hz in the two doublets seen in the ZZ Ceti star R548 (ZZ Ceti itself), Jones et al. suggest this object should have a 10^5 G magnetic field. G185–32 is another ZZ Ceti to show some doublets in its power spectrum, one with a splitting of $\Delta f = 27 \times 10^{-6}$ Hz and another of $\Delta f = 18 \times 10^{-6}$ Hz, which would imply an even stronger fields of around 4×10^5 G. We saw in these stars an opportunity to test Jones et al. predictions. The confirmation of Jones et al. hypothesis (that these stars had magnetic fields of the order of 10^5 G) would then prove the hypothesis of suppression of pulsations by magnetic fields to be incorrect.

We surveyed three different types of stars for magnetic fields: 1) non-pulsators in the instability strip; 2) pulsators in the instability strip —

especially those presenting doublets (rather than triplets); 3) non-pulsators cooler than the red edge (11,000 K) of the instability strip.

2. The Observational Technique

Magnetic fields lift the degeneracy of atomic levels of same n, ℓ and different m . For weak fields this implies that spectral lines be split in triplets. The splittings are proportional to the field strength, where the elements of these triplets are separated by $\Delta\lambda = 4.67 \times 10^{-13} \lambda^2 B z$, where $\Delta\lambda$ is the Zeeman splitting; λ is the wavelength; B is the magnetic field and z is the Landé factor. These three components are polarized. The short wavelength component varies from total left handed circular polarization when \mathbf{B} is pointing straight at us to total linear polarization (in a direction perpendicular to \mathbf{B} when \mathbf{B} is pointing 90° from the line of sight. In intermediate positions we see elliptical polarization. The central component is always linearly polarized in a direction parallel to the field. The long wavelength component behaves in the same way as the short component.

Among the approximately 2,000 spectroscopically identified white dwarfs (McCook and Sion, 1987), forty are known to be magnetic (Schmidt and Smith, 1995). Of these, 37 have fields above 1 MG and most have been identified thanks to the Zeeman splitting of their absorption lines. Due to the broadness of absorption lines on white dwarfs, this is not a very sensitive technique. But for the hydrogen atmosphere white dwarfs it is possible to use the core of the H_α line (and in some cases $H_{\beta\text{et}h\alpha}$ as well). Due to the high densities and relatively low temperatures in white dwarf atmospheres collisions dominate the transitions and LTE is a good approximation. However,

because of the strong opacity in the line center the line cores are formed at the outermost part of the stellar atmosphere where radiative processes dominate over collisions and non-local thermodynamic equilibrium (NLTE) best describes the thermodynamic conditions of the gas. NLTE atmospheric models (Wesemael et al., 1980, Koester and Herrero, 1988) show a strong overpopulation of the $n = 2$ level of the hydrogen atom at the top of the atmosphere. The higher Balmer lines are much less affected because they are formed deeper in the atmosphere where densities are much higher. These line cores are on average 1 Å wide. Compared to the tens or even hundreds of Ångstroms that hydrogen lines have on white dwarfs, the line cores provide higher sensitivity for detection of magnetic fields in white dwarfs. Koester and Herrero (1988) have observed 7 white dwarfs with high resolution spectroscopy and found an upper limit of 25 kG to their magnetic fields.

Lines which are 1 Å wide may be broadened by rotation or by the presence of magnetic fields. If we attribute the broadening only to magnetic fields then we see from the previous equation for $\Delta\lambda$ that this implies in a splitting of 0.5 Å either side for a field of 25 kG. Figures 4.1 to 4.3 show three situations. First a line 1 Å wide where it is being assumed that all broadening is caused by rotation. In figure 4.2 a magnetic field of 25 kG is applied and this 1 Å wide line is split in three, producing a broader line. This new broader line has a full width at half maximum of 1.5 Å, which would imply in an upper limit of 37.5 kG — instead of the real 25 kG, if we were to assume no rotational broadening. A field of 50 kG would produce an even stronger effect, as shown in figure 4.3, and high signal to noise spectrum would even allow one to see the Zeeman triplet at the bottom of the line, instead of seeing only

the broadening. We are however dealing with low signal to noise spectra and the quantity we can reliably measure is the full width at half maximum which would in this case be 2.8 \AA and imply in an upper limit of 71 kG for the magnetic field, again if we assumed no rotational broadening.

The spectrum of the pulsating star G29-38 is shown in figure 4.4. Superposed to the stellar spectrum we plot a gaussian fit to the line to illustrate how good an approximation a gaussian is to the line core. The measured full width at half maximum is approximately 1 \AA , implying an upper limit of 25 kG to the magnetic field. It is true that the measured line is a convolution of the real line and the instrumental profile and that affects our measurement of the real width of the line. However, the effect of that is negligible in these spectra because the typical width of the lines being measured (1 \AA) is much larger than the instrumental profile width (0.2 \AA maximum). Another effect that needs consideration is the signal to noise ratio in our spectra. The spectrum of G29-38 shown has a high signal to noise ratio (50); what happens if a spectrum at a lower signal to noise ratio is taken? To answer that question we decided to run Monte Carlo simulations to study the effect of noise on the determination of the full width at half maximum of the lines. The typical line width at these temperatures is 1 \AA and the line bottom is approximately 20% lower than the surrounding broad wings of H_α — from stars observed at high signal to noise ratio. Using these values we computed 1,000 gaussians adding noise to them. We ran Monte Carlo simulations for a signal to noise ratio of 20, the same as our worst spectrum. For data with such low signal to noise we find that all of the 1,000 simulated spectra have measured widths from 0.9 to 1.1 \AA . We can therefore assign a very conservative error to our line width

measurement as being 0.1 \AA . This translates into a magnetic field uncertainty of 2.5 kG .

Using circular polarization measurements Schmidt and Smith (1995) have recently surveyed 169 hydrogen atmosphere white dwarfs (DAs) — every DA on the white dwarf catalog brighter than B magnitude 15.0 and north of -30° . Using 3σ as a safe estimate of their measurements we can say they have set an upper limit of $\approx 25 \text{ kG}$ to the presence of longitudinal magnetic fields among the objects which are the subject of this paper.

There was still the possibility that these objects are unfavorably oriented for detecting a magnetic field through circular polarization measurements. Most magnetic white dwarfs seem to be slow rotators. We know of four which have their rotation and magnetic axis unaligned. The fastest rotator has a period of ten minutes while the slowest has a period of a few days. It is impossible to know whether the other stars have very slow rotational periods or if their magnetic and rotation axes are aligned — something which is not found elsewhere in nature — but the fact is that their circular polarization has not changed in years. Our point here is that due to slow rotational periods it is possible that a magnetic star be missed in a circular polarization survey if it is observed at the wrong moment in time. The mean surface magnetic field B_s is defined by:

$$B_s = \frac{\int B I dA}{\int I dA}$$

and is what dictates the amount of splitting observed in the Zeeman triplet. I is the light intensity, B the magnetic field and dA the area element. For dipole

fields B can vary by a factor of at most 2 from equator to pole, therefore the biggest possible difference in B_s for the same star seen pole on and equator on is a factor of 2 as well. Now the longitudinal field is defined by:

$$B_e = \frac{\int B \cos \gamma I dA}{\int I dA}$$

where γ is the angle between the magnetic field line and the line of sight. Because of this $\cos \gamma$ factor B_e is much more strongly dependent on the geometry than is B_s . For a centered dipole field and a limb darkening coefficient $u = 1$ ($I_\theta/I_0 = 1 - u + u \cos \theta$) Schmidt and Smith (1995) computed the relation between B_e and B_d (B_d is the polar strength of a dipole field) and found $B_e = 0.4B_d \cos i$, where i is the angle between the magnetic field axis and the line of sight. For a single observation there is a probability P_m that a field of polar strength B_d be missed:

$$P_m = \int_{\cos^{-1}(2.5B_{lim}/B_d)}^{\pi/2} \sin i di = 2.5B_{lim}/B_d,$$

where B_{lim} represents the sensitivity of the measurement.

Another reason for spectroscopic measurements is the fact that tangled magnetic fields — as expected to be if generated by the convective motions — have no net longitudinal component as different parts of the star will have different orientations with respect to the observer and cancel each other out. Yet such a field would still broaden the line cores and be detected in a spectroscopy survey.

3. Observations

Our observations were carried from January 1994 to October 1994 using the cross dispersed coude echelle spectrograph of the 2.7 m reflector at McDonald observatory (Tull et al, 1995). In one instance the 2.1 m telescope was used, the spectrograph used in the run was the Sandiford spectrograph, a cassegrain instrument with a resolution of 60,000 (McCarthy et al, 1993).

For most of our work we used a Tektronics 512x512 $24\mu\text{m}$ CCD binning it in 2x2. This binning factor implies in a dispersion of approximately 0.12 \AA per pixel. This resolution is plenty for the measurements we intended and is still low enough to provide us with enough light to take spectra down to 14th magnitude. In table 4.1 we present all the details of the observing setup.

Our data reduction was carried using the standard path: bias level subtraction, flat field corrections, and aperture extractions. All this was done using the tasks of the Image Reduction and Analysis Facilities (IRAF) developed at the National Optical Astronomical Observatories (NOAO).

4. Results

We now show the spectra of the observed stars dividing them in three groups: the non-variables in the strip, the variables and, the non-variables below (cooler) the instability strip. On table 4.2 we quote our upper limits as well as those of Schmidt and Smith. Column “prob. miss” in that table shows the probability that the circular polarization measurement might miss a 50 kG field (polar strength). Figures 4.5 to 4.14 show the spectra we obtained for all objects we observed. The vertical scale is in arbitrary units while the horizontal scale is in Angstroms and has been transformed to the lab reference

frame.

With the exception of G19–20, which has a 1.4 \AA core, all other observed stars have cores as narrow, or narrower, than 1 \AA implying none has a magnetic field stronger than 25 kG. Because there is a different motivation for each group, it is useful to discuss each of these groups separately.

The absence of observable magnetic fields in the non-pulsating stars proves that magnetic fields are not the cause for the lack of pulsations among these objects.

Because our limiting magnitude was around 14 we were unable to observe any of Dolez et al. non variables. Schmidt and Smith observed the two stars brighter than 15th magnitude finding an upper limit of 20 kG for the presence of any magnetic field in them (see table 4.3).

As discussed in the introduction, the variable stars we were particularly interested in testing the presence of a field were G185-32 and R548 because of the doublet structure in their pulsation spectrum. No magnetic field has been detected in either object. Since the driving of pulsations happens deep below the photosphere, it is possible, though very unlikely, that a magnetic field is confined to deeper portions of the star and cannot be spectroscopically detected. G29-38 is another star of special interest; along the years its pulsation spectrum has been changing (Kleinman, 1995a). Given the results of Winget et al. (1994), we thought it was possible that a cyclic dynamo was in action in G29-38, sometimes allowing the star to pulsate freely, sometimes constraining the motions. However, thanks to the special interest raised by its infrared excess several groups have obtained high resolution spectroscopy

on this object with the intention of detecting radial velocity variations caused by the orbital motion of the putative brown dwarf companion. All these observations show a narrow H_α core implying that no field above 25 kG has been present in G29-38, even when we see its pulsations changing in amplitude. Yet another star was important to observe: G226-29. Angel et al. (1981) had a 2σ detection of a 10^5 G field in this star. If that is true, then the pulsation spectrum should be affected accordingly: either the triplets should not be as symmetric as they are (Kepler et al, 1983) or the star should not pulsate. We then reobserved G226-29 to try to have a better limit on its magnetic field. We do not see any evidence of a field up to our limit of 25 kG. Schmidt and Smith find $B = -0.7 \pm 2.0$ kG for this star.

Among the cooler objects the same result is found. The three cool stars observed display narrow H_α cores. L870-2 is a special case as it is a double white dwarf. The width of the core can only be reliably measured in one of the components and we find it to be 0.7 \AA implying in an upper limit of 18 kG for this star. In figure 4.7 five spectra of L870-2 can be seen. The wavelength shift between the two line cores is obvious during the 2.5 hours of observations. In addition to the spectroscopic data from this work all the cool stars observed photometrically (see chapter 2) and for which Schmidt and Smith attempted spectropolarimetric measurements are presented on table 4.4. This table expands the number of observed cool DAs to 7. No magnetic fields are found in any of these objects. This rules out the creation of magnetic fields by convection as a possible explanation for the location of the red edge of the ZZ Ceti instability strip.

5. Temperatures

We decided to test the validity of claims on the presence of non-variables in the instability strip by cross examining temperature tables produced by different authors. Current state of the art temperature determinations are described in Bergeron et al., 1995. The method for determination of mass and temperature consists in fitting synthetic line profiles to the observed hydrogen lines of these objects. Thanks to the high pressure sensitivity of the high Balmer lines, they are very useful as gravity indicators, while the lower order lines are sensitive to temperature. Using a grid of synthetic models varying in $\log g$ and T_{eff} one finds which model best matches the observed spectrum. Tables 4.5 and 4.6 show the T_{eff} for all ZZ Ceti stars in every temperature determination we are aware of. An entry 00000 means no temperature determination is available for that star in that particular study. A similar comparison has been done before by Wesemael (1991) where he concentrated mostly on the determination of the blue edge. We here are not concerned with the positioning of the instability strip on an absolute temperature scale but rather on the relative position of one star with respect to another. In order to do that we have chosen one star as our fiducial point and computed the temperature differences (ΔT) between it and all other stars. We have many different ways to assess the situation now. The simplest consists in finding $\langle \Delta T \rangle$ and $\sigma_{\Delta T}$ for each star and from there to use the average $\sigma_{\Delta T}$ to find the average uncertainty in each temperature determination. We have done that using three different stars as our fiducial points: G117-B15A, G226-29 and BPM 37093. These three are the stars for which most temperature determinations are available. G117-B15A is present in every sample and would be the ideal star as the fiducial point; however, it

falls exactly in that region where two solutions, one hotter and one cooler, are possible (Daou et al, 1990). This makes the scatter in ΔT much worse than it really is. In tables 4.7, 4.8, 4.9 the average ΔT and $\sigma_{\Delta T}$ for each star is shown for each reference star. It is easily seen that using G117-B15A as a reference gives us the biggest scatter. Because of the lower scatter produced by either G226-29 or BPM 37093 we decided to use them as reference stars. From the values of $\sigma_{\Delta T}$ it can be safely said that the uncertainty in *relative* temperatures is of the order of 300 K. This uncertainty figure agrees with that of Kepler and Nelan (1993) and we therefore can trust their individual probabilities for each of their objects to be outside the strip as well as their composite probability that the strip is completely pure.

6. Conclusion

We have proven that the non pulsating stars in the ZZ Ceti instability strip are not magnetic stars, down to a limit of 25 kG. This limit is roughly what is expected to shut off convection and pulsation on white dwarfs. This puts the magnetic field hypothesis to rest. Another cause must be found for the lack of pulsations in those stars.

Bradley and Winget (1994) found in their pulsation models that the temperature for the blue edge of the instability strip is mass dependent. Low mass objects start pulsating at lower temperatures than higher mass objects. They do not find the same dependence for the red edge, basically because they do not find a red edge. Giovannini (1996) has tested their hypothesis observationally and his results for the blue edge are in agreement with their predictions. In figure 4.16 we show the results of Giovannini. The open

circles represent the variable ZZ Ceti stars for which he determined mass and temperature. The filled circles the non-variables. The line represents the theoretical blue-edge of Bradley and Winget. It is plotted as a vertical line for masses above $0.8 M_{\odot}$ for the simple reason that the theoretical models only go to $0.8 M_{\odot}$. Projecting this plot in one dimension in order to get rid of the mass information one ends up with a large number of non-variables mixed with the variables. Back to the two dimensional plot the separation between variables and non-variables is excellent. The agreement between the theoretical and the observed blue edges is quite good if one is willing to move the theoretical line by 300 K towards higher temperatures (the dotted line). One variable star still stays bluewards of the shifted theoretical blue-edge, it is G226-29. It needs to be ignored as some sort of misfit — either assuming the star itself is peculiar in some way or its temperature and mass determinations are in error. Two non-variables stay inside the shifted blue edge. As discussed in the previous section their temperature and masses may be in error and it can easily be argued that they belong outside the instability strip. While this is so far the best explanation for non-variables within the strip we would like to draw attention to a few points which still need to be addressed.

Between the shifted blue edge and G226-29 there is not a single star observed in the mass interval $0.55 M_{\odot}$ to $0.80 M_{\odot}$. In the same mass range, the next star hotter than G226-29 is more than a thousand degrees away. This is the region where the slope of the blue edge is defined. Therefore while the data strongly suggest the slope to be real the amount of data is really not enough to prove it. Finding new stars between the shifted blue edge and G226-29 as well as between G226-29 and the hotter stars will allow us to definitely know

whether the slope of the blue edge is real. It is interesting to note that in the analysis of Bergeron et al (1995) they also find a slope to the blue edge and, in their analysis, G226-29 has a higher mass, and therefore follows the blue edge line. Their analysis is based only on variable stars. Lacking observations of non-variables one is left to ask what is the situation on the right side below the dividing line. It could either be that stars in that region are actually not variable, it could be that stars there are variable. Stars in this region need to be found and observed photometrically to decide the question.

Another point to be considered is the gap in temperature in Giovannini's sample. The coolest DAV in the sample is 12,000 K. The next cool DA is 11,300 K. Bergeron et al (1995) have shown how different treatments of convection lead to such temperature gaps in the distribution of stars. The ML2 (this notation for different convective "recipes" is from Fontaine et al, 1981) prescription does not create any visible gap in their distribution of stars with temperature, ML1 and ML3 do. They have then used ML2 models for the temperature and mass determinations. In order to have a better agreement between the ultraviolet and optical temperatures, they chose a ML2 model with $\alpha = 0.6$ ($\alpha \equiv l/H_p$, that is the ratio of the mixing length with the pressure scale height). Giovannini uses models developed by Koester. These models use ML1 with $\alpha = 2$ which is very similar to the normal ML2. It may be that the gap in Giovannini's sample is caused by problems in the way convection is treated in the models he used. Elimination of this temperature gap will allow a better assessment of the shape of the red edge.

Markiel et al. (1995) have published models of dynamos for DA stars. They predict very weak fields should be generated by the convective motions

in the ZZ Ceti temperature range, with a maximum of 370 G at 11,000 K. This limit is much lower than our detection limit of 25,000 G and our non-detection of fields is consistent with their prediction. Their models also produce stronger magnetic fields for cooler stars but those fields are still below our detection limits. Future measurements using circular polarization measurements on 4 m class telescopes will allow us to probe for fields of order 1 kG as Schmidt and Smith (1995) have demonstrated to be possible for a few brighter stars using a 2.1 m telescope.

It would be interesting to see what sort of fields their models produce for different combinations of convective efficiency and differential rotation. We could then confront our measurements with their models to put limits on convective efficiency and differential rotation.

In this work we observed three of the cooler DA stars and found no magnetic fields in them. This result eliminates the hypothesis of strong magnetic fields created by convection and differential rotation as a cause for the location of the red edge at a temperature of 11,000 K.

It is unfortunate that no magnetic white dwarf is known in the temperature range where we see the ZZ Ceti stars because only then we will be able to measure what effects magnetic fields may have on pulsations. Hopefully future surveys for magnetic white dwarfs will eventually produce some magnetic white dwarfs in this temperature range.

Table 4.1. Observing Log

WD	alias	m_V	Int. Time	S/N
April 1994 (2.7 m)				
1022+050	PG1022	14.2	2.0h	30
1716+020	G19-20	14.3	2.0h	20
1647+591	G226-29	12.1	2.0h	30
August 1994 (2.1 m)				
2246+223	G67-23	14.4	3.0h	20
0133-116	R548	14.1	3.0h	30
2326+049	G29-38	13.0	2.0h	15
October 1994 (2.7 m)				
1935+276	G185-32	13.0	3.0h	30
0133-116	R548	14.2	2.5h	30
0401+250	G8-8	13.8	2.5h	45
2326+049	G29-38	12.9	3.0h	50
0101+048	G1-45	14.0	3.0h	30
0135-052	L870-2	12.8	3.0h	70

Table 4.2. Results.

WD	alias	spectroscopy (kG)	circ. polar. (kG)	prob. miss
Non-variables:				
0401+250	G8-8	25	1.3 ± 6.6	0.33
1022+050	PG	25	-5.1 ± 6.2	0.31
2246+223	G67-23	25	1.5 ± 13.8	0.69
ZZ Ceti:				
0133-116	R548	25	11.5 ± 10.9	0.58
1647+591	G226-29	25	-0.7 ± 2.0	0.10
1935+276	G185-32	16	-8.5 ± 10.5	0.53
2326+049	G29-38	28	2.8 ± 12.8	0.64
Cooler stars				
0101+048	G1-45	21	-9.7 ± 7.6	0.38
0135-052	L870-2	18	-1.6 ± 6.1	0.31
1716+020	G19-20	35	-2.1 ± 7.4	0.37

Note. — The spectroscopy column shows the upper limit for the presence of a magnetic field. The worst case uncertainty in line width measurements determined from Monte Carlo simulations on data with signal to noise ratios of 20 is 0.1 \AA which translates in 2.5 kG in magnetic field strength. The circular polarization entry comes from Schmidt and Smith (1995). The fifth entry — probability of missing — is computed for a polar field strength of 50 kG and using a 2σ limit for B_{lim} and represents the probability that such a field be not detected due to geometrical cancellation effects.

Table 4.3. Dolez et al. non variables in the strip.

WD	alias	mv	B(kG)
WD 0231-054	GD 31	14.5	8.9 ± 7.1
WD 0302+621	GD426	15.2	1.4 ± 7.1
WD 0339+523	Rubin 70	15.8	NO
WD 0348+339	GD 52	15.3	NO
WD 1636+160	GD 202	15.7	NO
WD 2311+552	GD 556	16.0	NO
WD 2347+128	G 30-20	15.9	NO

Note. — NO means not observed

Table 4.4. Cool DAs

WD	Alias	Temperature	B(kG)
0032-175	G266-135	9980	10.3 ± 11.7
0101+048	G001-045	8750	-9.7 ± 7.6
0135-052	L870-002	8700	-1.6 ± 6.1
1537+651	GD348	9910	-7.7 ± 9.7
1655+215	G169-34	9578	-3.0 ± 5.8
1840-111	G155-34	10389	-1.8 ± 5.1
2246+223	G067-023	11131	11.0 ± 11.4

Note. — Cool DAs observed photometrically. The magnetic field measurements come from Schmidt and Smith, 1995.

Table 4.5. ZZ Ceti temperatures.

WD#	1	2	3	4	5
0104-464	00000	10315	00000	00000	00000
0133-116	11117	12550	11830	12400	12800
0341-459	00000	12870	00000	00000	00000
0416+272	10739	13010	00000	00000	00000
0417+361	10990	11900	00000	00000	00000
0455+553	10964	00000	00000	00000	00000
0517+307	00000	00000	00000	00000	12450
0858+363	11297	13350	11100	12000	11750
0921+354	11668	13640	11840	13150	13200
1159+803	10964	00000	00000	00000	00000
1236-495	00000	00000	11200	11560	00000
1307+354	10495	00000	10300	11740	11320
1350+656	0.000	00000	00000	00000	13140
1422+095	0.000	00000	00000	00000	13420
1425-811	00000	12520	12230	12640	00000
1559+369	10990	11730	10880	11560	00000
1647+591	11066	00000	12120	12260	11840
1855+338	00000	00000	12040	12060	00000
1935+276	11117	00000	11970	12370	00000
1950+250	11694	00000	00000	00000	00000
2303+242	00000	00000	00000	00000	00000
2326+049	11402	12630	11380	11780	11570

Note. — 1) Greenstein (1982) (g-r) 2) McGraw (1979) (strömgren) 3) Kepler and Nelan (1992) SWP (IUE) 4) Kepler and Nelan (1992) LWP (IUE) 5) Daou, et al (1990)

Table 4.6. ZZ Ceti temperatures (continued).

WD#	7	8	9	10	11	12	13
0104-464	00000	00000	12355	00000	00000	00000	11270
0133-116	12200	12770	12692	00000	00000	00000	11990
0341-459	00000	00000	12057	00000	00000	00000	11540
0416+272	00000	00000	00000	00000	00000	00000	11440
0417+361	00000	00000	00000	00000	00000	00000	11180
0455+553	00000	00000	00000	00000	00000	00000	11420
0517+307	00000	00000	00000	00000	00000	00000	11980
0858+363	00000	00000	00000	11218	00000	00000	11820
0921+354	12460	13000	13196	11862	11862	11548	11620
1159+803	00000	00000	00000	00000	00000	00000	11430
1236-495	00000	00000	12690	11299	11435	11696	11730
1307+354	11360	11740	00000	10173	00000	00000	11180
1350+656	00000	00000	00000	00000	00000	00000	11890
1422+095	00000	00000	00000	00000	00000	00000	11980
1425-811	12030	12620	13150	00000	00000	00000	12100
1559+369	00000	00000	12000	00000	00000	00000	11160
1647+591	11760	12390	13563	11985	11849	12044	12460
1855+338	00000	00000	00000	11572	00000	11660	11960
1935+276	11820	12510	00000	11690	00000	11651	12130
1950+250	00000	00000	13002	00000	00000	00000	11710
2303+242	00000	00000	12253	00000	00000	00000	11480
2326+049	11530	12080	13323	00000	00000	00000	11820

Note. — 7) Wesemael et al. (1986) (Model Nelan Wegener 1985)
8) Wesemael et al. (1986) (Model Koester et al. 1985) 9) Giovannini
(1996), models Koester $ML1/\alpha = 2.0$ 10) Koester and Allard (1993)
 $\log g=8$ 11) same as 10 but X^2 is minimum 12) same as 10 but consistent
with parallax + mass radius relationship 13) Bergeron et al (1995)
 $ML2/\alpha = 0.6$

Table 4.7. ZZ Ceti temperatures relative to G117–B15A.

WD	ΔT	$\sigma_{\Delta T}$
WD0133-11	-223.50	501.2
WD0858+36	-563.33	692.1
WD1236-49	-484.17	633.0
WD1307+35	-1130.00	601.1
WD1425-81	78.50	454.6
WD1559+36	-1051.50	472.3
WD1647+59	180.00	593.7
WD1855+34	-109.50	660.4
WD1935+27	-9.25	546.4
WD2326+04	-375.75	725.7

Note. — the average and standard deviations (of the standard deviations) are: $588 \text{ K} \pm 93 \text{ K}$.

Table 4.8. ZZ Ceti temperatures relative to G226-29.

WD	ΔT	$\sigma_{\Delta T}$
WD0133-11	-372.75	419.3
WD0858+36	-640.00	380.0
WD0921+35	-180.00	593.7
WD1236-49	-664.17	235.5
WD1307+35	-1206.67	653.1
WD1425-81	-70.75	381.5
WD1559+36	-1200.75	362.1
WD1855+34	-291.00	187.2
WD1935+27	-190.75	225.4
WD2326+04	-525.00	218.1

Note. — the average and standard deviation are: $354 \text{ K} \pm 156 \text{ K}$.

Table 4.9. ZZ Ceti temperatures relative to BPM 37093

WD	ΔT	$\sigma_{\Delta T}$
WD0133-11	433.00	374.2
WD0858+36	143.33	273.9
WD0921+35	484.17	633.0
WD1307+35	-423.33	551.0
WD1425-81	735.00	371.9
WD1559+36	-395.00	305.1
WD1647+59	664.17	235.5
WD1855+34	383.50	374.8
WD1935+27	483.75	397.9
WD2326+04	280.75	241.0

Note. — the average ΔT and standard deviation are: $376 \text{ K} \pm 129 \text{ K}$.

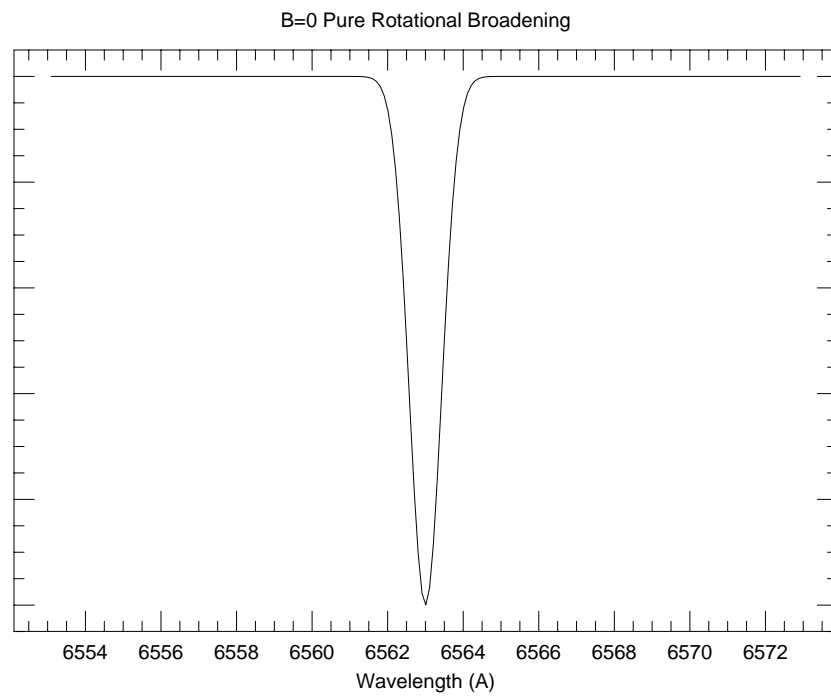


Fig. 4.1.— A gaussian with a full width at half maximum of 1 Å looks very similar to the absorption core of H_α in a white dwarf. Such a line can have the width it has either because of rotation or a combination of rotation and a magnetic field.

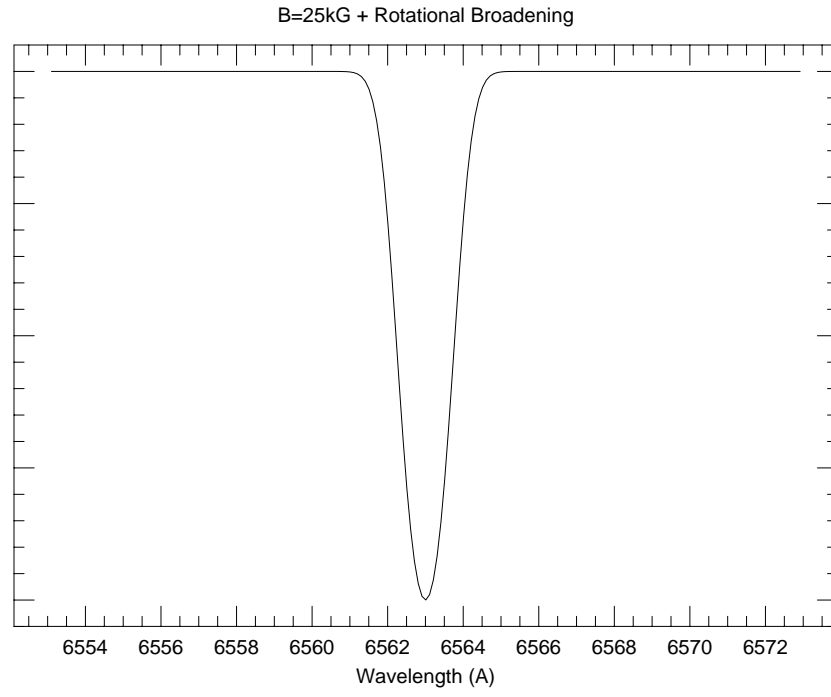


Fig. 4.2.— The sum of three 1 \AA wide lines split by a 25 kG magnetic field (0.5 \AA in both directions) produces a wider line whose full width at half maximum is 1.5 \AA . Measuring this width it is possible to set an upper limit of 37.5 kG to the presence of a magnetic field.

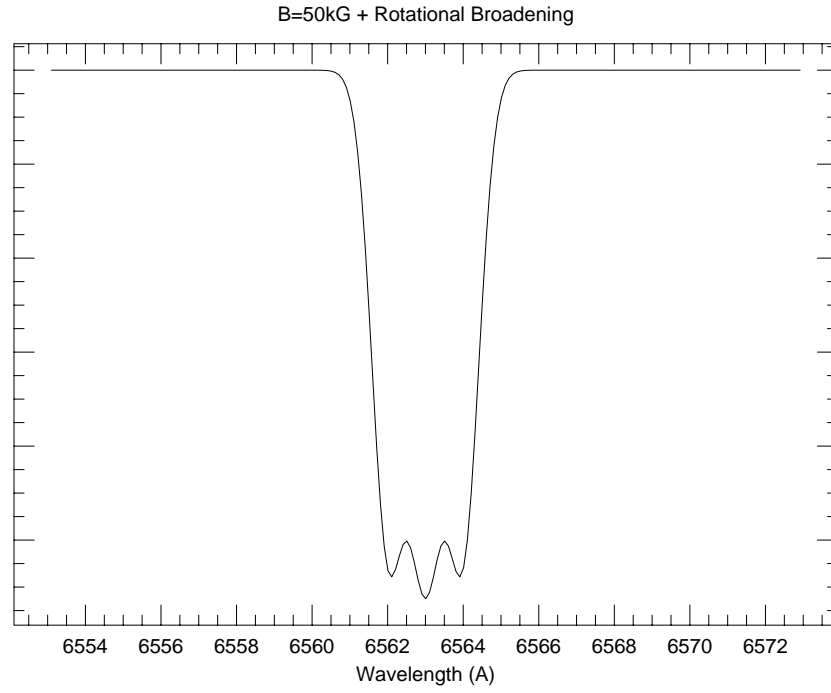


Fig. 4.3.— The sum of three 1 \AA wide lines split by a 50 kG magnetic field (1 \AA in both directions) produces a wider line whose full width at half maximum is 2.8 \AA . Measuring this width it is possible to set an upper limit of 71 kG to the presence of a magnetic field. In very high signal to noise spectra it would be possible to see the triplet at the bottom of the line, however this would not be the case with our low signal to noise spectra.

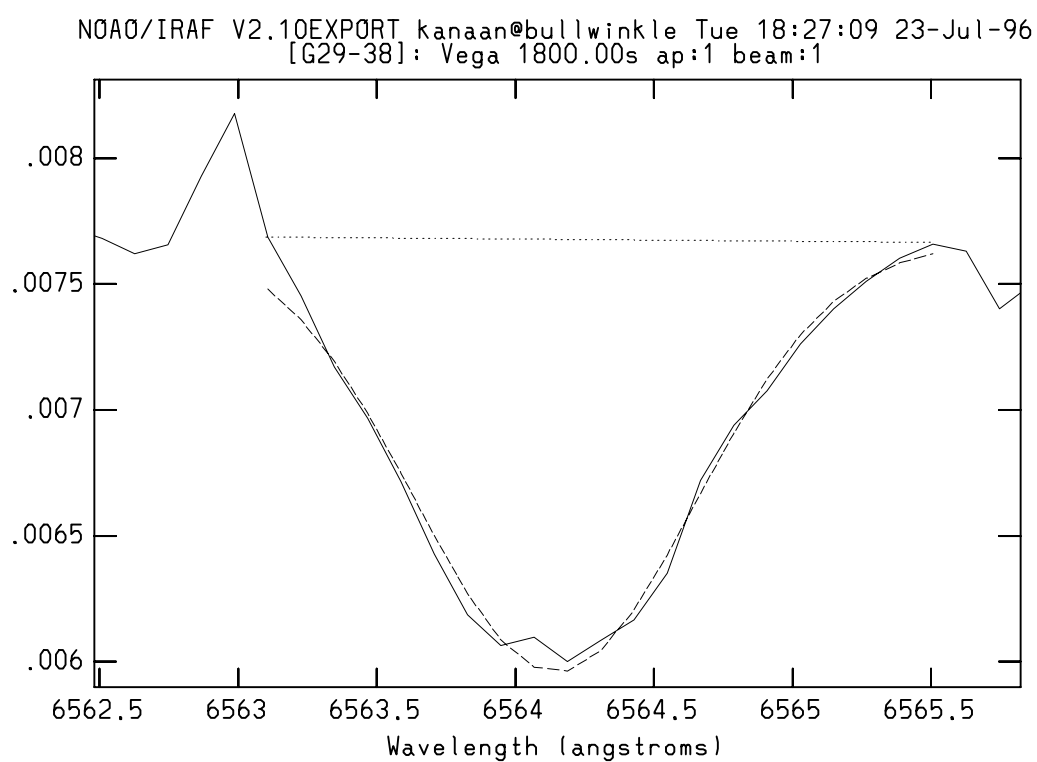


Fig. 4.4.— The ZZ Ceti G29-38.

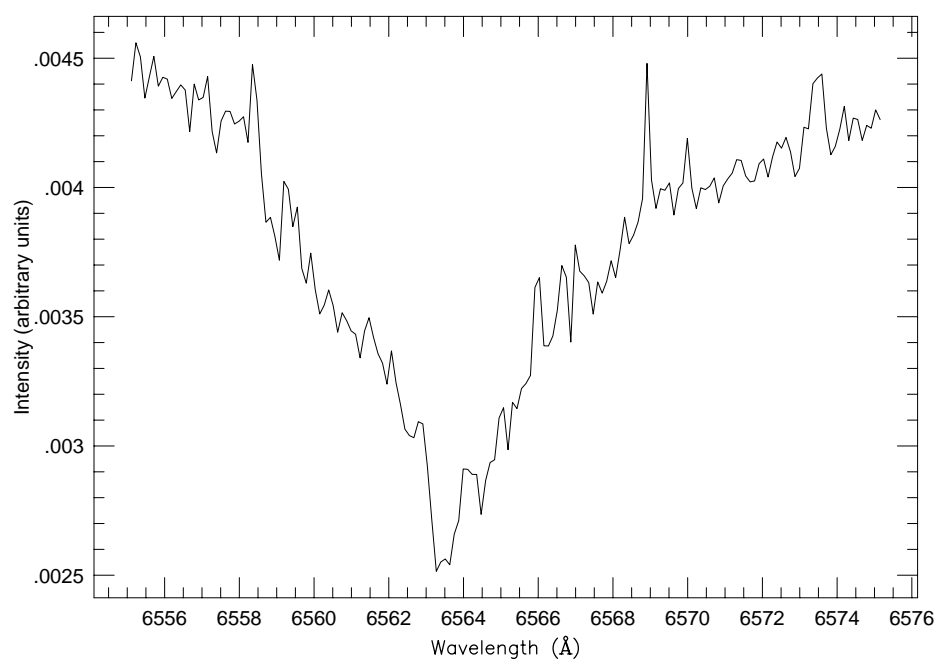


Fig. 4.5.— The spectrum of the cool DA G1-45.

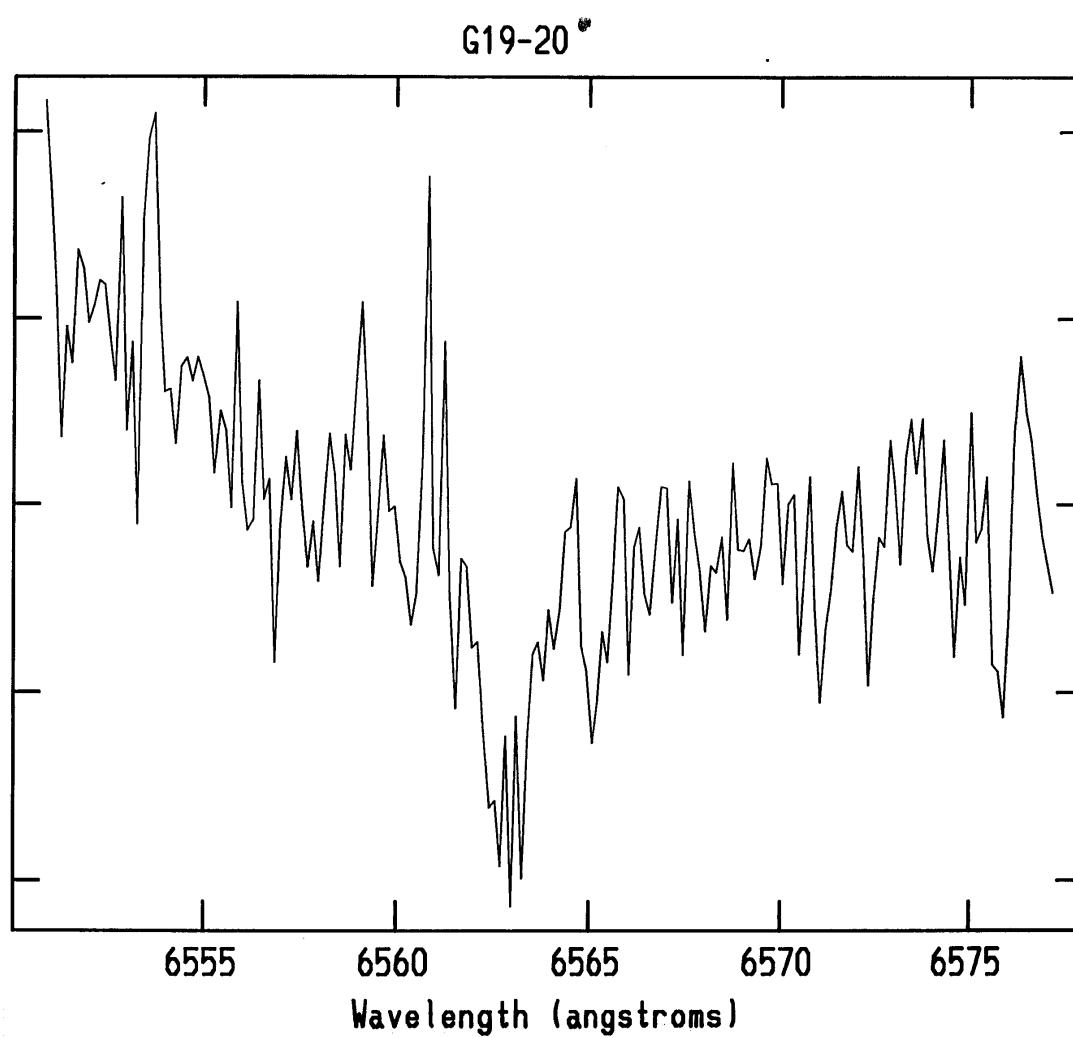


Fig. 4.6.— The spectrum of the cool DA G19-20.

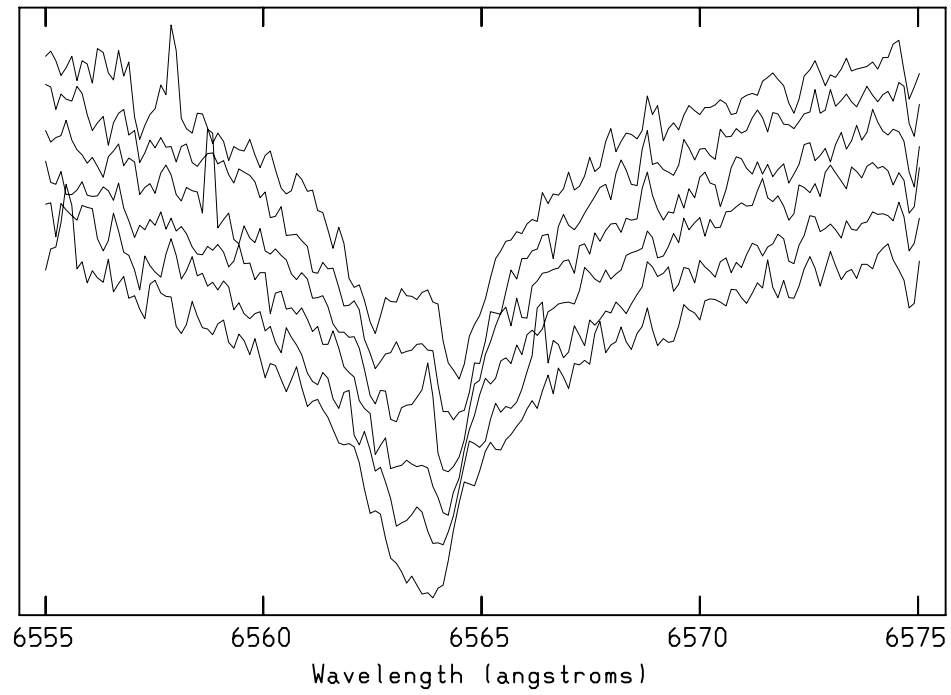


Fig. 4.7.— The cool binary degenerate L870-2. Spectra are separated by 0.5h intervals, beginning at the bottom.

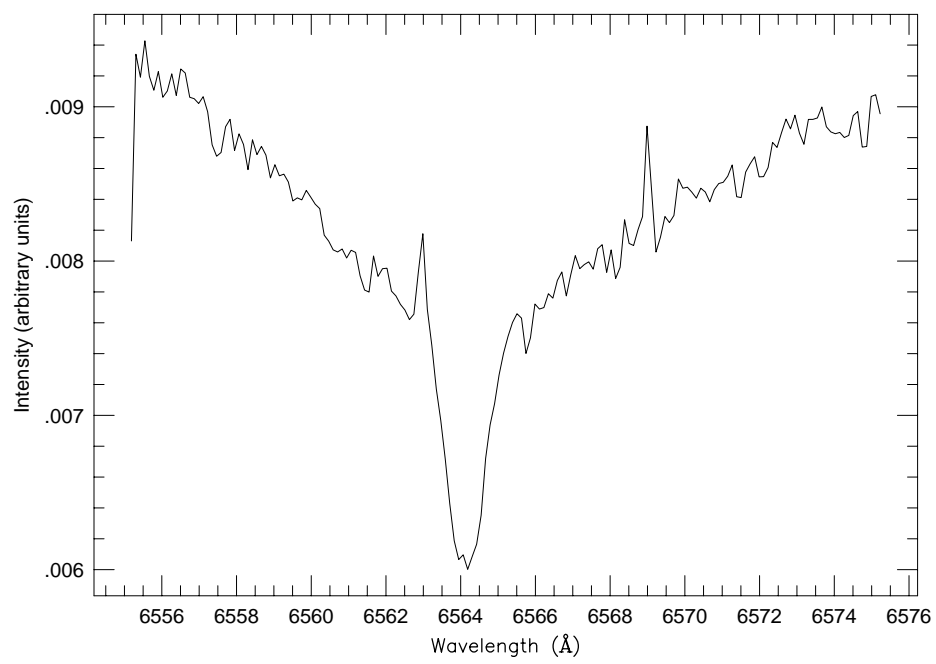


Fig. 4.8.— The ZZ Ceti G29-38.

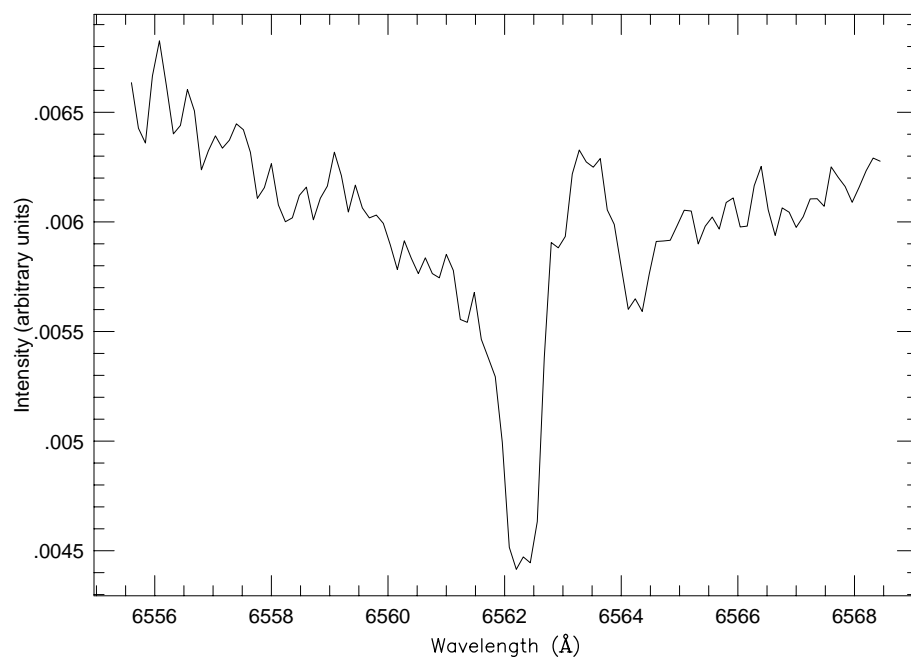


Fig. 4.9.— The ZZ Ceti G185-32.

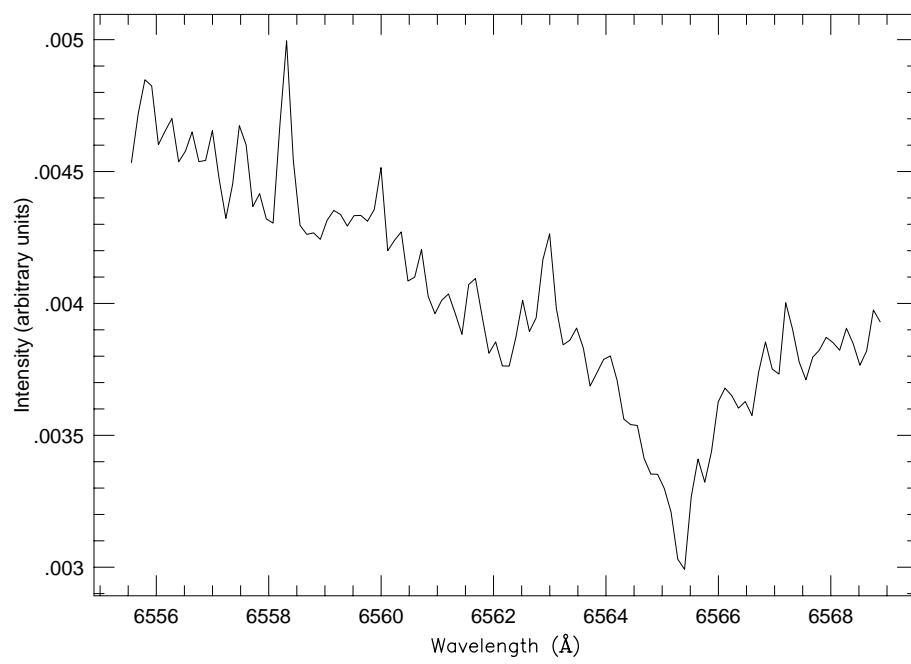


Fig. 4.10.— The ZZ Ceti R548.

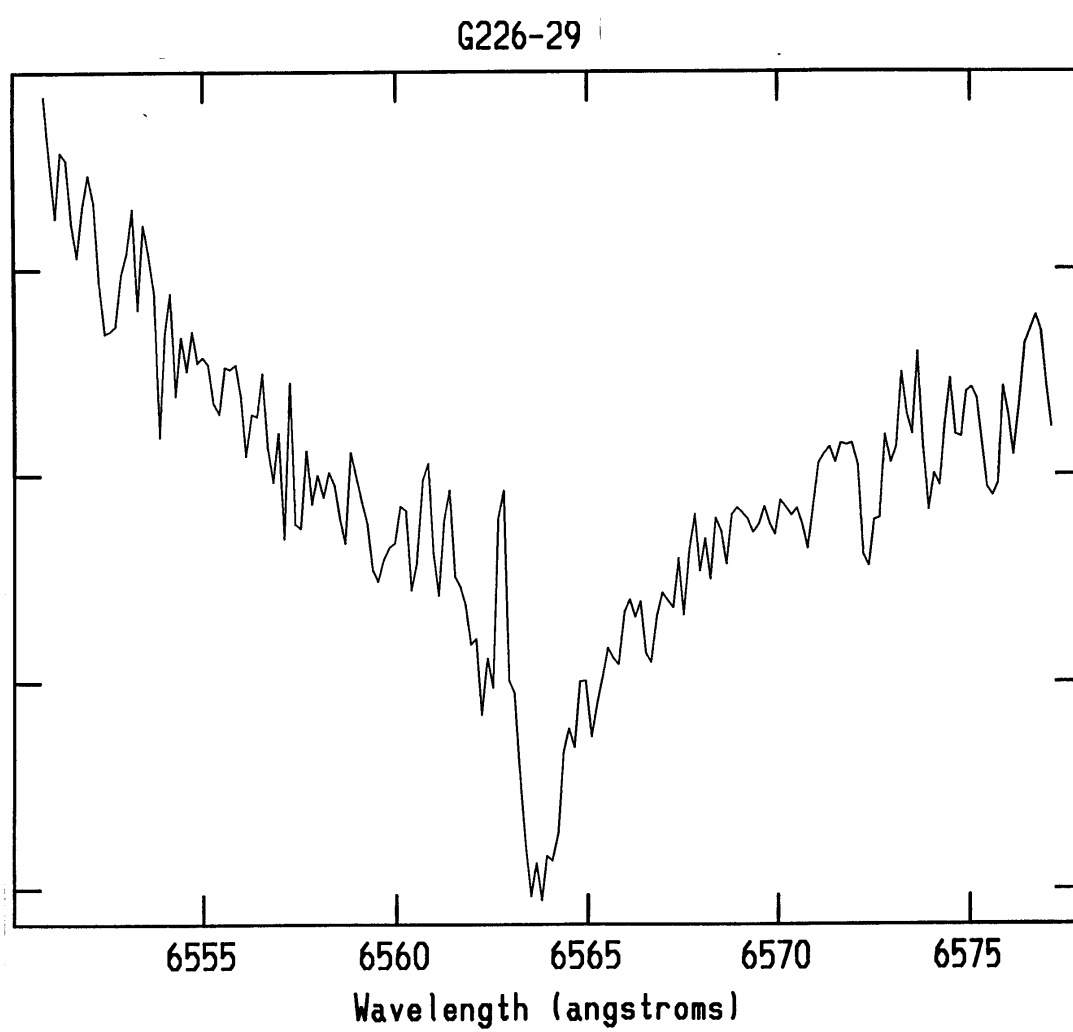


Fig. 4.11.— The ZZ Ceti G226-29.

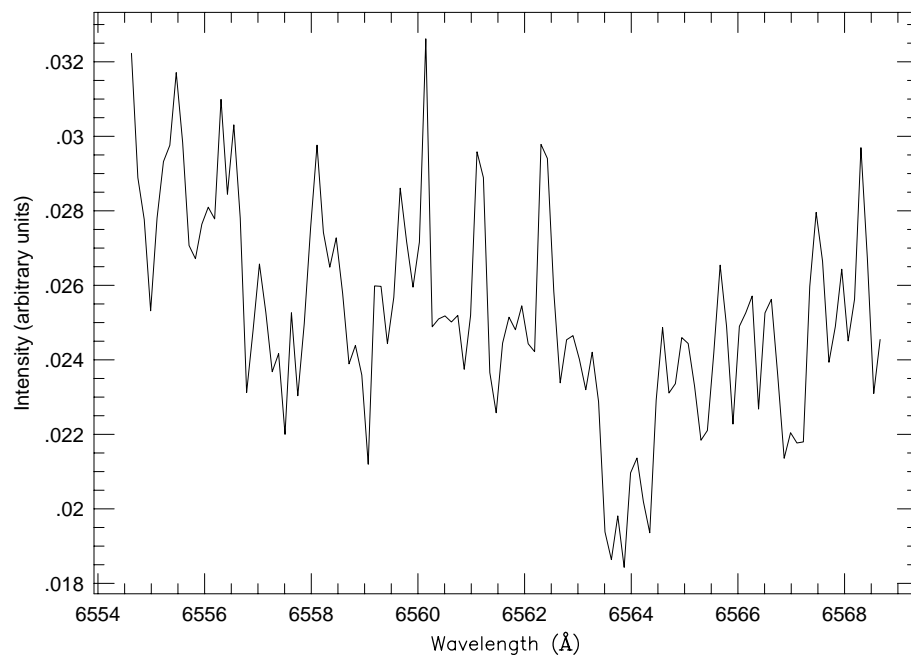


Fig. 4.12.— The non-variable G67-23.

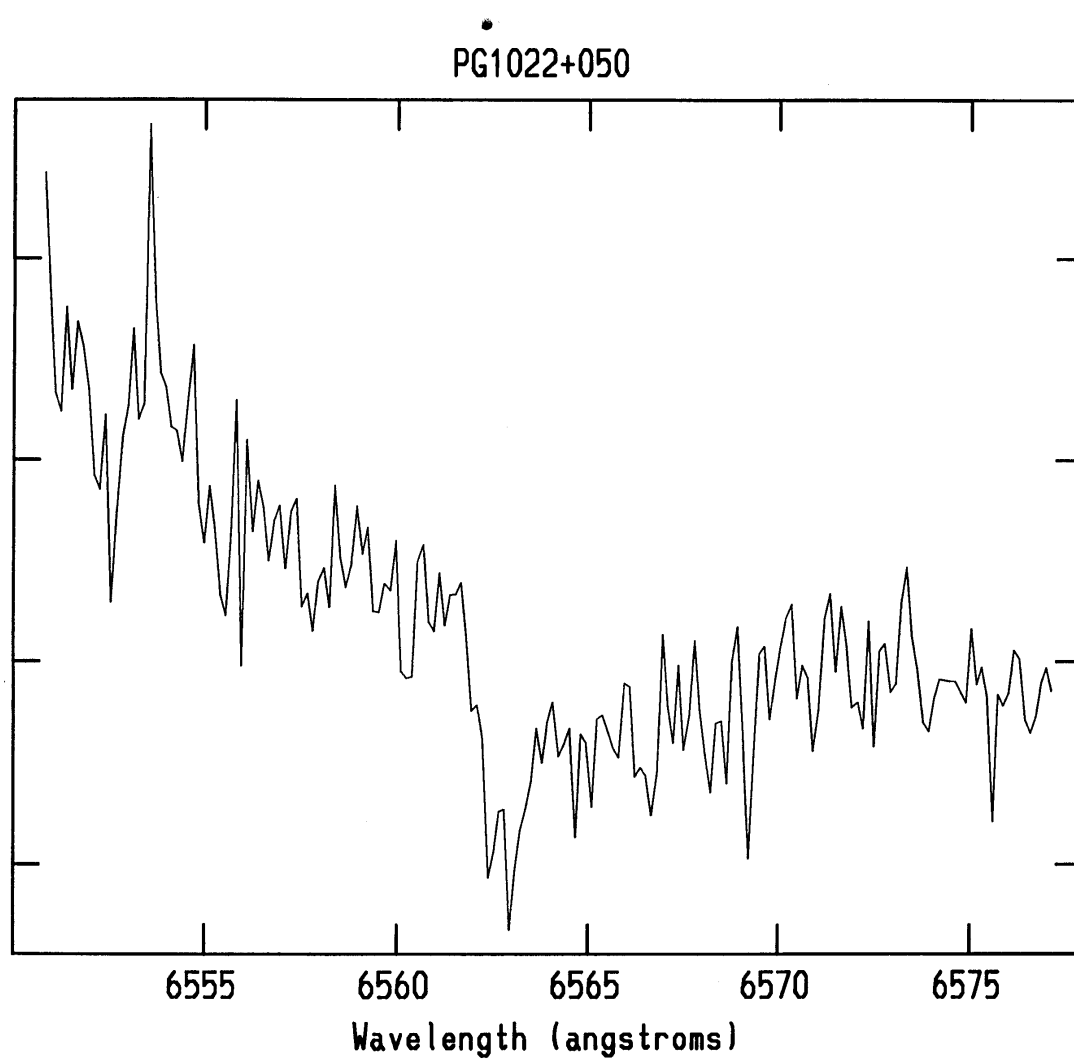


Fig. 4.13.— The non-variable PG1022+050.

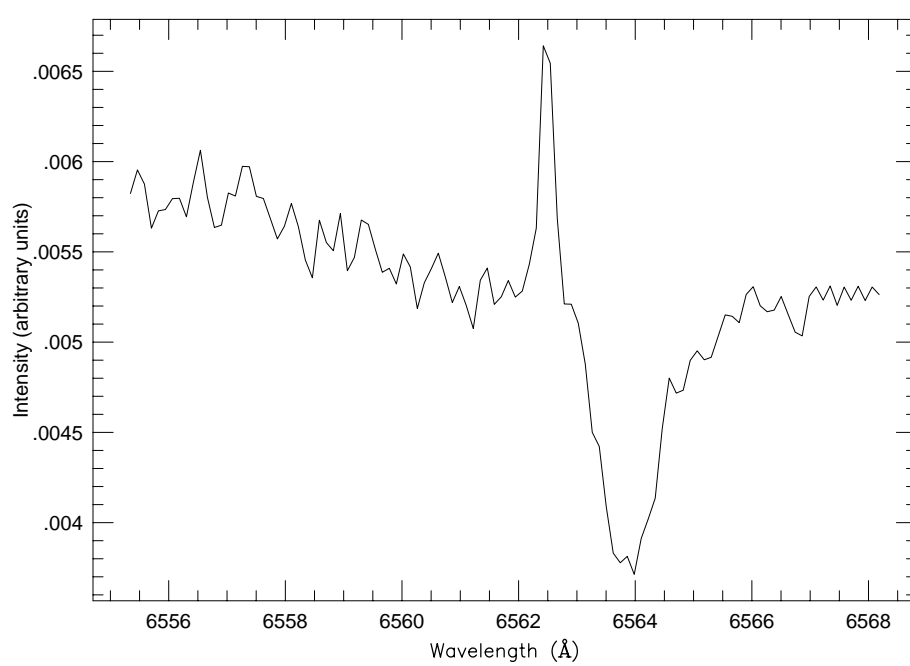
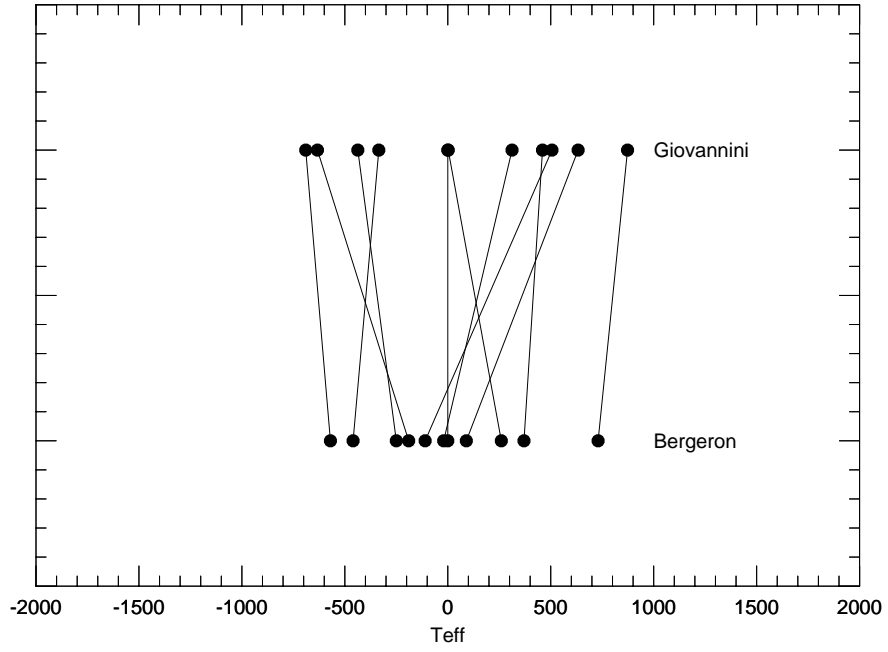


Fig. 4.14.— The non-variable G8-8.



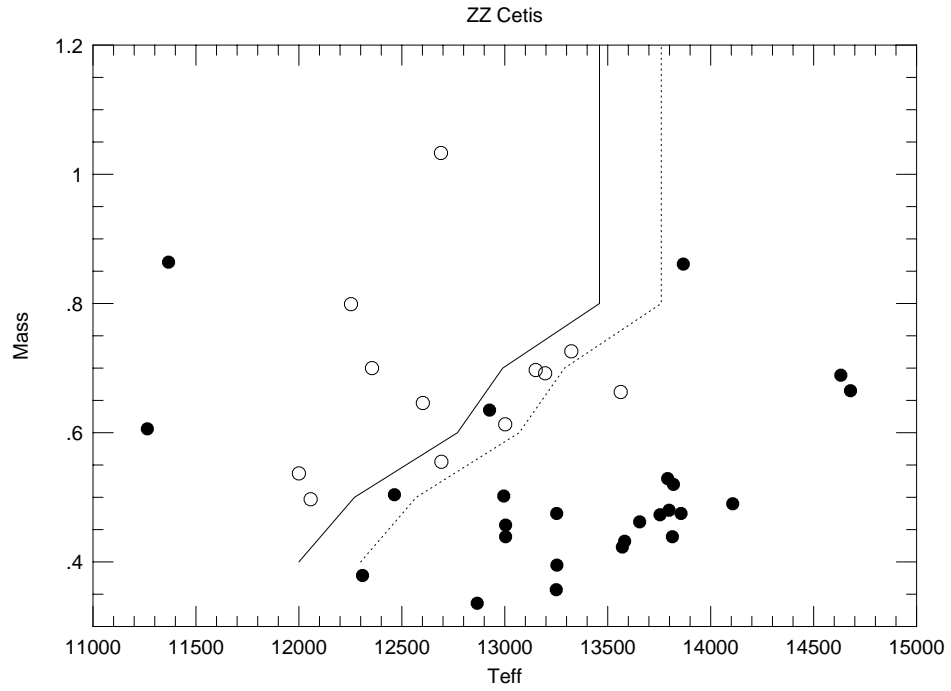


Fig. 4.16.— The ZZ Ceti instability strip according to Giovannini (1996). The Solid line represents the computations of Bradley and Winget. The dashed line is the same but shifted by 300 K to include all the variable stars. Open circles represent the pulsating ZZ Ceti stars. Filled circles are non variable stars. Theoretical models were computed only till $0.8 M_{\odot}$, this is why the line becomes vertical at $0.8 M_{\odot}$.

Chapter 5

Pulsations and Radial Velocity Variations in Magnetic Pulsating Ap Stars. Analysis of γ Equulei

1. Introduction

The Ap stars are a group of chemically peculiar stars which show spectral, photometric, and magnetic field (\sim kilogauss) variations modulated with the rotation period of the star. Stibbs (1950) proposed that all of these variations could be explained by the oblique rotator model — a dipole magnetic field whose axis is inclined to the rotation axis of the star. Michaud (1970) proposed the diffusion model where the rare earths are brought up to the surface by radiation pressure while other elements sink to stellar interior. The magnetic field modifies the vertical diffusion by forcing ions to travel only along field lines. This can account for the enhancements near the magnetic poles of such elements as the rare earths.

The rapidly oscillating Ap stars (roAp) are a subclass of these objects that exhibit low-amplitude photometric variations (0.5–13 mmag) with periods ranging from 6 to 15 min. The photometric amplitude of the oscillations is modulated in phase with the magnetic field variations (*i. e.* rotational

phase). To explain this behavior Kurtz (1982) proposed the oblique pulsator model where these variations are explained as low-order ($\ell < 4$) high-overtone ($k > 10$) nonradial p -mode pulsations whose axis of symmetry for the pulsations is aligned to the magnetic axis rather than the rotational axis of the star.

The evolutionary status of Ap stars is not well understood, it is not known to this date whether they are pre-main sequence, main sequence or post-main sequence stars. Their position on the Hertzsprung-Russell diagram is suggestive that they be somehow related to δ Scuti stars in the sense that the same driving mechanism, HeII partial ionization zone, may be responsible for the pulsations in both objects. If that is the case it is expected that the ratio of radial velocity amplitudes to luminosity amplitudes (normally called $2K/\Delta m$) should be roughly the same.

Estimates of the $2K/\Delta m$ ratio have been done for only 3 roAp stars and with confusing results. Matthews et al, 1988 measured a RV peak-to-peak amplitude ($2K$) of 400 m s^{-1} from this and the photometric amplitude (measured by them in the same night) they found $2K/\Delta m$ of $59 \text{ km s}^{-1} \text{ mag}^{-1}$. This value is consistent with *radially* pulsating δ Scuti stars. Libbrecht (1988) claimed the detection of RV variations with a $2K$ amplitude of 84 m s^{-1} in the roAp star γ Equ and inferred a $2K/\Delta m > 30 \text{ km s}^{-1} \text{ mag}^{-1}$ (without simultaneous photometry), while Matthews and Scott (1995) found for the same star that $2K/\Delta m > 625 \text{ km s}^{-1} \text{ mag}^{-1}$. Recently, Hatzes and Kürster (1994), searched for radial velocity variations in the roAp star α Cir and placed an upper limit of $2K < 60 \text{ m s}^{-1}$ for any variations. This resulted in $2K/\Delta m < 10 \text{ km s}^{-1} \text{ mag}^{-1}$. At present the $2K/\Delta m$ measurements are

too few to confirm or deny any link of roAp stars with the δ Scuti stars. The available results are however different, either in the total radial velocity amplitude measured by different observers for the same star, or for the ratio $2K/\Delta m$ between different stars. It has not been clear what has caused the observed differences.

We felt that at McDonald observatory we have the right tools to establish what is the problem with these conflicting results. During the last decade a search for planets around solar type stars has been undertaken by Cochran et al (Cochran and Hatzes, 1994). With use of an iodine cell at the coudé spectrograph of the 2.7 m telescope at McDonald Observatory the authors have been able to measure radial velocities with a precision as good as 10m/s over periods of years. We decided then to use the same equipment to observe several known roAp stars. The difference between our observations and theirs is our use of a cross dispersed echelle coudé spectrograph, allowing us a much wider wavelength coverage. The idea was to observe, reduce and analyze data on different objects all through the same techniques, therefore eliminating the possibility that the discrepant results obtained by other authors were caused by differences in the data acquisition/analysis process. Here we present our initial results on the analysis of the roAp star γ Equulei.

γ Equ is the brightest of all the roAp stars. It is also the slowest rotator of all roAp stars, having a rotational period of 78 years (Bonsack and Pilachowski, 1974, Leroy et al, 1994). Furthermore, its variability is dominated by a single pulsation mode of relatively long period (12.44 minutes — Kurtz, 1983). These characteristics make it the best target for the kind of measurements we are interested. Its slow rotation implies very narrow

absorption lines which are ideal for radial velocity measurements, and the light curve being dominated by a single, relatively long period, pulsation mode allows us to sample the light curve with several points per period and without having to worry about the effects of mode superposition.

2. Observations

To compare the radial velocity variations amplitude to the photometric amplitude, spectroscopic and photometric observations were planned simultaneously using the coude spectrograph of the 2.7 m telescope and a 3-channel photoelectric photometer at the 0.9 m telescope, both located at McDonald Observatory. Unfortunately, observing conditions were not photometric (out of three allocated nights, data were gathered for only 2 hours) and only spectroscopic data are presented here.

The spectroscopic observations were made using the F3 focus of the 2-d coude spectrograph of the 2.7 m telescope (Tull et al, 1995). This prism cross-dispersed echelle provides complete coverage from 4,000 Å to 10,000 Å when used with a large enough chip. At the time of the observations only a 800×800 TI CCD with $15 \mu\text{m}$ pixels was available. This provided a limited (5,000Å – 6,000Å) and incomplete coverage (see figure 5.1).

Radial velocity measurements were made using an iodine (I_2) gas absorption cell. Stellar observations were made with this device placed in front of the entrance slit of the spectrograph. This superimposes a set of iodine absorption lines on top of the stellar spectrum. As all radial velocity shifts of the star are made with respect to the iodine lines instrumental shifts are

minimized and a highly accurate radial velocity results.

To allow for good sampling of the γ Equ pulsation curve, whose period is 12 minutes, spectra were taken every 80 seconds (60 seconds exposure time + 20 seconds readout).

3. Analysis

Figure 5.1 shows the spectrum of γ Equulei in the 10 useful echelle orders. The radial velocity measurements of each individual spectral order (using all spectral lines together) were Fourier analyzed and the resulting transforms are shown in figure 5.2. Inspecting that figure, one immediately sees that the pulsational amplitude seems strongly dependent on the spectral region of the measurements. As an additional illustration of our results we show phase diagrams of our radial velocity measurements in Figure 5.3.

Note that there appears to be a trend in this plot: spectral orders dominated by strong lines have lower amplitude. To investigate this further radial velocity measurements were made using individual lines rather than the full spectral order. With the help of line identification lists produced by Bidelman (Cowley private communication), we identified as many lines in the stellar spectrum as possible. Because only one line is used in this radial velocity measurement, the velocity precision of our radial velocity measurements is drastically reduced. Even so we still are able to measure the radial velocity variations with very high precision, especially for the deeper lines. Figure 5.4 shows the Fourier transform of one deep and a shallow line. In Appendix A we present the identification of all lines we used for the radial

velocity measurements.

The pulsation frequency derived from the Fourier transform of radial velocity measurements of individual lines is, within measurement errors, the same for every line and identical to the previously determined photometric frequency. Based on that, a sine curve of fixed period but variable amplitude and phase was fit for the radial velocity measurements of each individual line. Radial velocity amplitude measurements are shown from the spectral lines of two elements; chromium and iron, primarily because they are the dominant species found in the spectra. It is well known that the line strengths of some elements in Ap stars vary with rotation phase. Because of the suspected long rotation period of 78 years for γ Equ it is not known what the exact phase behavior of the line strength for chromium and iron is. However, for other Ap stars it is found that chromium is concentrated towards the magnetic poles, whereas iron is more evenly distributed across the surface (Wolff, 1983). If this is true for γ Equ, then the radial velocity variations of the chromium line would be dominated by the motions in regions near the pole.

The fact that integrated radial velocities from echelle orders dominated by strong lines have a lower amplitude than for orders dominated by weaker lines suggests searching for correlations between radial velocity amplitudes and equivalent width of spectral lines.

Figure 5.5 shows the radial velocity amplitudes as a function of equivalent width for all of the CrI and CrII lines that could be identified. The trend of decreasing amplitudes with equivalent width is obvious and significantly greater than the mean error of the measurement. A word of caution is in order at this point. Line identifications on stars like γ Equ is a

risky business, many lines are blended with other lines and often it is hard to tell if one is a blend of two lines or if only one of the two lines is present. We used only those lines for which we were sure of their identification as well as of their being not blended with any other line. The measurement of equivalent widths is also tricky for the same reason, the large amount of lines present in the spectrum makes it almost impossible to define a continuum, and therefore the equivalent widths are highly uncertain. We consider our equivalent widths to have an uncertainty of 0.01 \AA .

Figure 5.6 shows the amplitudes as a function of equivalent width for all the FeI lines and Figure 5.7 for the FeII lines. On Figure 5.7 the point of maximum amplitude seems to be an iron line, however it is a line at 6044 \AA and at about $5,500 \text{ \AA}$ Bidelman's list of line identifications is not complete anymore. As our data does not provide complete wavelength coverage this line is the only one belonging to multiplet #350 of FeII, therefore its identification is uncertain. No obvious trend can be seen here and the few detections of any amplitude modulation all have lower amplitudes than most of the chromium lines.

We present the amplitudes as well as phases and their uncertainties are on tables 5.1. Even though some of the phase measurements do differ by more than the uncertainty we are unable to see any correlation between the phases and any other quantity. It is included on the table in case somebody can see any correlation missed.

4. Discussion

The radial velocity measurements presented so far seem to give the following picture: chromium lines show a higher mean velocity than iron, neutral chromium a higher mean velocity than once ionized chromium. This behavior also seems evident in another species, titanium. After chromium and iron titanium has the most lines in the spectral region covered by our data, but this is only 5 lines (4 once ionized, 1 neutral). Figure 5.8 shows the amplitudes of TiI and TiII lines as a function of equivalent width. Because of the small absolute amplitudes the error bars (relative to the absolute value of the amplitudes) are large and it can be argued that the amplitude is constant for the 4 lines. However, there is a visible trend: larger equivalent widths, smaller amplitudes. The one line of TiI shows a velocity of 557 ± 135 m/s, again consistent with the behavior of chromium lines, that is neutral lines show higher amplitudes.

Looking at Figure 5.2 it is possible to imagine that what we actually have is a wavelength dependent modulation in amplitude rather than element and equivalent width. In Figures 5.9 to 5.12 we show the velocity modulation amplitudes as a function of wavelength for chromium, iron and titanium. It is clear that the iron lines all have low amplitudes. Chromium lines appear in high and low amplitude at different wavelengths, and the same can be said about titanium.

In formulating one hypothesis for the radial velocity variations of the various lines presented one must account for the following observed properties: i) elemental differences, why do chromium and titanium seem to have much higher average velocities than iron; ii) the equivalent width dependence, lines of small equivalent widths have higher amplitudes than lines of large equivalent

widths. Tentatively these can all be explained by a non-uniform distribution of elements moving in the presence of a magnetic field, their motion being influenced by the Lorentz force. We now explain how this idea can explain each of the above items.

i) The elemental differences. Most of the chromium (and titanium) we see on the surface of Ap stars is concentrated on the magnetic poles. Whatever motion these atoms have is the motion seen on the spectral lines. Now, at these regions the magnetic field direction is perpendicular to the surface, and so is the motion of particles undergoing p-mode oscillations. Chromium should therefore be free to move up and down over most of the region where it is abundant. Iron, on the other hand, is spread over the whole surface and should be able to move freely at the poles and have “difficulty” at the equator, this would then cause the iron lines to have smaller amplitudes than chromium.

ii) The equivalent width dependence. Lines of large equivalent width are formed closer to the surface, and lines of small equivalent width are formed deeper down the photosphere. At small depths in the atmosphere the magnetic pressure dominates over the gas pressure and therefore all motions are dictated by the magnetic field geometry. The reverse is true deeper in the atmosphere. We suggest that as we look at lines formed closer to the surface the magnetic field becomes more important in restraining the motions of the gas. An even simpler explanation is possible: lines of large equivalent width are probably formed in a larger area than the ones of small equivalent. If the latter come from regions close to the pole then the same explanation used for the elemental differences applies here.

The radial velocity measurements presented here clarify some of the

confusing results for $2K/\Delta m$ measurements found by previous authors. The measured $2K$ amplitude depends on which spectral region one observes. If that region is dominated by weak lines, particularly by those elements concentrated at the poles, then one would get a grossly different answer than if one used a region dominated by strong lines of an element uniformly distributed across the stellar surface. A measurement of the mean $2K/\Delta m$ ratio is thus largely meaningless and may not be useful in elucidating the excitation mechanism for pulsation in roAp stars.

We have gathered strong evidence that elements concentrated towards the magnetic poles display higher amplitudes while elements uniformly distributed over the surface show smaller velocities. We also see a correlation between equivalent width and velocity amplitudes. We advanced a qualitative model to explain what is observed. If our simple model is correct one important prediction of it is that the amplitudes of the rare earths should diminish when the magnetic field is in quadrature (the moment we see the least of the poles), unfortunately this is also the moment at which the photometric amplitudes are at a minimum because of cancellation between the two poles. Still, if our model is correct the relative amplitude between the chromium lines and the iron lines should be a function of rotational phase. The ratio should be at a maximum when the magnetic pole is pointing towards us and a minimum when pointing 90° away. Gamma Equulei is obviously not the object of choice for such a measurement as its rotational period is very long. Other stars of shorter rotational periods (2-3 days) would be ideal, but their lines are a little too broad and we lose precision in our determination of radial velocities. HR1217 with a rotational period of 12 days ideal from the viewpoint of radial

velocity measurements but a little over the tolerance of most time allocation committees.

Table 5.1. Radial velocity amplitudes for Cr lines.

Wavelength (Å)	Amplitude (m/s)	σ (m/s)	Time of Maximum (BJED)	σ (days)	Equivalent Width
Chromium I					
5151.84	224.16	26.21	9608.707861	0.000162	0.0900
5212.27	1052.22	192.27	9608.707030	0.000253	0.0279
5224.96	88.62	18.98	9608.707422	0.000298	0.0828
5296.80	24.19	15.85	9608.712816	0.000901	0.0610
5297.20	7.99	23.80	9608.706964	0.004125	0.0700
5308.30	27.31	16.48	9608.708421	0.000836	0.0709
5387.00	161.17	68.41	9608.714424	0.000574	0.0520
5844.30	451.23	41.96	9608.708144	0.000128	0.0306
Chromium II					
5210.84	31.45	26.43	9608.709436	0.001132	0.0500
5306.00	57.18	13.73	9608.707077	0.000333	0.0583
5310.80	86.07	22.56	9608.714315	0.000357	0.0609
5478.30	18.97	12.87	9608.713266	0.000920	0.0730
5566.00	141.78	24.63	9608.707611	0.000242	0.0823
Iron I					
5137.41	28.09	23.42	9608.712470	0.001144	0.1145
5139.48	40.54	14.76	9608.707102	0.000501	0.1054
5141.77	31.21	16.21	9608.707128	0.000721	0.0453
5142.55	2.90	57.00	9608.707197	0.027306	0.085
5142.96	270.02	121.90	9608.714071	0.000608	0.040

Table 5.1—Continued

Wavelength (Å)	Amplitude (m/s)	σ (m/s)	Time of Maximum (BJED)	σ (days)	Equivalent Width
.18	32.69	16.45	9608.708292	0.000684	0.0771
5216.29	13.05	9.22	9608.708065	0.000976	0.0624
5217.40	11.02	15.69	9608.714937	0.001945	0.0610
5217.88	29.05	23.53	9608.713585	0.001117	0.0300
5226.80	186.80	261.61	9608.707968	0.001939	0.1200
5227.10	89.99	84.42	9608.714342	0.001267	0.1000
5228.10	60.84	16.95	9608.707154	0.000387	0.0380
5229.80	29.81	15.21	9608.713641	0.000688	0.0700
5295.20	123.80	47.74	9608.715043	0.000528	0.0224
5302.10	75.85	19.51	9608.714545	0.000358	0.0785
5373.50	18.67	24.23	9608.706875	0.001794	0.0477
5379.50	21.28	24.57	9608.710695	0.001580	0.0333
5383.20	7.33	9.75	9608.714408	0.001798	0.1220
5463.00	3.05	11.46	9608.713775	0.005060	0.0618
5464.00	54.48	33.58	9608.714478	0.000834	0.0290
5474.00	23.33	16.26	9608.713437	0.000942	0.0570
5476.30	31.51	38.86	9608.710647	0.001686	0.0800
5553.20	69.94	27.42	9608.714775	0.000534	0.0300
5555.00	29.14	13.59	9608.714027	0.000628	0.0740
5558.00	65.51	22.49	9608.714898	0.000471	0.0290
5560.10	23.86	33.12	9608.709275	0.001957	0.0300
5562.80	24.20	27.35	9608.712860	0.001554	0.0454
5563.50	63.59	26.02	9608.706845	0.000557	0.0500
5565.40	10.37	18.78	9608.711925	0.002516	0.0600
5567.20	20.82	40.88	9608.706669	0.002728	0.0235
5638.10	27.55	20.34	9608.714228	0.000996	0.0480
5641.30	20.52	19.52	9608.713378	0.001286	0.0370
5649.80	42.17	19.49	9608.712583	0.000636	0.0230
5658.50	15.76	15.31	9608.714842	0.001313	0.1100
5848.00	80.74	37.10	9608.713447	0.000621	0.0186
6034.00	257.56	64.46	9608.707186	0.000348	0.0290
6042.00	18.63	17.92	9608.714750	0.001321	0.0358
Iron II					
5143.89	41.49	43.68	9608.713332	0.001425	0.019
5144.42	82.38	107.76	9608.708068	0.001808	0.027
5146.13	38.65	16.86	9608.714585	0.000590	0.034
5147.15	40.30	35.29	9608.711387	0.001215	0.018
5148.06	11.89	16.36	9608.713729	0.001854	0.060
5149.47	64.43	20.51	9608.714570	0.000428	0.028
5150.89	3.09	13.38	9608.711933	0.006026	0.065

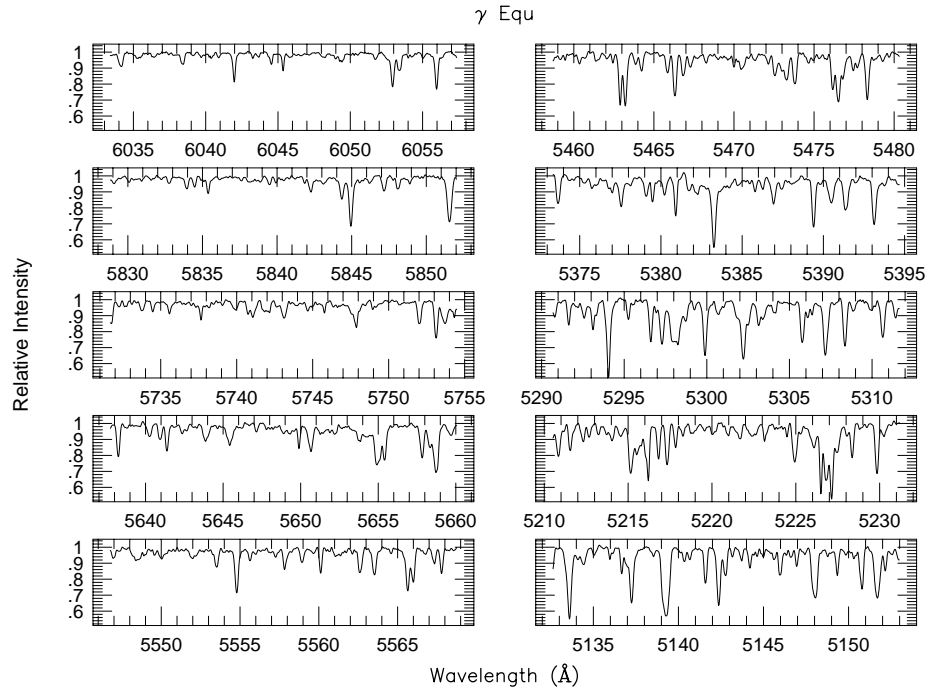


Fig. 5.1.— On this figure we show the part of the spectrum of γ Equulei which was accessible to us with our instrument. Due to small size of our detector we do not have complete wavelength coverage.

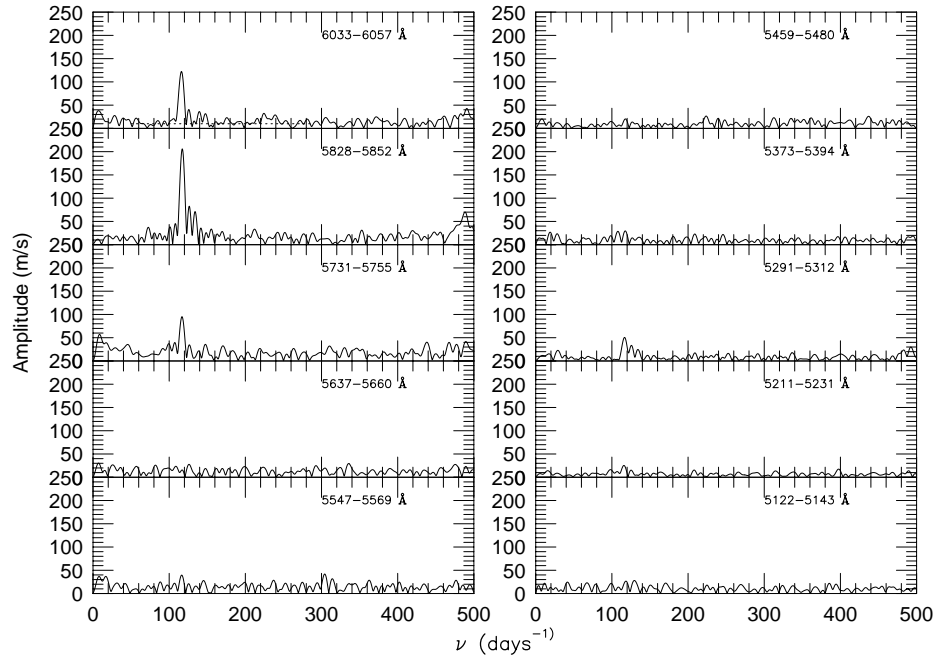


Fig. 5.2.— The Fourier transforms at each spectral order is shown on this figure. All boxes have the same scale. This is the first clear proof of our point: different spectral regions do have different velocities.

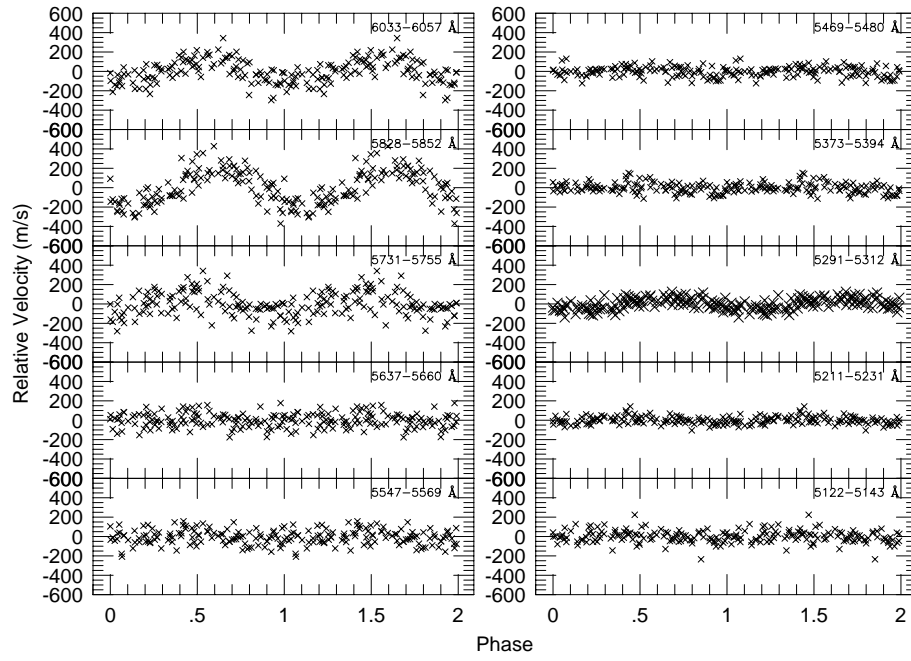


Fig. 5.3.— The phase diagrams for the radial velocity measurements on each spectral order.

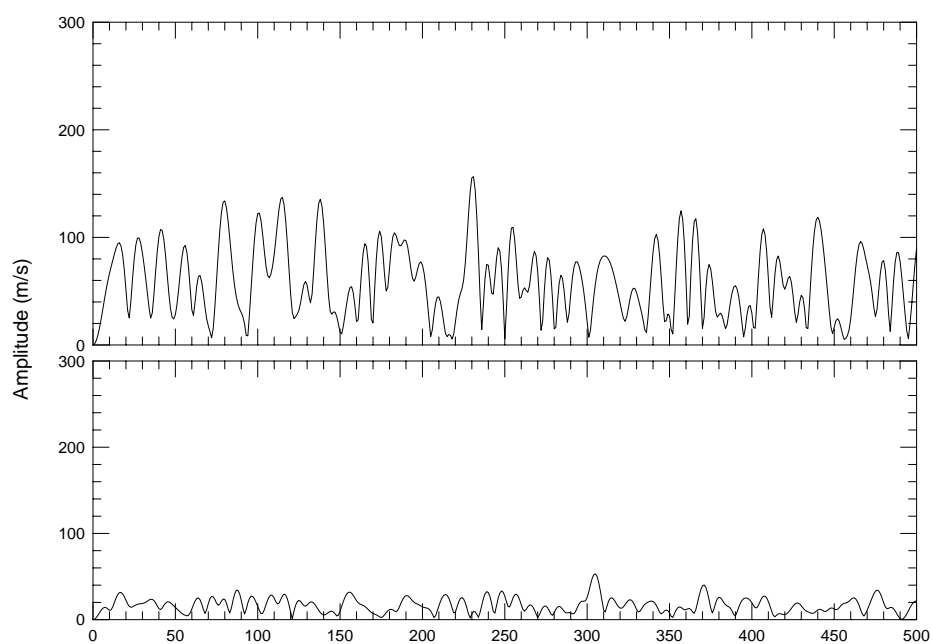


Fig. 5.4.— Fourier transforms for two iron lines. Iron 5555.00 and iron 5295.20. Note the big difference in the noise between each.

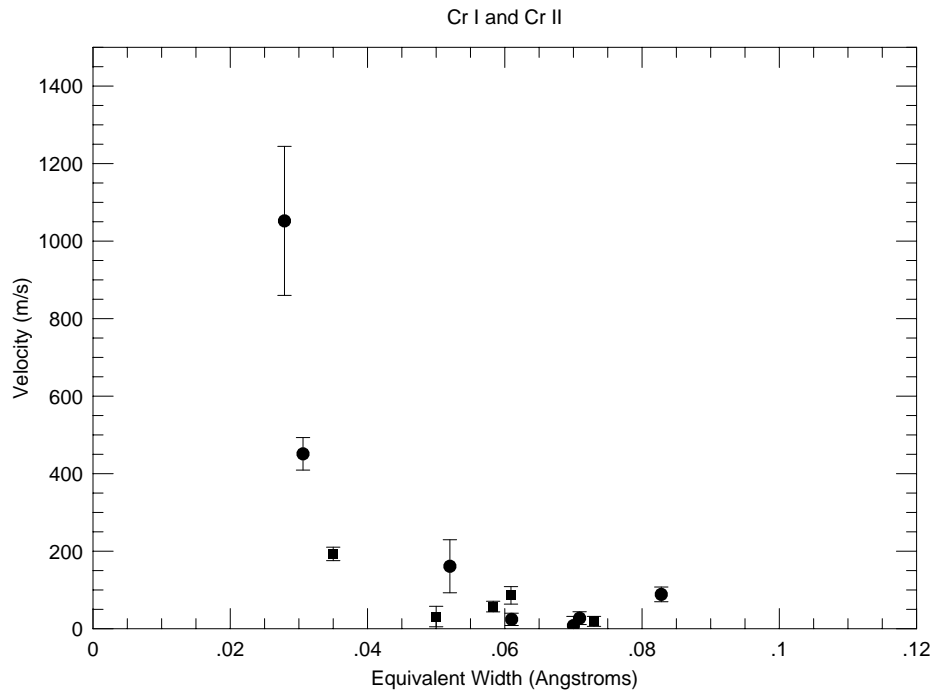


Fig. 5.5.— The amplitudes of all unblended CrI and CrII lines as a function of equivalent width. The filled are circles are lines of CrI. The open circles are lines of CrII.

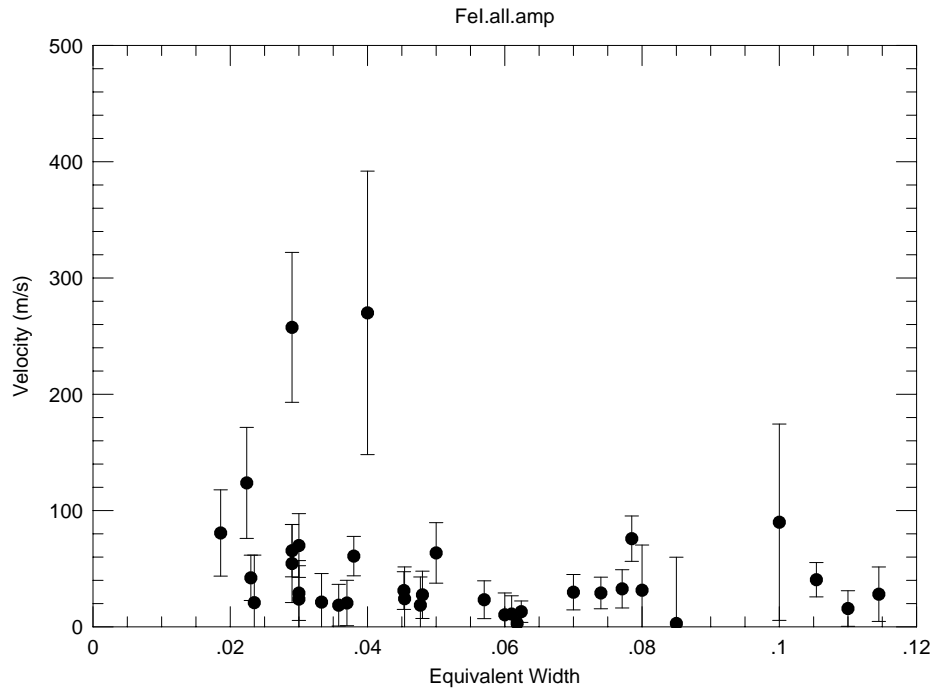


Fig. 5.6.— The amplitudes of all unblended FeI lines as a function of equivalent width.

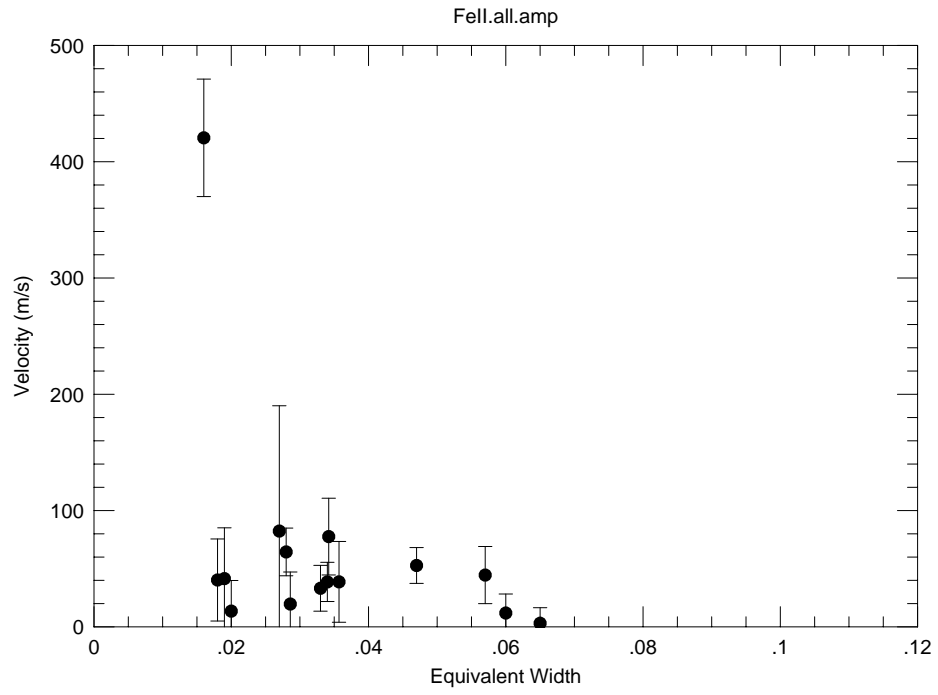


Fig. 5.7.— The amplitudes of all unblended FeII lines as a function of equivalent width.

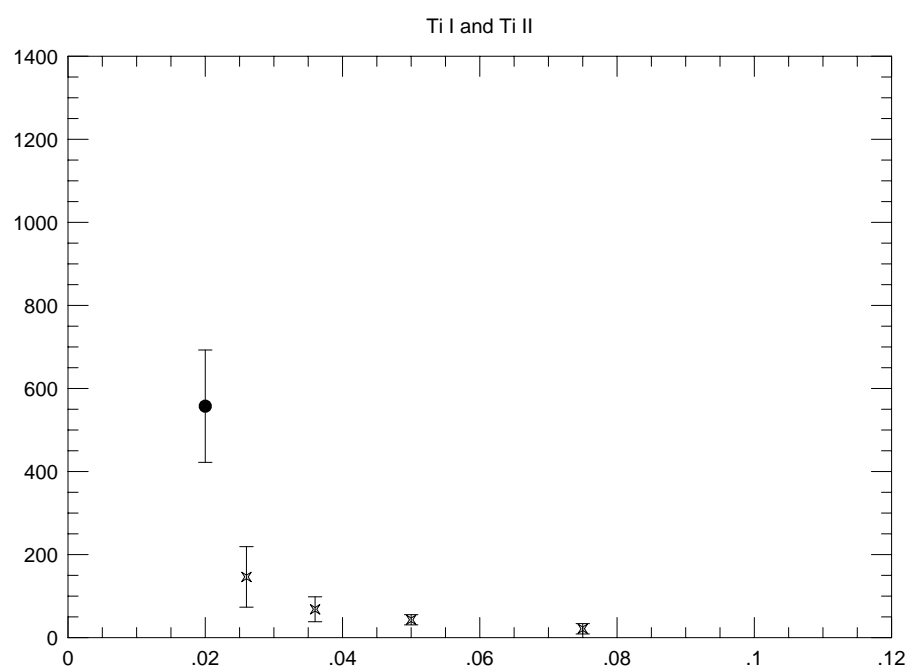


Fig. 5.8.— The amplitudes of all unblended TiI and TiII lines as a function of equivalent width.

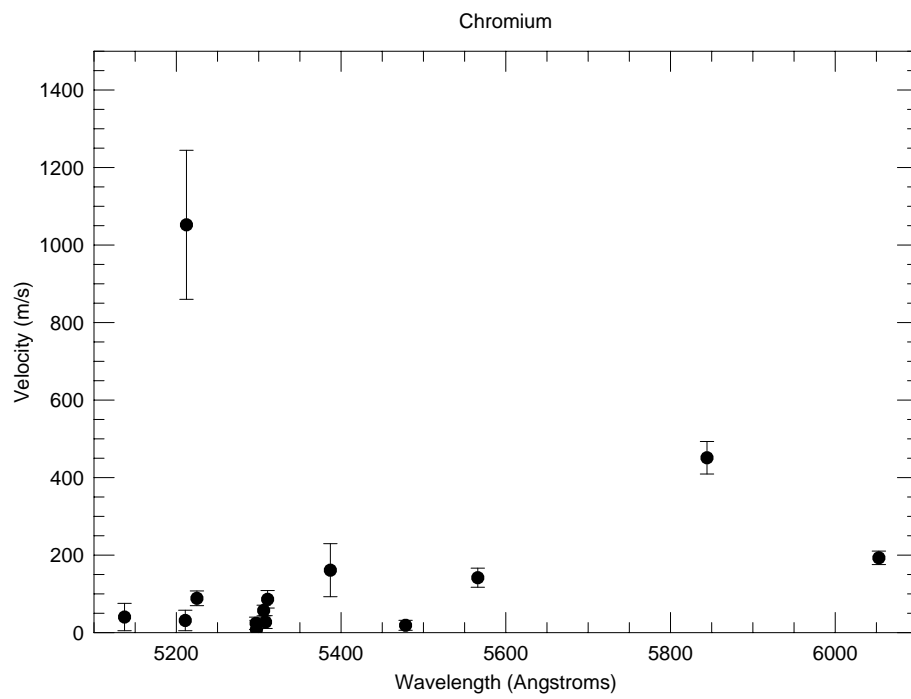


Fig. 5.9.— The amplitudes of all unblended CrI and CrII lines as a function of wavelength.

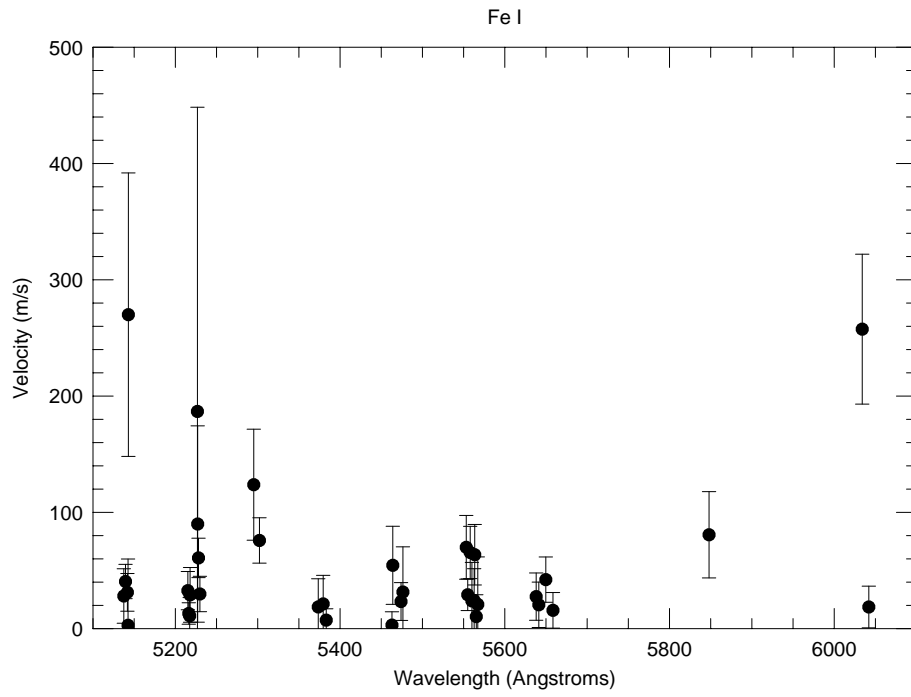


Fig. 5.10.— The amplitudes of all unblended FeI lines as a function of wavelength.

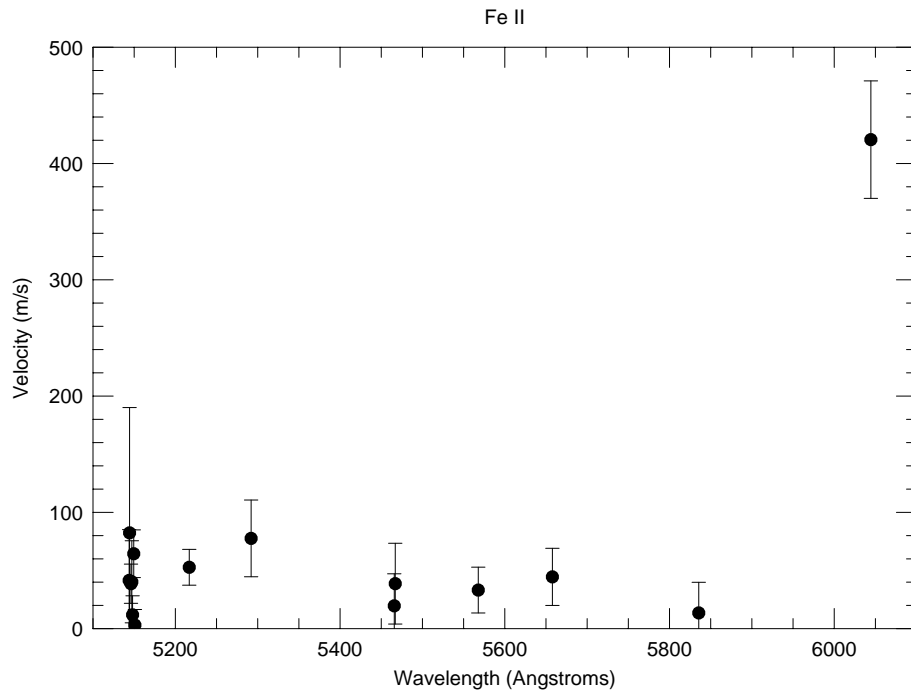


Fig. 5.11.— The amplitudes of all unblended FeII lines as a function of wavelength.

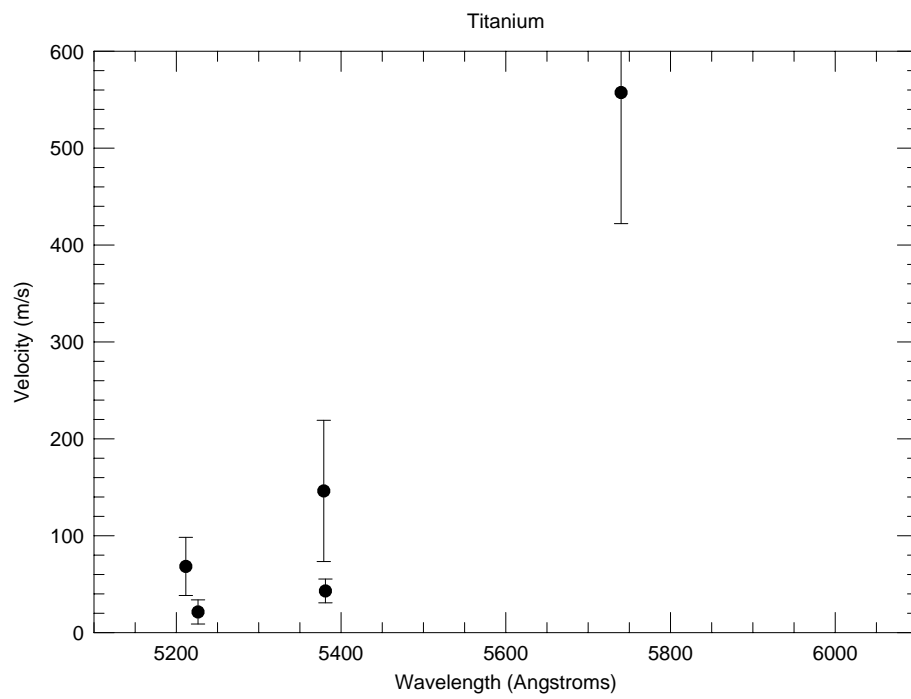


Fig. 5.12.— The amplitudes of all unblended TiI and TiII lines as a function of wavelength.

Chapter 6

A Proposed Test of Models for the Origin of Magnetic White Dwarf Stars

1. Introduction

The origin of magnetic fields in white dwarf stars has been an unsolved problem for several decades. As we believe white dwarfs to be a very uniform class of stars — in the sense of having the same physical characteristics, not life histories — it is hard to imagine how some of these objects can have fields stronger than 10^6 G while the majority does not show any field up to $10^3 - 10^5$ G, a limit which depends on the sensitivity of the survey done to study them. It is a general belief that white dwarfs with strong magnetic fields do not have any additional special characteristic distinguishing them from other white dwarfs. They are found at almost any spectral types (Schmidt and Smith, 1995), temperatures and masses typical of white dwarfs, having some skew towards more massive objects ¹ (Liebert, 1988).

These characteristics are very different from magnetic main sequence stars. On the main sequence magnetic fields come in very well defined groups.

¹I will come back to question this in section 5

All the magnetic main sequence stars are upper main sequence stars. It is true though that among the A and B stars we do find magnetic stars and still do not know what distinguishes them from the other non magnetic A stars. Magnetic fields have also been advocated for cool spotted main sequence stars. We have inferred the presence of spots on those stars but have not yet measured a magnetic field associated with those spots (Borra et al, 1984).

The origin of these strong fields is a mystery. Are they primordial or are they self-generated? As discussed in the literature, models for self-generated fields always encounter some fundamental difficulty and invariably have some prediction in contradiction with observations. The typical decay time for magnetic fields in white dwarfs is of the order of 10^{10} years (Wendell et al, 1987), this is one of the main reasons why fossil fields are a popular explanation for the fields in white dwarfs.

In 1981 Angel made an important connection which will be the subject of this chapter. He realized that, if one assumes conservation of magnetic flux, the magnetic fields of white dwarfs are consistent with the magnetic fields of main sequence stars. That is, if an Ap star contracted to the size of a white dwarf then its magnetic field would be amplified by a factor of $(R_{\text{Ap}}/R_{\text{WD}})^2$, which is roughly 10^4 . Given that Ap stars magnetic fields range from 10^2 G to 10^4 G this agrees nicely with the range of magnetic fields we encounter on the magnetic white dwarfs: 10^6 G to 10^9 G. Angel also noted that the spatial density of magnetic white dwarfs is about the same as we expect for the remnants of Ap stars — assuming a constant star formation rate in the last 10 Gyr.

If their hypothesis is correct it will have some impact on our

understanding of white dwarf formation. All magnetic white dwarfs being formed from very similar stars and yet displaying a wide range of masses and spectral types.

2. Our Method

We have devised an observational project to test if the magnetic white dwarfs descend from Ap stars. The idea is a very simple test using star clusters. Star clusters whose main-sequence turnoff point is above the region where Ap stars lie should contain no magnetic white dwarfs. Star clusters whose turnoff point is below the region where the Ap stars lie should have some magnetic white dwarfs. If that is not the case we have proved that the fossil field hypothesis is not correct. If after having observed many stars we only find magnetic white dwarfs among the older clusters then we have gathered strong evidence supporting the fossil field hypothesis. One conspiracy may play against us. Suppose the magnetic fields of white dwarfs are developed some time after the main sequence. Now suppose these fields only develop in stars whose main sequence mass was in the same mass range as the Ap stars. The only way to check this very contrived possibility would be searching for magnetic fields in the intermediate phases, that is, the red giant and planetary nebula phases. We dismiss that possibility for now. If we find that the magnetic white dwarfs originate from stars occupying the same region on the HR diagram as the Ap stars, then we will examine the possibility of that being a coincidence instead of having a causal relation.

We can actually do better than just a binary test as proposed in the previous paragraph. We do have a good idea of cooling times for white dwarfs

so we can actually map any particular white dwarf back to a narrow range of possible main sequence progenitors. By taking advantage of that we can use any star cluster for our tests and then decide what part of the white dwarf cooling track corresponds to main sequence stars which are in the A spectral type vicinity. If there is any correlation between white dwarf magnetism and some other region of the main sequence this will also be evident in our data.

Thompson and Duncan (1993) have proposed that while in the red giant phase magnetic fields can be created. They suggest that a dynamo operating in the convective core of a red giant will create an observable magnetic field only if the convective core encompasses the material which will be at the white dwarf surface. They find this to happen only for stars with masses above $3 M_{\odot}$. Given the luminosity function for the main-sequence this implies that approximately 5% of all white dwarfs should be magnetic, a number consistent with the observed 4%. According to this model every white dwarf in young clusters should be magnetic, a very strong prediction which will be easily testable.

3. Feasibility

How many stars do we need to observe to reach a significant conclusion? The ratio of magnetic/non-magnetic white dwarfs is close to 4%. The ratio of magnetic A to non-magnetic A stars is close to 10% (Wolff, 1983). We will have our white dwarf sample divided in two, one where no magnetic stars should be found if the fossil field hypothesis is correct. The other sample for the clusters where the Ap stars have already evolved and therefore we expect to find a fraction of about 4% magnetic white dwarfs. Now let us suppose

that the magnetic fields in white dwarfs are not fossil fields. That being the case we should find magnetic white dwarfs in both samples, that is the one including and the one not including Ap star descendants. The question then is: what is the probability of choosing a sample of N stars (where only 4% are magnetic) and not finding any magnetic star (therefore having the impression that no magnetic stars are present in that group). This is a trivial case of the binomial distribution and we find $P = 0.96^N$. For $N=60$, $P < 10\%$, to reach $P < 1\%$ we need $N=120$. On the other hand, selecting white dwarfs who must be descendants from A type stars we expect 10% of them to be magnetic.

We plan to observe 60 stars in one sample and 60 in the other. First of all let us ask ourselves how many do we have. 53 white dwarfs are currently known in star clusters close enough for the faintest white dwarf to be observable spectroscopically — $m_V < 22$. Spectra and/or circular polarization measurements are available for 19 stars, in the Praesepe or in the Hyades. The available spectra for the other stars are too noisy to look for Zeeman splitting. For these stars we need to obtain medium resolution (8\AA per pixel) and medium signal-to-noise (> 30) spectra to be able to detect the Zeeman triplets whenever they exist. On table 6.1 we show all of the known white dwarfs in clusters.

All these objects account for a little less than half the total we need. We need then to find more objects. Our strategy involves three main components:

- 1) Finding blue objects in clusters. To avoid confusion with other blue objects we select only clusters of low galactic latitude, $b < 10$, insuring obscuration by the Galaxy will make more distant objects invisible. Foreground blue objects will be present, but in many cases will be discarded even before a

spectrum is taken because of their excessive brightness. We will be using the primary focus camera at McDonald Observatory and the Schmidt telescope at Cerro Tololo to do this part of the project. U and R frames are all we need to select blue objects. This exact same technique has been used in the past by Romanishin and Angel (1980) and Koester and Reimers (1994) in their series of papers have found spectroscopically that approximately 50% of the selected blue objects are white dwarfs.

2) Finding white dwarfs among the blue objects. Once we have a big sample of blue objects we will then start taking spectra of each candidate to decide whether they are white dwarfs or not. These spectra can be of very low resolution (35\AA per pixel) and signal-to-noise (4). This is feasible on a 2m class telescope — with a reliable pointing and guiding system.

3) Finding magnetic white dwarfs among the white dwarfs. Zeeman splitting is approximately 20 \AA at H_α and 10 \AA at H_β for a field strength of 1 MG. A dispersion of 8\AA per pixel and signal-to-noise ratio of 30 would be enough for detecting a 2 MG field. On figure 6.1 we show the spectrum of the magnetic white dwarf EG 61 ($B=2\text{MG}$) at a dispersion of 8.6\AA per pixel. We degraded the spectrum from its original signal-to-noise of 100 to 50, 30 and 20. Down to $S/N = 30$ the signature of a magnetic field is still easy to recognize. To further prove that a S/N of 30 is sufficient for this purpose we then plotted the spectra of three stars all at the same dispersion (8.6 \AA) and S/N (30). These stars are, EG 61 (21,000 K / $0.9 M_\odot$), GD 31 (16,600 K / $1.0 M_\odot$) and 40 Eri B (16,000 K / $0.4 M_\odot$). The spectrum of the magnetic star is significantly different, the main difference being that the bottom of the hydrogen lines is flat. The massive GD 31 display broad lines compared to the

low mass 40 Eri B but the line core is still very well defined unlike EG 61.

Will we ever find that many white dwarfs in clusters?

Yes but they will be fainter and fainter as we have to start looking at more distant clusters. We show on tables 6.2 and 6.3 the next clusters we will observe in search of white dwarfs. For the first sample we do have a good luminosity function and can compute the expected number of evolved stars between the main sequence turnoff point and $6 M_{\odot}$. $6 M_{\odot}$ is used as a lower limit for the mass of the most massive main sequence star which may turn into a white dwarf. Using $6 M_{\odot}$ instead of higher values gives a lower limit for the number of evolved stars in the cluster which may already be white dwarfs. To really get the expected number of white dwarfs in the cluster we still need to take into account the post main sequence lifetime of each of these evolved stars. Here as a lower limit we argue that half of the evolved stars should have turned into white dwarfs. Therefore for this first sample we expect to find at least 45 new white dwarfs. If we assume the other sample of clusters is not too different from the first then at least another 30 stars should be found. These new 75 stars added to the known 53 stars is more than the 120 we need.

4. First Results

We have set out to find new white dwarfs in clusters as well as doing spectroscopy of the known ones. Our luck with the weather has been terrible on the photometric front, and no new white dwarf candidates have yet been found. On the spectroscopic front Chuck Claver and James Liebert obtained spectra of the Praesepe white dwarfs using the Steward Observatory Multiple

Mirror Telescope (MMT). And, low and behold, found one magnetic white dwarf of which I show a spectrum next (see figure 6.3). The original spectrum was taken with a dispersion of 1.2\AA per pixel and I have rebinned it to 8.4\AA per pixel.

What do we learn from this observation?

The Praesepe turnoff point is at $2.2M_{\odot}$ (van den Berg, 1990). Ap stars are found on the main sequence with masses ranging from 2 to $3 M_{\odot}$. Precise determination of temperature and mass for this star has not yet been done based on our data. We use next the mass and temperature determinations from Reid (1996). Assuming EG 61 to have the same radial velocity as the average velocity of the cluster, Reid then measures the redshift of the H_{α} line and finds a mass of $0.912 \pm 0.020 M_{\odot}$. A temperature of around 21,000 K can be derived from the B-V photometric index. According to Wood (1990) these numbers imply in an age between 180 to 230 Myrs, depending on what core composition (O, C/O, C) is assumed. The Praesepe has an estimated age around 1.0 Gyr (Claver, 1994, van den Berg, 1990). Therefore this star has had a pre-white dwarf lifetime of 0.8 Gyr. This corresponds to the lifetime of stars between 2 and $3 M_{\odot}$ (Cox & Giuli, 1968). The mass range where the Ap stars are most frequent.

A word of caution is in order here. The gravitational redshift mass of Reid has probably been underestimated. At strong magnetic fields ($> 1 \text{ MG}$) even the central components of a triplet are shifted (the π lines), not only the two satellite lines (the σ components). Using the tables of Wunner et al (1985) it can be seen that a 2 MG field, like the one in EG 61, displaces the central component of H_{α} (the $3p0-2s0$ transition) by 0.085\AA towards the

blue. Correcting the value of Reid for the gravitational redshift ($62.5 \text{ km/s} + 3.9 \text{ km/s}$) and using the same radius quoted by him increases the estimated mass to $0.96 M_{\odot}$.

From preliminary analysis of the data on the Praesepe white dwarfs, it is evident that one of them (WD 0836+201) is a low mass star while the other stars seem to have a normal mass (around $0.6 M_{\odot}$). It is tempting to speculate on the possible effect the magnetic field may have on the mechanisms of mass loss. As this star is the only massive white dwarf in this cluster it may be that strong magnetic fields inhibit the mass loss mechanism. However, in a cluster like the Hyades, with roughly the same age as the Praesepe other massive white dwarfs are found and none of them are magnetic. It is also true that massive white dwarfs are slightly more abundant among magnetic white dwarfs than among normal white dwarfs. There is a weak correlation between white dwarf mass and progenitor mass as can be seen from the mass distribution of white dwarfs found in young open clusters. This, and the fact that magnetic white dwarfs tend to be more massive than non-magnetic white dwarfs, has led investigators to propose that magnetic white dwarfs are descendants of massive main sequence stars, in agreement with Thompson and Duncan models. EG 61 comes from an intermediate mass main sequence progenitor and is therefore more consistent with the idea of mass loss inhibition than descendance from massive stars. Finding more magnetic white dwarfs in clusters will answer this question in a definite way.

5. A Closer Look at the Distribution of Magnetic White Dwarfs

We now return to the point alluded to in the footnote in the beginning of this chapter. Figure 6.4 shows the field intensities as a function of T_{eff} for all the magnetic white dwarfs for which a temperature is available. A quick inspection of this plot will convince anyone that the previous statement saying magnetism does not correlate with any physical characteristic is not real. We know this may be a little dangerous to say given the small numbers we are dealing with, however, we now know the temperature of 36 magnetic white dwarfs and this plot is at least intriguing.

For $T_{\text{eff}} < 16,000$ K many stars with $B > 100$ MG are found. For temperatures higher than that only one star has such a strong field. A simple statistical test helps to evaluate the significance of this excess of objects with strong fields. To make the counting of objects we now plot \mathbf{B} on a log scale (figure 6.5). Very few objects are found at field strengths lower than 10 MG. This is most probably a selection effect because strong magnetic fields are easier to find than weak ones. Counting the number of stars with fields between 10 and 100 MG and then with fields between 100 and 1,000 MG we will see that for temperatures below 16,000 K there are 10 of each. For temperatures above 16,000 K there are 7 below 100 MG and only one above 100 MG. What is the probability of finding only one strong field star above 16,000 K if the hotter stars follow the same distribution as the cooler ones? This is yet another case of the binomial distribution:

$$P(1) = \binom{8}{1} (0.5)^1 (1 - 0.5)^7 \simeq 3.1\%$$

which is a very small number indeed. However, it only means that this distribution is very unlikely to happen by chance. What could cause it then?

The first important point to stress here is that of all magnetic white dwarfs only the ones from Schmidt and Smith survey come from a uniform set of stars. They observed all DA stars brighter than 15th magnitude from subclass 8 to 2 (the subclass being defined as the ratio $T/5040$). DA9 stars were not observed because their hydrogen lines are too weak. Many other magnetic white dwarfs are identified in classification spectra. Very strong magnetic fields disturb the hydrogen lines so much that sometimes recognizing the spectrum as belonging to a DA is a hard task. It is easier if the hydrogen lines are strong but harder as they become weaker. This might be the explanation. Because most of the strong field stars are seen at the temperatures where the hydrogen lines are at a maximum. However, the most probable effect of washing out the hydrogen lines with a strong magnetic field is to make a DA look like a DC (featureless continuum spectrum), and we do not know of any DC stars at temperatures above 13,000 K.

It is hard to imagine what selection effect may lead to the observed distribution of B with T_{eff} . However, it is easy to think that this distribution may be caused by one. The only way to really answer this question is by observing a large, magnitude limited, sample of white dwarfs, with no preference for spectral types.

An obvious correlation between what is seen in this distribution and the physics we know is that the peak field intensities happen exactly where convection begins. This may be a clue to the understanding of this. It is also true that at lower temperatures, where convection is even stronger the fields are not as intense as around the temperature of 15,000 K. It is also important to remark that weaker fields are equally as likely as strong ones in the vicinity

of 15,000 K. Therefore, all we can say is (if this distribution turns out to be real) is that strong fields are more likely in this temperature range than in others.

6. Other Connections

When this project is concluded we will know whether or not the magnetic fields of white dwarfs are fossil. However, what do we know about the the origin of magnetic fields of Ap stars? Nothing.

We here outline an observational project, on the same lines as for the white dwarfs, to try to determine when Ap stars develop their magnetic fields.

Abt (1979) and Abt and Cardona (1983) have collected strong evidence that the Ap phenomenon is related to stellar age. The authors have first observed open clusters of varied ages and found that the fraction Ap/A stars increases with the group's ages reaching the same value as among the field stars at an age of 10^8 years. To further test this hypothesis they then studied A stars in binary systems. They found that the ratio Ap/A is larger for binaries composed of A + cool star than for binaries composed of A + hot star. Their idea being that the A + hot systems, on average, have to be younger than the A + cool systems. Subsequent investigations have cast doubt on many of Abt's results (see *e. g.* North, 1993). However, their method of identification of Ap stars is not as reliable as Abt's. Abt has identified Ap stars based on high resolution spectroscopy. North and the others have used the $\lambda 5200$ depression as an indicator of peculiarity as well as magnetic field strength. In order to identify a star as Ap they use Geneva photometric indices to isolate the peculiar

stars in color-color diagrams. While this is an ingenious method it may also be dangerous because i) borderline cases between normalcy and peculiarity are hard to distinguish even spectroscopically; ii) differential reddening (known to happen) may affect the color-diagrams. For entertainment we will in the next paragraphs assume Abt to be right. Then we will come back and propose observations to decide who is right.

It is widely accepted that magnetic fields play an important role in the rise of chemical peculiarities on Ap stars, for the simple reason that whenever we see the latter we see the former. We want to know whether these stars have had a magnetic field since they were formed and diffusion worked slowly making the peculiar abundances arise as the stars sat on the main sequence or, was the magnetic field generated during the main sequence phase and the rare earths were quickly carried to the surface by diffusion? We propose a simple test to answer this question.

We must survey all A stars, normal and peculiar, in the clusters studied by Abt for the presence of magnetic fields. If the ratio magnetic-A/nonmagnetic-A shows the same rise as the ratio Ap/A shows with increasing age then we know that the magnetic fields are turned on during the main sequence phase and, that diffusion is a quick process. If the ratio magnetic-A/nonmagnetic-A turns out to be constant (and high) in time we know that the stars already have a magnetic field when they reach the main sequence, implying diffusion is a slow process. Of course these are two of the simplest outcomes, it is conceivable that the distribution of magnetism does not follow any nice distribution and we will be left to scratch our heads trying to make up new models to make some order out of chaos.

Using modern multi-fiber spectrographs we can redo all the observations previously done by Abt and by Cramers et al in a few nights. Gathering all these data will provide us with an uniform set of data on all these clusters. This would once and for all settle the controversy of whether there is an increase in the ratio A_p/A with age, which per se is a very important result. If the ratio A_p/A increases with age then we will search for magnetic fields on all A stars in some of the clusters

6.1. A Few More Ideas

If magnetic fields of Ap stars can be fossilized and kept through the white dwarf stage, why can't the same happen to Ap stars belonging to binary systems? It is our point here that this could well be. And they would of course become one of the two magnetic kinds of cataclysmic variables, either polars, or intermediate polars, depending on the field strength.

Both polars ($B \simeq 1 - 3 \times 10^7$ G) and intermediate polars ($B \simeq 2 - 10 \times 10^6$ G) seem to have fields strengths similar to the field strengths of single white dwarfs. One immediate problem with this picture is the large abundance of polars and intermediate polars compared to normal cataclysmic variables. In Ritter's catalog (1990) there are 17 polars and 13 intermediate polars out of a total of 170, or a fraction a little higher than $1/6$, four times higher than the ratio of magnetic single white dwarfs to nonmagnetic single white dwarfs. This much higher ratio may be a selection effect because the magnetic cataclysmics are much brighter X-ray sources than their counterparts and therefore are detected much more easily in X-ray surveys.

A better test is to compare the space densities of the magnetic cataclismic variables to that of binaries containing an Ap star. We now do not have reliable numbers for either of these densities.

The next step in a more rigorous test is again through the observation of stellar clusters. However, because these are binary systems an additional complication is added. Simply observing two samples of clusters, as in the white dwarf case, is not sufficient. It is possible to have a cluster with a main-sequence turn-off mass at, say $1.8 M_{\odot}$ and have a white dwarf whose progenitor is $4.0 M_{\odot}$ having a $2.5 M_{\odot}$ companion. In this case the white dwarf cannot be descendant from an Ap star. It is also possible (and actually more likely, because of the shape of the mass distribution on the main sequence) to have a white dwarf originated from a $2.8 M_{\odot}$ accompanied by a $2.2 M_{\odot}$ star. Here the white dwarf can be descendant from an Ap star.

We currently know of only one cataclismic variable which may be part of a galactic and this test is far from being a practical one at this point. However, with the possible use of color sensitive detectors in a not too distant future we will be able to perform spectroscopy on objects of magnitudes as faint as 28 using the Hubble Space Telescope. By then the number of clusters available to our eyes will be immensely increased.

7. Conclusion

Among the 53 dwarfs known in star clusters we have 28 that could be remnants of Ap stars. Among these we know for sure that one has a magnetic field of approximately 2 MG, 24 have no magnetic fields stronger than 1 MG, and we

know nothing about the other 3, for which we will need to obtain spectra in the near future.

Another 25 stars cannot be descendants of Ap stars. The available spectra for most of these stars has a very low signal to noise ratio and are not useful for magnetic field detection. We plan to use a 4 m class telescope to obtain spectra on these objects.

The fossil field theory survived our test at this very early stage. Its survival is a positive one in the sense that we found one magnetic star where it was expected, another form of survival would have been finding no magnetic star anywhere. We are confident we will be able in the future not only to answer the question whether the magnetic fields are fossil or not as well as showing, if it exists, any correlation between main sequence original position and white dwarf magnetism.

Table 6.1. White Dwarfs in Clusters.

Name	$\log L/L_{\odot}$	$\log T_{eff}$	Cluster	Turnoff
EG 059			Praesepe	2.0
LB 5893			Praesepe	2.0
LB 1876			Praesepe	2.0
EG 061			Praesepe	2.0
NNW1145			Praesepe	2.0
SE-664			Praesepe	2.0
EG 060			Praesepe	2.0
LB6072			Praesepe	2.0
LB1839			Praesepe	2.0
NNW-13			Praesepe	2.0
LB6037			Praesepe	2.0
EG 026	-2.10	4.21	Hyades	2.0
EG 028	-2.26	4.17	Hyades	2.0
EG 029	-2.44	4.20	Hyades	2.0
EG 030	-2.15	4.16	Hyades	2.0
EG 031	-1.52	4.34	Hyades	2.0
EG 036	-1.88	4.32	Hyades	2.0
EG 037	-1.36	4.42	Hyades	2.0
EG 039	-1.66	4.34	Hyades	2.0
EG 042	-1.15	4.47	Hyades	2.0
EG 076	-2.04	4.21	Hyades	2.0

Table 6.1—Continued

Name	$\log L/L_{\odot}$	$\log T_{eff}$	Cluster	Turnoff
EG 079	-3.17	3.94	Hyades	2.0
EG 139	-1.49	4.36	Hyades	2.0
LP475-242	-2.29	4.20	Hyades	2.0
EG 025	-1.05	4.66	Pleiades	5.0
SiriusB	-1.25	4.51	Sirius	3.0
EG 130	-2.34	4.16	Sirius	3.0
EG 131	-2.26	4.28	Sirius	3.0
EG 162	-2.47	4.17	Sirius	3.0
EG 050	-1.46	4.40	61 Cyg	1.0
EG 145	-2.12	4.15	61 Cyg	1.0
EG 178	-3.54	3.73	61 Cyg	1.0
EG 135	-3.33	4.05	γ Leo	1.0
2			NGC2287	3.9
3			NGC2287	3.9
5			NGC2287	3.9
1			NGC2422	5.0
1		4.47	NGC2516	4.8
2		4.56	NGC2516	4.8
5		4.53	NGC2516	4.8
1		4.20	IC2391	5.8
1		4.20	NGC2451	5.8

Table 6.1—Continued

Name	$\log L/L_{\odot}$	$\log T_{eff}$	Cluster	Turnoff
		4.17	NGC2451	5.8
6		4.49	NGC2451	5.8
1		3.98	NGC2168	5.3
3		4.57	NGC2168	5.3
4		4.64	NGC2168	5.3
1		4.45	NGC3532	4.0
5		4.45	NGC3532	4.0
6		4.45	NGC3532	4.0
8		4.38	NGC3532	4.0
6		4.46	NGC3532	4.0
6		4.25	NGC3532	4.0

Table 6.2. Clusters to be observed I

Cluster	Age (Myr)	RA	Dec	Size (')	dm	Nev.	$m_{V_{fd}}$	U	R
NGC1342	302.00	0331.7	3720	14.0	8.7	11	20.6	1.25	36
NGC1647	213.80	0446.0	1905	45.0	8.7	3	20.4	1.25	36
NGC1662	302.00	0448.4	1056	20.0	8.0	3	19.9	0.50	15
NGC2168	107.15	0608.8	2420	28.0	9.7	18	21.2	2.00	36
NGC2301	107.15	0651.8	0029	12.0	9.4	3	20.9	1.25	36
NGC6633	660.69	1827.7	0634	27.0	7.5	5	19.9	0.50	15
NGC6940	1096.48	2034.6	2819	31.0	9.5	45	22.0	3.20	36
NGC7243	107.15	2215.3	4953	21.0	9.7	4	21.2	2.00	36

Note. — dm is the cluster's distance modulus. Nev. is the number of evolved stars in the cluster. $m_{V_{fd}}$ is the magnitude of the faintest white dwarf expected for a cluster with that age. U and R are the integration times in U and R to detect the faintest white dwarf.

Table 6.3. Clusters to be observed II.

Cluster	Age (Myr)	RA	Dec	Size (')	dm	N_{MS}	$m_{V_{fd}}$	U	R
NGC0559	1258.93	0129.5	6319	4.4	9.8	60	22.6	6.60	72
NGC0752	1096.48	0157.8	3741	49.0	8.0	60	20.7	1.25	36
NGC6811	537.03	1938.2	4634	12.0	9.8	70	21.0	2.00	36
Col0463	151.36	0148.4	7157	36.0	8.9	40	20.5	1.25	36
NGC1039	194.98	0242.0	4247	35.0	8.2	60	20.9	2.00	36
NGC1513	426.58	0410.0	4931	9.0	9.6	50	21.7	2.60	36
NGC6709	77.62	1851.5	1020	13.0	9.9	40	21.4	2.00	36
NGC7039	125.89	2111.2	4539	24.0	9.2	50	20.7	1.00	36
NGC7261	39.81	2220.4	5805	5.0	9.8	30	20.6	1.00	36

Note. — dm is the cluster's distance modulus. N_{MS} is the number of main sequence stars in the cluster. $m_{V_{fd}}$ is the magnitude of the faintest white dwarf expected for a cluster with that age. U and R are the integration times is U and R to detect the faintest white dwarf.

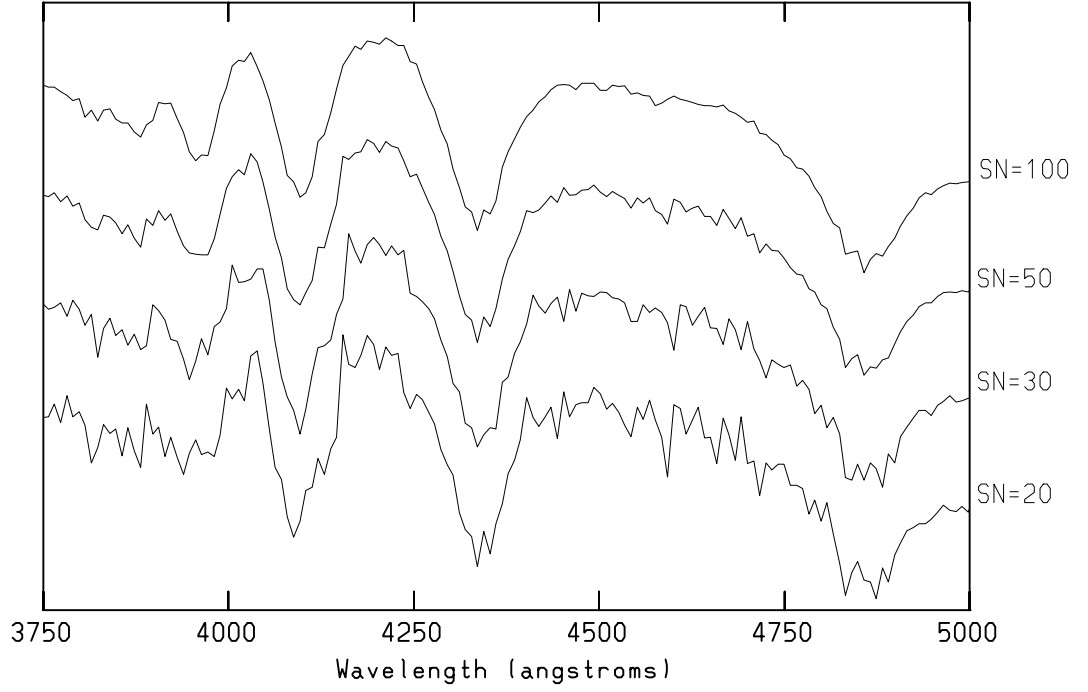


Fig. 6.1.— Spectra of a magnetic white dwarf (2 MG) at different signal-to-noise ratios. All spectra have a dispersion of 8.6\AA per pixel.

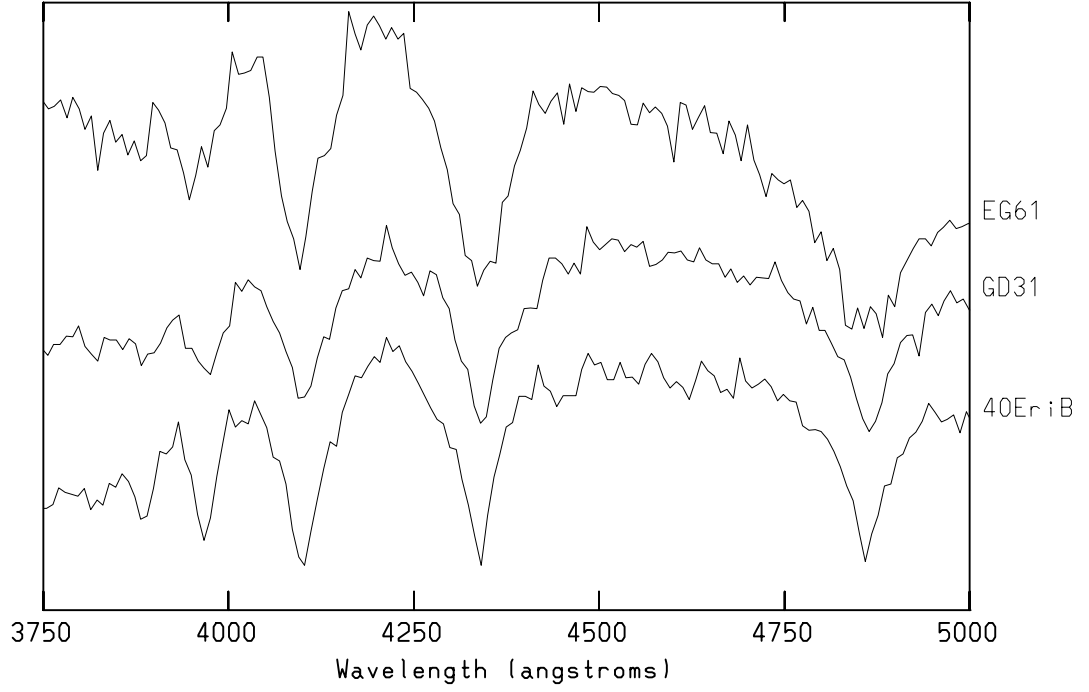


Fig. 6.2.— Spectra of three white dwarfs. 40 Eri is a $0.4 M_{\odot}$ and 16,000 K. GD 31 is $1.0 M_{\odot}$ and at 16,600 K. EG 61 is $0.9 M_{\odot}$ and 21,000 K and has a magnetic field of 2 MG.

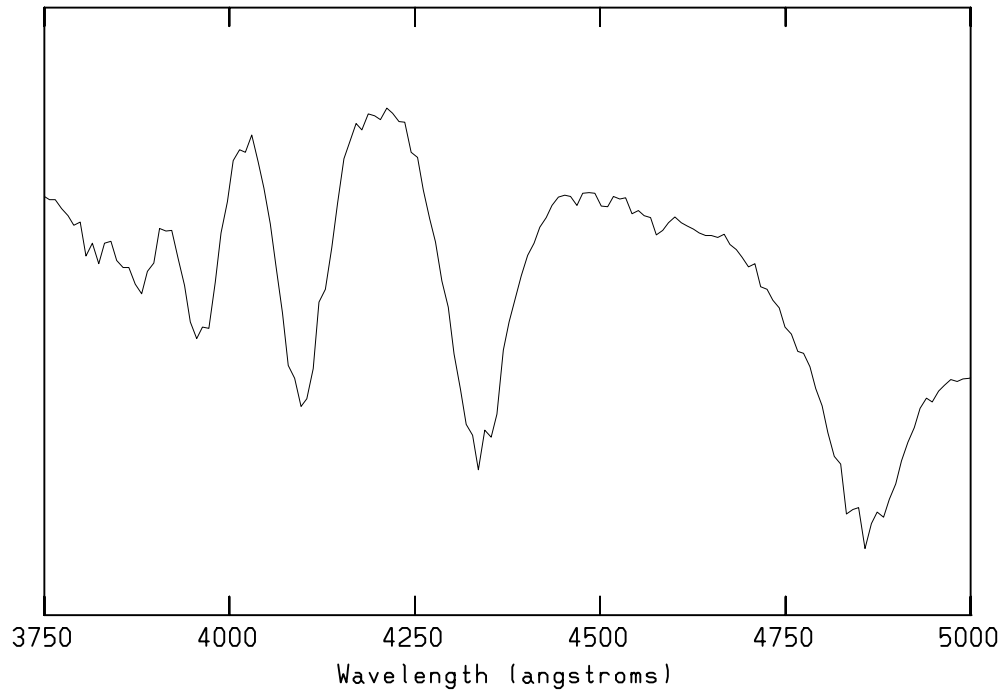


Fig. 6.3.— Spectrum of the recently discovered white dwarf in the Praesepe. A field of 2 MG has been derived for this star from the splitting at the bottom of H_{β} and H_{γ} .

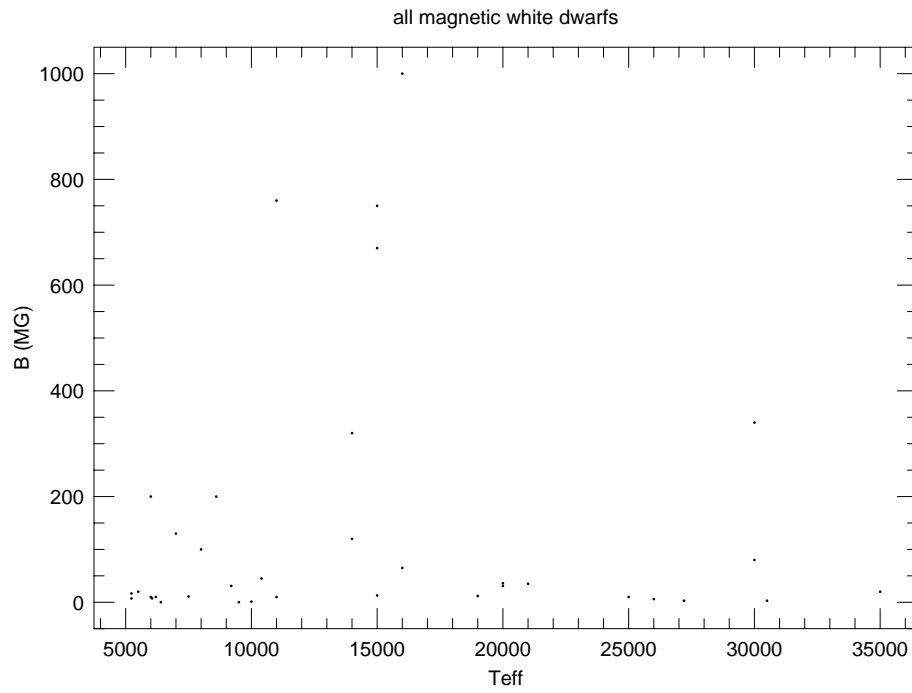


Fig. 6.4.— The distribution of magnetic field strengths as a function of effective temperature.

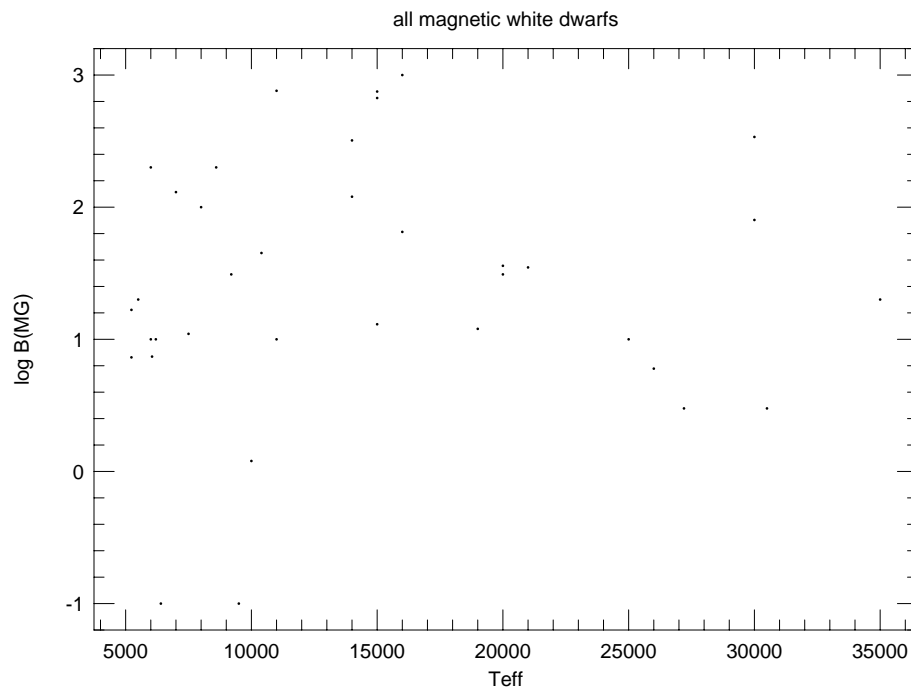


Fig. 6.5.— The distribution of magnetic field strengths as a function of effective temperature (log plot).

Chapter 7

Conclusions

In this work I have approached two fundamental problems with the ZZ Ceti instability strip. First, I have proven that the lack of pulsating stars below the temperature of 11,000 K is real. There are no more doubts of its origin as observational selection effects. In the past there claims that long period variations might simply follow the trend to longer and longer periods and be not undected. My observations using a CCD photometer allow for the constant monitoring of extinction variations by continuously looking at some comparison star in the field of view of the detector. This ability greatly increases the accuracy for longer periods and I was able to demonstrate that none of these objects pulsates with amplitudes larger than 5 mmag and periods longer than 2 hours.

Among the ZZ Ceti stars BPM 37093 is a black sheep. It has a long period and very low amplitude pulsations, unlike all other ZZ Ceti stars where there is a correlation between period and amplitude. Our first conjecture to explain its behavior was that it may be a star reaching the red edge of the instability strip. This would explain the long period, because the thermal scale at the partial ionization zone is long, and the low amplitude would be a consequence of the turning off of the pulsations. Along this work we came to

realize that BPM 37093 has such a high mass that at least some, and maybe most of it, is crystallized. That spurred another idea to pursue. We now have the possibility of studying for the first time the effects of crystallization on a pulsating star. I have already shown that this star has a very different behavior from other pulsating ZZ Ceti stars. We need in the near future, preferably before we observe it again so that we have predictions instead of explanations, to develop better pulsation models which include the effect of a crystallized core in a pulsating star.

This is the first time since crystallization was theoretically “discovered” we have a chance to test the predictions made. In the future with production of better luminosity functions signatures of crystallization will (or not) be seen in the white dwarf luminosity function. BPM 37093 is so far the only object we can, through the use of asteroseismology, hope to test the predictions of crystallization theory on a single star.

The second problem with the ZZ Ceti instability strip is the presence of non-pulsating stars in the same temperature range as the pulsating ones. Not this be a big problem as we see this in all other instability strips. The question is that, because the contamination with non-variables is much lower among the ZZ Ceti stars and because these objects are physically simpler and more homogeneous than the other known pulsating stars, we had a hope to actually find what was the physical characteristic distinguishing the variables from the non-variables. One possibility raised was the presence of magnetic fields in the non-variable stars. I then surveyed 3 of the 4 non-variables and found no magnetic fields in them, down to my detection limit which was 25 kG. In the meantime Schmidt and Smith (1995) published a survey for magnetic fields

among 169 DA stars. Their results also shown that other non-variables do not have magnetic fields with about the same limits as my results. The magnetic fields as supressors of pulsations has now been buried by these works.

Bradley and Winget (1994) produced models showing that the temperature at which a DA star starts pulsating is mass dependent. Bergeron et al. (1995) has presented temperature and mass determination for most ZZ Ceti stars. Their result agrees with Bradley and Winget's prediction, however, the lack of non-pulsating stars in their analysis leaves room for speculation. Giovannini (1996) has observed many variables as well as non-variables and his results are also in agreement with the theoretical predictions. From Giovannini's data it can be seen that there is a nice separation (however not perfect) between variables and non-variables when we make a diagram of mass against temperature. Because most of the non-variables observed by Giovannini are low-mass stars, and only one variable is a low mass star the division between variables and non-variables is not as clear at higher masses ($0.5 M_{\odot}$) where most of the variables are. It will be interesting to see in the future when more non-pulsating stars are added to Giovannini's sample how clean this division remains, and especially how clear the mass-temperature trend in the blue edge is.

One excellent laboratory to study the interactions of magnetic fields with pulsations is the rapidly oscillating Ap stars. I have observed one of these stars using time resolved high resolution spectroscopy and found very puzzling results. There had been a few reports before our observations of different values for the radial velocity modulations caused by pulsations in these objects. We now understand why that was. Different spectral lines

show different modulations. The amplitude of the modulations seems to be anti correlated with the equivalent width of the lines. It is also true that some elements systematically have larger amplitude than others. And it is also apparent that different ionization stages of the same element also have consistently different amplitudes. We offered a qualitative model based on the oblique pulsator model and the effect the Lorentz force has on moving charges. Further testing of our model will have to wait for more data on other roAp stars to be analyzed. And ideally in the near future we will be able to observe one of these objects throughout its rotational cycle.

Finally, I propose an observational program to test unambiguously the validity of the old claim that all magnetic white dwarfs are descendants from the magnetic Ap stars. The first magnetic white dwarf in a cluster has now been found and pursuing this program, I am trying to identify more white dwarfs in several clusters not previously searched for white dwarfs and doing spectroscopy on the known stars to verify whether or not they have a magnetic field.

Appendices

Appendix A

Line Identifications for γ Equulei

In this Appendix I present the line identifications for γ Equulei. Only the lines used for radial velocity measurements are presented.

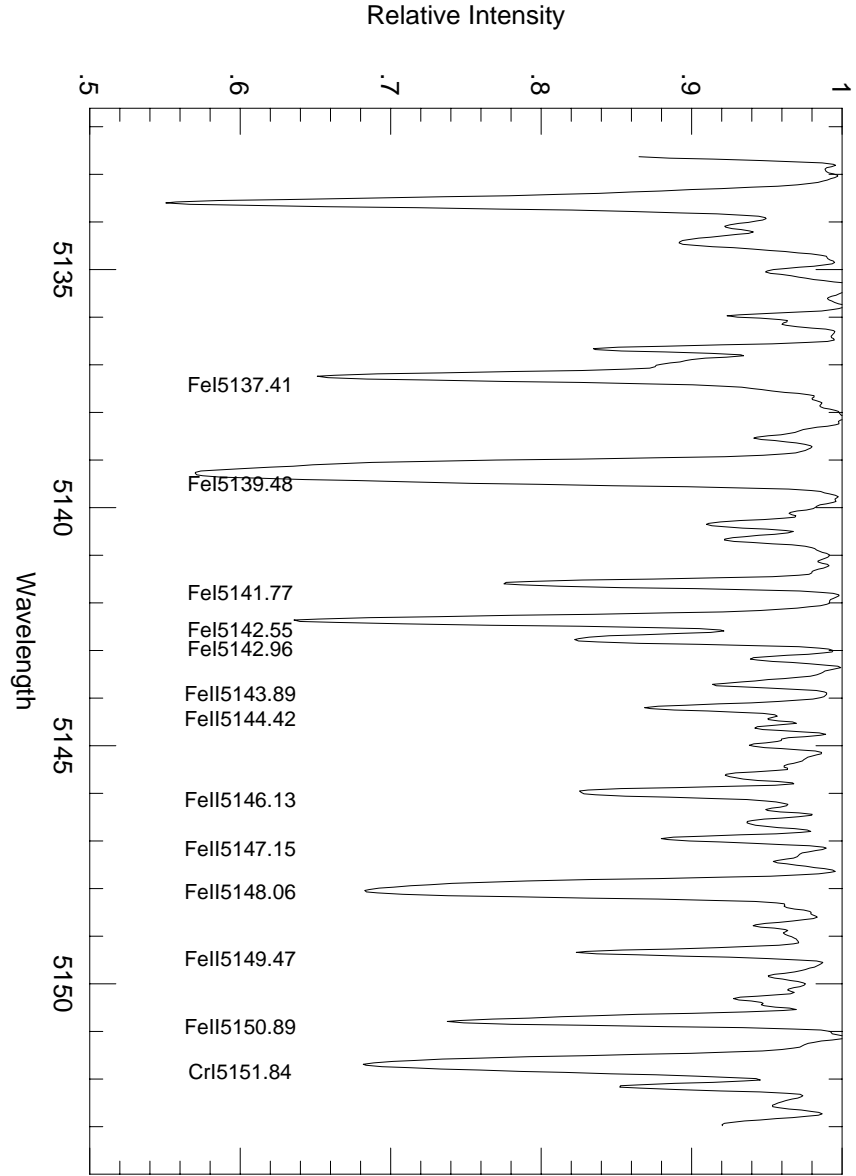


Fig. A.1.— Line identifications in the region from 5132 Å to 5153 Å. In this figure we mark the lines used in our analysis. All of the Fe, Cr and Ti lines studied are marked on the spectra from figure

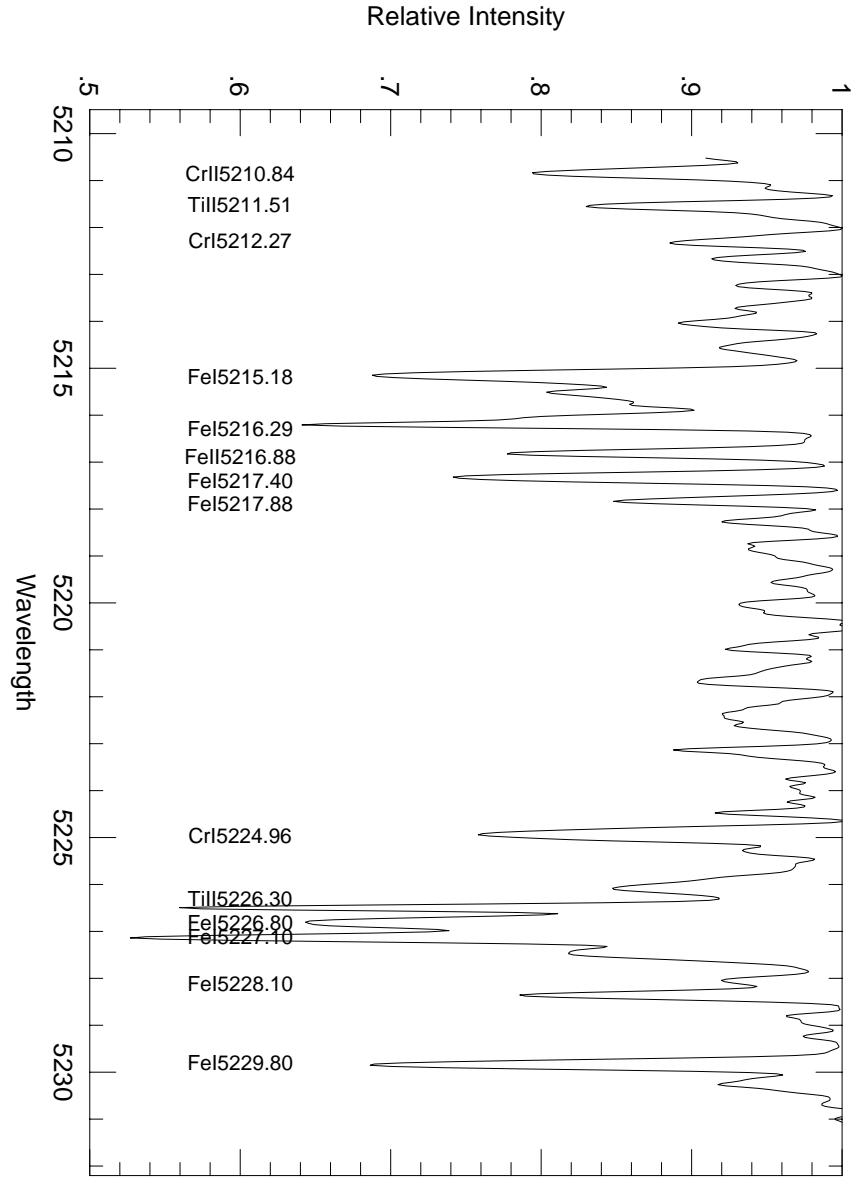


Fig. A.2.— Line identifications in the region from 5210 Å to 5231 Å.

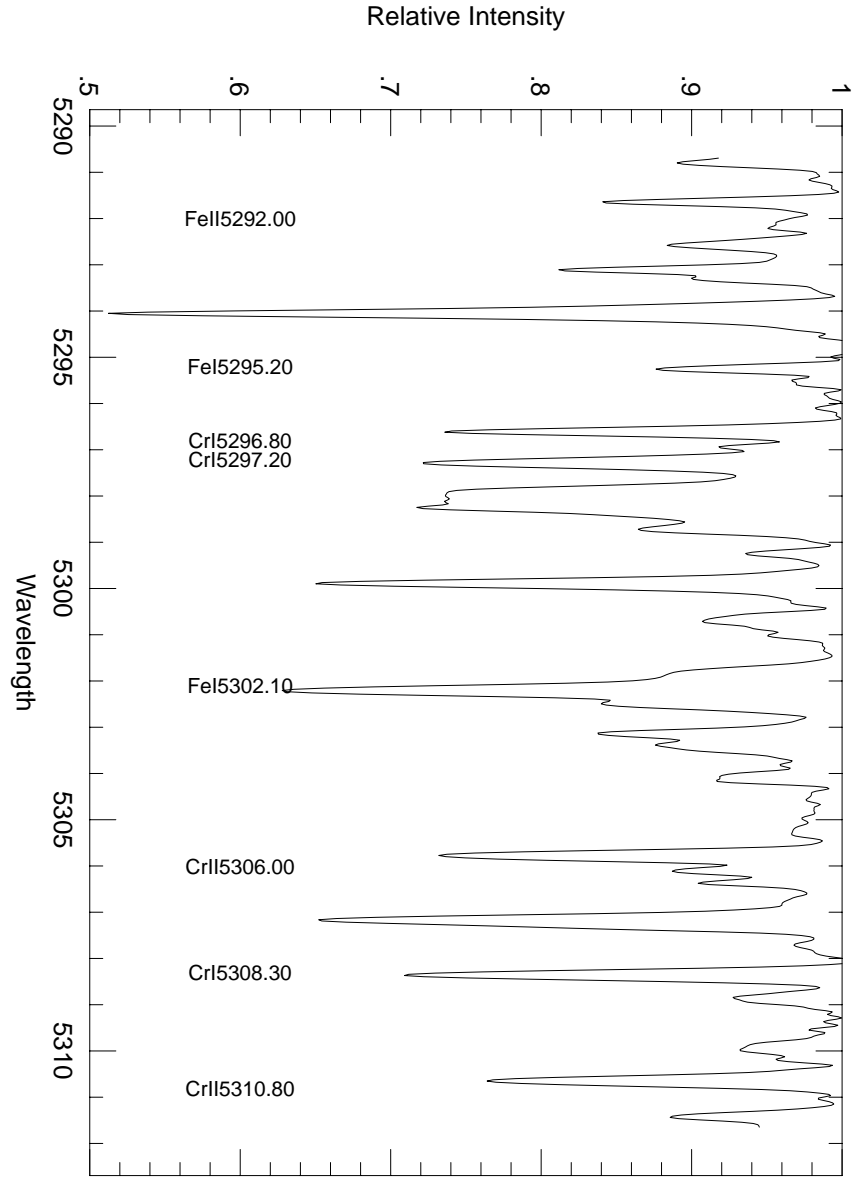


Fig. A.3.— Line identifications in the region from 5290 Å to 5310 Å.

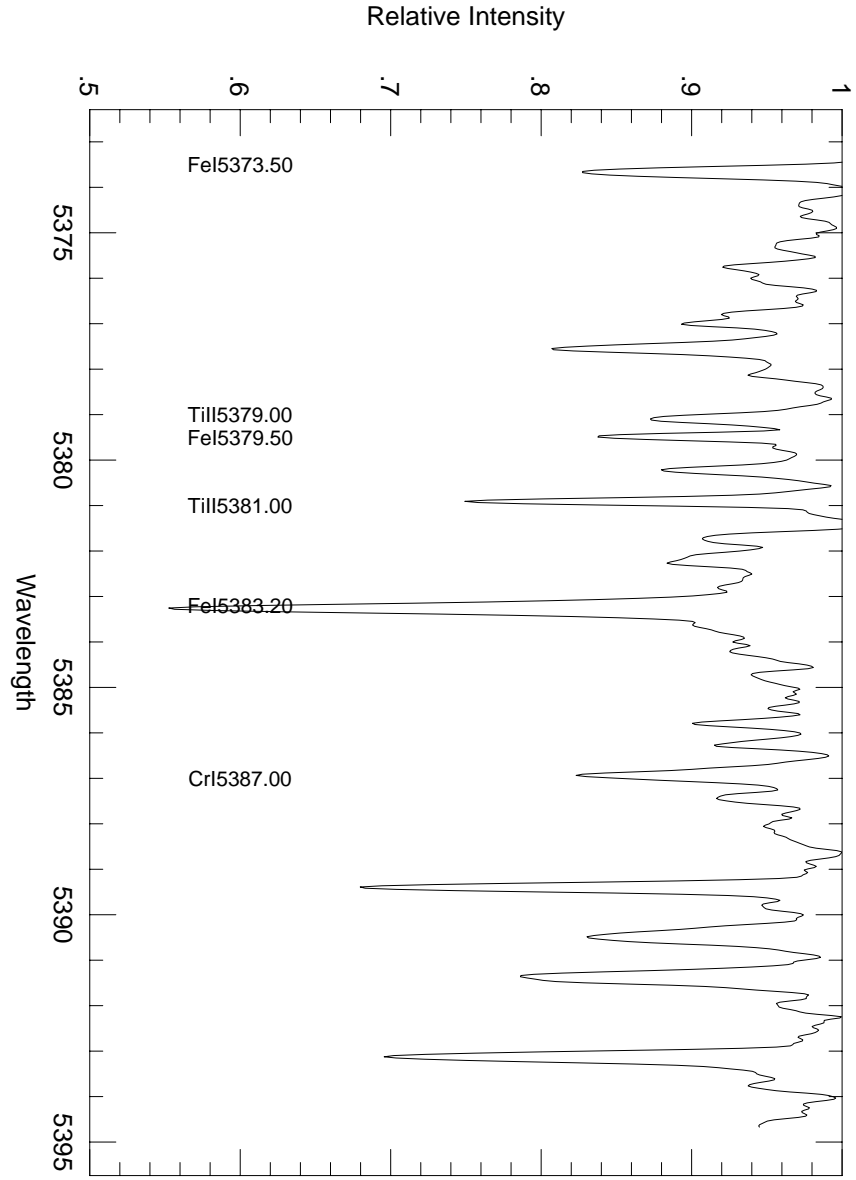


Fig. A.4.— Line identifications in the region from 5374 Å to 5395 Å.

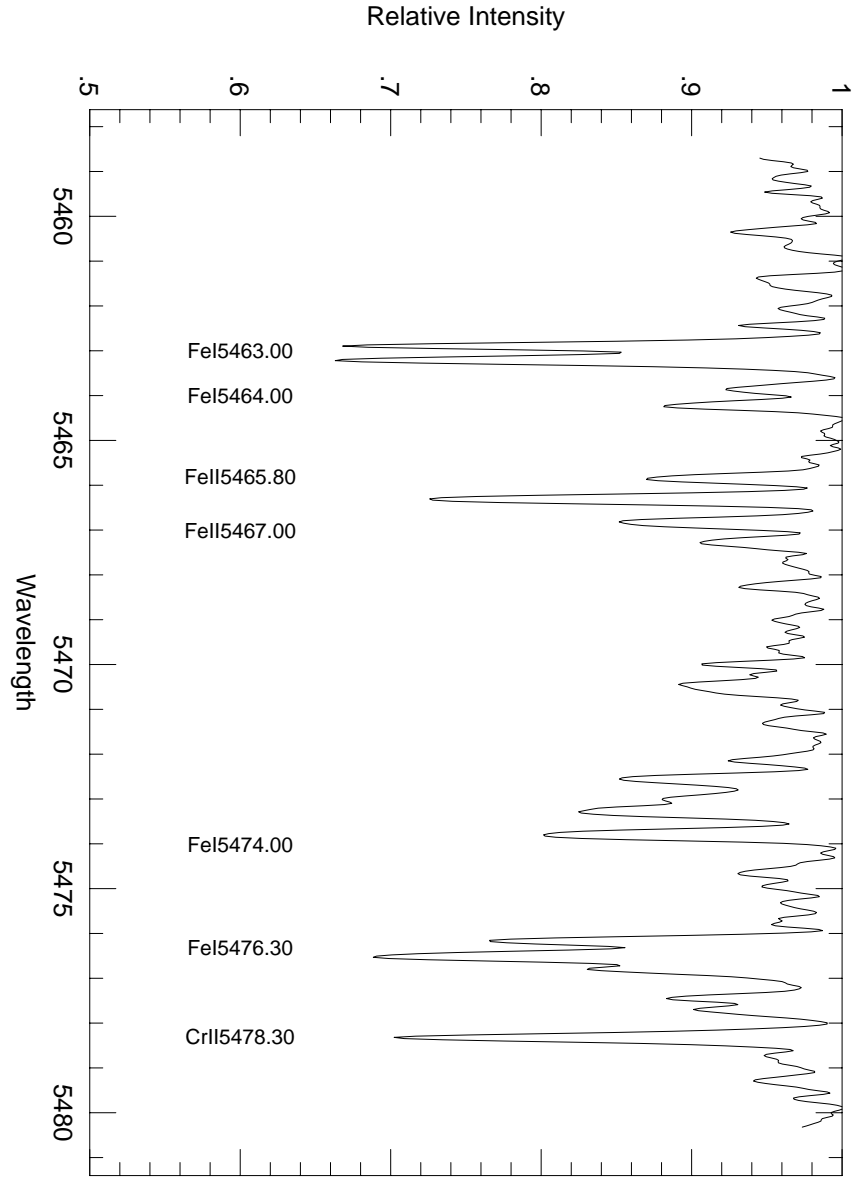


Fig. A.5.— Line identifications in the region from 5459 Å to 5481 Å.

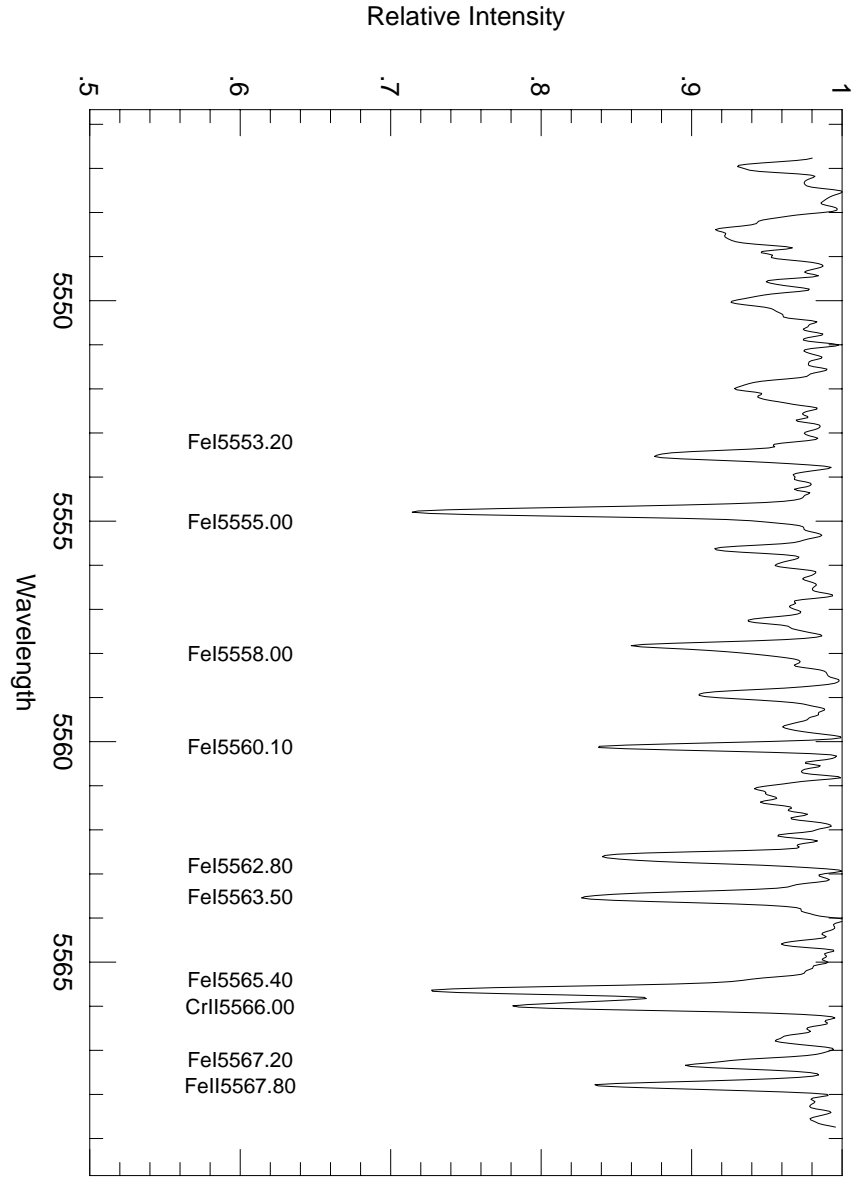


Fig. A.6.— Line identifications in the region from 5547 Å to 5568 Å.

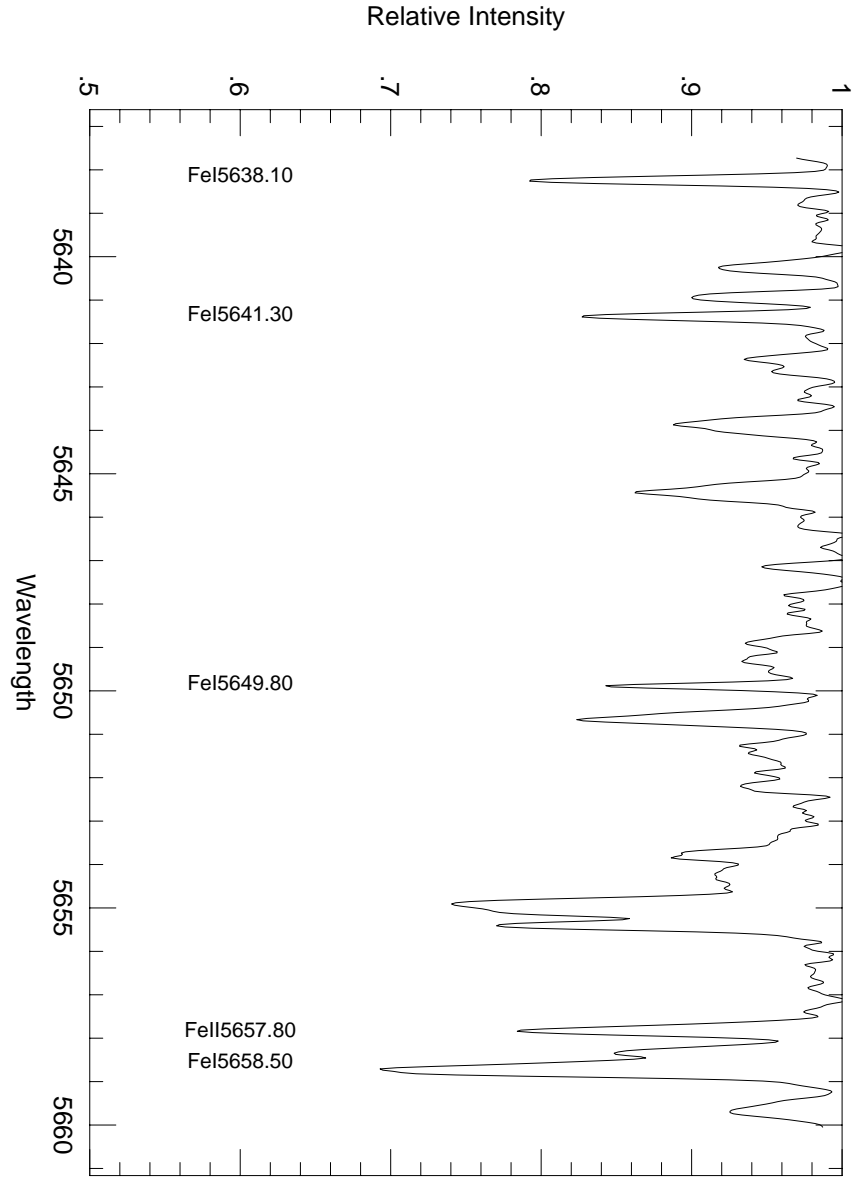


Fig. A.7.— Line identifications in the region from 5638 Å to 5660 Å.

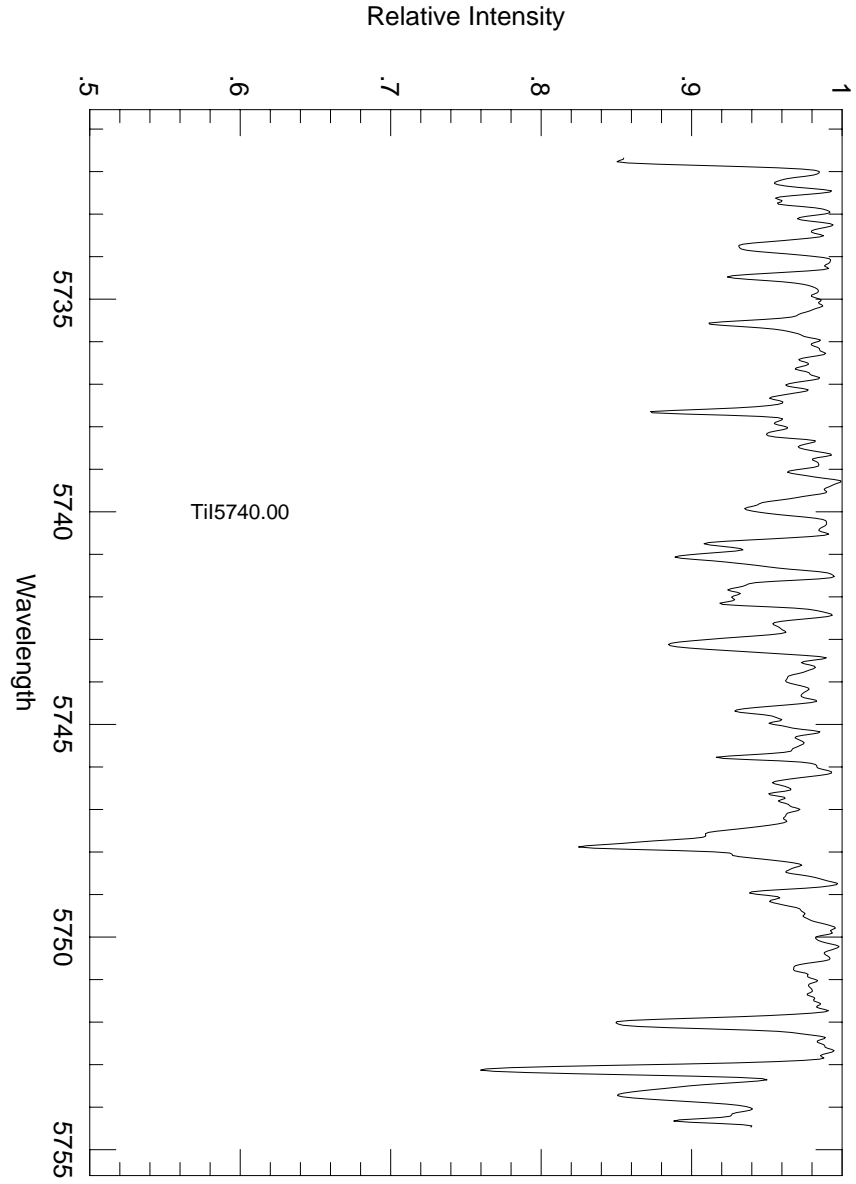


Fig. A.8.— Line identifications in the region from 5732 Å to 5755 Å.

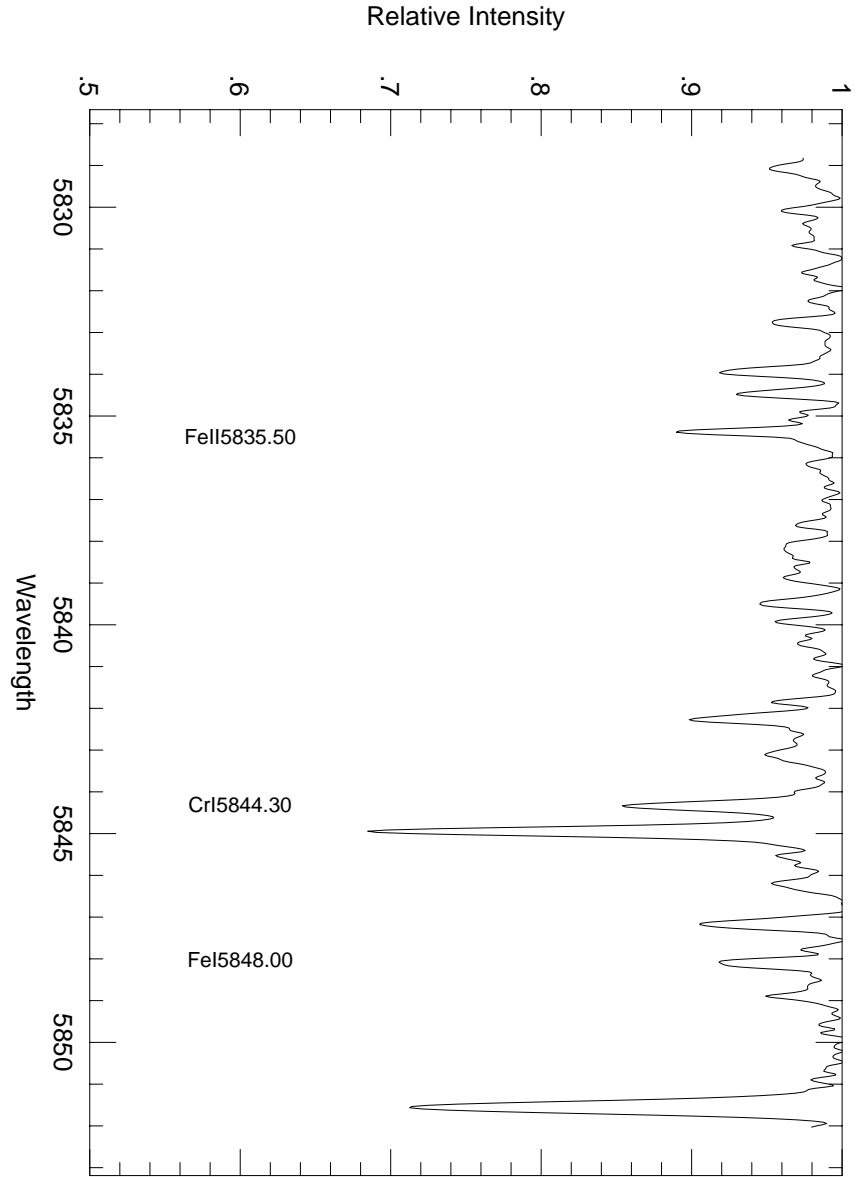


Fig. A.9.— Line identifications in the region from 5830 Å to 5852 Å.

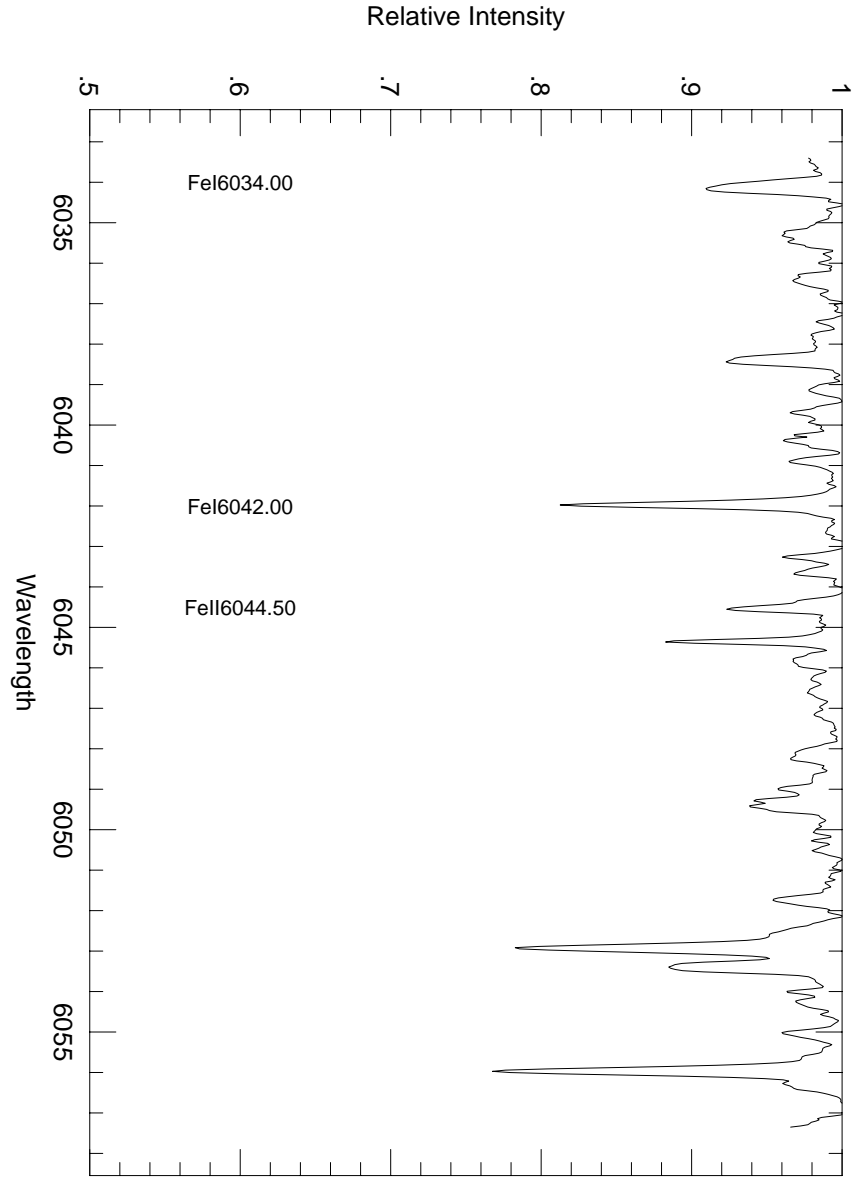


Fig. A.10.— Line identifications in the region from 6034 Å to 6057 Å.

Bibliography

- Abbott, T.M.C., 1992, Ph. D. Thesis University of Texas at Austin.
- Abrikosov, A., 1961, Soviet Phys, 12, 1254
- Angel, J.R.P., Borra, E.F. and Landstreet, J.D., 1981, ApJS, 45, 457
- Angel, J.R.P., Borra, E.F., and Landstreet, J.D., 1981, ApJS, 45, 457
- Liebert, J., Saffer, R.A. and Bergeron, P. 1995, ApJ, 357, 216
- Bergeron, P., Wesemael, F., Fontaine, G. and Liebert, J., 1990, ApJ, 351, L21.
- Bergeron, P., Wesemael, F., Lamontagne, R., Fontaine, G., Saffer, R.A. and Allard, N.F. ApJ, 449, 258
- Bidelman, W.P., 1985, in “Cepheids: Theory and Observations”.
Proceedings of the IAU colloquium no. 82 (ed. Barry F. Madore) Cambridge
University Press p. 83
- Bonsack, W.K. and Pilachowski, C.A., 1974, ApJ, 190, 327
- Borra, E.F., Edwards, G. and Mayor, M., 1984, ApJ, 284, 211
- Bradley, P., Winget, D.E. and Wood, M.A., 1992, ApJ, 391,L33
- Bradley, P. and Winget, D.E. 1994, ApJ, 421, 236

- Breger, M. 1979, PASP, 91, 5.
- Claver, C.F., 1994, Ph.D. Thesis, University of Texas at Austin
- Clemens, C. 1994, Ph.D. thesis University of Texas at Austin
- Cochran, W.D. and Hatzes, A.P., 1994, Ap&SS, 212, 281
- Cox, J.P. and Giuli, R.T., 1968, Principles of Stellar Structure (N.Y.: Gordon and Breach)
- Cox, J.P. 1980, "Theory of Stellar Pulsation", Princeton
- Daou, D., Wesemael, F., Bergeron, P., Fontaine, G. and Holberg, J.B., 1990, ApJ, 364, 242
- Deupree, R.G., 1977, ApJ, 211, 509
- Deupree, R.G., 1980, ApJ, 236, 225
- Dolez, N., and Vauclair, G. 1981, A&A, 102, 375
- Dolez, N., Vauclair, G. and Koester, D., 1991 in "White Dwarfs", Seventh European Workshop on White Dwarfs, Eds. G. Vauclair and E. Sion, Kluwer Academic Publishers, Netherlands, p. 361
- Fontaine, G., McGraw, J.T., Dearborn, D.S.P., Gustafson, J. and Lacombe, P., 1982, ApJ, 258, 661
- Fontaine, G., Villeneuve, B. and Wilson, J., 1981, ApJ, 243, 550
- Fontaine, G., Villeneuve, B. and Wilson, J., 1981, ApJ, 243, 550

- Fontaine, G., McGraw, J.T., Dearborn, D.S.P., Gustafson, J. and Lacombe, P., 1982, ApJ, 258, 661
- Fontaine, G., Bergeron, P., Lacombe, R., Lamontagne, R. and Talon, A., 1985, AJ, 90, 1094
- Gilliland, R. L. and Brown, T. M., 1988, PASP, 100, 754
- Giovannini, O., 1996, Ph.D. thesis Universidade Federal do Rio Grande do Sul
- Gough, D.O. and Tayler, R.J., 1966, MNRAS, 133, 85
- Greenstein, J., 1982, ApJ, 258, 661
- Hansen, C. J., Winget, D. E., and Kawaler, S. D. 1985, ApJ, 297, 544
- Hatzes, A.H. and Kurster, M., 1994, A&A, 285, 454)
- Iben, I., 1991, ApJS, 76, 55
- Jones, P.W., Pesnell, W.D., Hansen, C.J. and Kawaler, S.D., 1989, ApJ, 336, 403
- Kanaan, A., Kepler, S.O., Giovannini, O. and Díaz, M. ApJ, 390, L89
- Kepler, S.O. and Nelan, E.P. 1993 AJ, 105, 608
- Kepler, S.O., Robinson, E.R., and Nather, R.E., 1983, ApJ, 271, 744
- Kepler, S.O., Robinson, E.L. and Nather, R.E., 1983, ApJ, 271, 744
- Kepler, S. O. et al., 1995, Baltic Astronomy, 4, 221

- Kleinman, S.J., 1995, Ph.D. thesis University of Texas at Austin
- Kleinman, S.J., 1996, PASP, 1996, 108, 356
- Kleinman, S.J., Nather, R.E. and Phillips, T., 1996, PASP, 108, 356
- Koester, D. and Herrero, A., 1988, ApJ, 332, 910
- Kurtz, D.W., 1982, MNRAS, 200, 807
- Kurtz, D.W., 1983, MNRAS, 202, 1
- Leroy J.L., Bagnulo S., Landolfi M. and Landi Degl’Innocenti, E., 1994, \AA , 284, 174
- Libbrecht, K.G., ApJ, 330, L51
- Liebert, J., 1988, PASP, 100, 1302
- Markiel, J.A., Thomas, J.H. and Van Horn, H.M., 1994, ApJ, 430, 834
- Markiel, J.A., Thomas, J.H. and Van Horn, H.M., 1995, ApJ, 453, 403
- Martinez, P., 1993, Ph.D. thesis University of Cape Town
- Matthews, J.M. and Scott, S., 1995 ASP Conf. Series, 83, 347
- Matthews, J.M, Wehlau, W.H. Walker, G.A.H. and Yang, S., ApJ, 324, 1099
- Mccarthy, J.K., Sandiford, B.A., Boyd, D., Booth, J., 1993, PASP, 105, 881
- McCook, G.P. and Sion, E.M. 1987, ApJS, 65, 603
- McGraw, J.T., 1976, ApJ, 210, L35

- McGraw, J.T., 1979, ApJ, 229, 203
- McGraw, J.T., 1979, ApJ, 229, 203
- Michaud, G., 1970, ApJ, 160, 641
- Moss, D., 1986, Physics Reports, 140, 1
- North, P., 1993, in “Peculiar Versus Normal Phenomena in A-Type and Related Stars”, ASP Conference Series, Vol. 44, M.M. Dworetsky, F. Castelli and R. Faraggiana (eds.), p. 577
- Reimers, D. and Koester, D., 1982, A&A, 116, 341
- Reimers, D. and Koester, D., 1982, A&A, 116, 341
- Reimers, D. and Koester, D., 1994, A&A, 285, 451
- Ritter, H., 1990 A&AS, 85, 1179
- Robinson, E.L., Stover, R.J., Nather, R.E. and McGraw, J.T., 1978, ApJ, 220, 614.
- Robinson, E.L., Kepler, S.O. and Nather, R.E., 1982, ApJ, 259, 219
- Robinson, E. L., Mailloux, T. M., Zhang, E., Koester, D., Stiening, R. F., Bless, R. C., Percival, J. W., Taylor, M. J., van Citters, G. W., 1995, ApJ, 438, 908
- Romanishin, W. and Angel, J.R.P., 1980, ApJ, 235, 992
- Salpeter, E., 1961, ApJ, 134, 669
- Scargle, J.D., 1982, ApJ, 263, 835

- Schmidt and Smith, 1995, ApJ, 448, 305
- Stetson, P., 1987, PASP, 99, 111
- Stibbs, 1950, MNRAS, 110, 395
- Thomson, C. and Duncan, R.C., 1993, ApJ, 408, 194
- Tull, R.G., MacQueen, P.J., Sneden, C. and Lambert, D.L., 1995, PASP, 107, 251
- van den Berg, D.A., 1990, AJ, 100, 445
- Wendell, C.E., Van Horn, H.M. and Sargent, D., 1987, ApJ, 313, 284
- Wesemael, F., Auer, L.H., Van Horn, H.M. and Savedoff, M.P., 1980, ApJS, 43, 159
- Wesemael, F., Bergeron, P., Fontaine, G. and Lamontagne, R., 1991, in “White Dwarfs”, eds. Gerard Vauclair and Edward Sion, proceedings of the Seventh European Workshop on White Dwarfs. Kluwer, Netherlands, p. 159
- Winget, D.E. 1981, Ph. D. Thesis, University of Rochester
- Winget, D.E. and Fontaine, G., 1982 in “Pulsations in Classical and Cataclysmic Variable Stars”, eds. John P. Cox and Carl J. Hansen, p. 46
- Winget, D.E., Van Horn, H.M., Tassoul, M., Hansen, C.J., Fontaine, G. and Carroll, B.W. 1982, ApJ 252, L65
- Winget, D.E., Robinson, E.L., Nather, E.R. and Fontaine, G., 1982, ApJ, 262, L11

Winget, D.E., Robinson, E.L., Nather, E.R. and Fontaine, G., 1982, ApJ, 262, L11

Winget, D.E., Hansen, C.J. and Van Horn, H.M., 1983, Nature, 303, 781

Winget, D.E. et al 1994, ApJ, 430, 839

Wolff, S.C., 1983. "The A-Stars: Problems and Perspectives". (CNRS, Paris and NASA, Washington, D.C.)

Wood, M.A., 1990, Ph.D. thesis University of Texas at Austin

Wood, M.A., 1990, Ph.D. thesis University of Texas at Austin

Vita

I was born on 29 March 1966, in the city of Bagé in the state of Rio Grande do Sul in Brasil. I spent too many evenings sitting by the sidewalk with my parents and two sisters watching the stars. By the time I was five I was already hooked on it. I started saying I wanted to be an Astronomer when I grew up. I attended public school for my elementary school years. I attended public school in high-school as well. In 1982 I moved to the state capital, Porto Alegre, and started my undergraduate studies in Physics. I graduated in Physics in the end of 1987 and soon started working on my masters degree, again in Physics but with a dissertation on White Dwarfs. That was the time when I met Lisi and my life was flooded with joy, and has been ever since. I graduated in July 1990. During this time I started collaborating with the Whole Earth Telescope and that collaboration culminated with my coming to Texas to become a graduate student. Gabriel was born in 1993 and has brought Lisi and I the wonders of the unexpected. His presence among us is a constant reminder how beautiful life can be if lived with love and curiosity, the two ingredients he has lots to spare.

Permanent address: Instituto de Física – UFRGS – AV. Bento
Gonçalves 9500 – 91501-900 – Porto Alegre – RS
– BRAZIL

This dissertation was typeset with L^AT_EX[†] by the author.

[†]L^AT_EX is a document preparation system developed by Leslie Lamport as a special version of Donald Knuth's T_EX Program.